# LINEAR QUADRATIC TRACKING OPTIMUM CONTROLLER MODEL DESIGN TO OPTIMIZE HIGH FREQUENCY POWER SUPPLY PERFORMANCE

by

Xiying Li

Submitted in Partial Fulfillment of the Requirements

for the Degree of

Master of Science in Engineering

in the

Electrical Engineering

Program

YOUNGSTOWN STATE UNIVERSITY

March, 1999

**Linear Quadratic Tracking Optimum Controller Model Design to Optimize High Frequency Power Supply Performance**

Xiying Li

I hereby release this thesis to the public. I understand this thesis will be housed at the Circulation Desk of the University library and will be available for public access. I also authorize the University or other individuals to make copies of this thesis as needed for scholarly research.

Signature:

Xiying Li 3/9/99

Student Date

Approvals:

03/10/99

Thesis Advisor Date

Robert H. Lorsbach 3-10-99

Committee Member Date

3/10/99

Committee Member Date

3/12/99

Dean of Graduate Studies Date

*To my wife, Xiaomei*

# Table of Contents

# ABSTRACT

The performance of the High Frequency Power Supply (HFPS) induction heating system is improved by building an optimum controller to achieve optimum closed loop control, using the Linear Quadratic Tracking (LQT) method. The optimum controller is designed to minimize the difference between the HFPS actual system output and the desired reference signal, while keeping the system control input minimized.

The utilization of switching devices in HFPS induction heating system results in high power loss, poor line power factor, and harmful harmonics. In this research, first a continuous-time linear system model is developed to simulate the HFPS induction heating system with a series-parallel resonant load. Second, the LQT optimum controller is developed to achieve optimum closed-loop control in both continuous and discrete time domains to optimize the system performance. Third, a desired pure sinusoidal reference signal is constructed with desired magnitude and frequency by programming devices. Fourth, the desired reference signal and HFPS induction heating system feedback as inputs to the LQT optimum controller are used to simulate the ideal and real system performance with the LQT optimum controller. By using the LQT optimum controller, the system output is forced to track the desired reference signal closely, in both continuous and discrete time domains. The simulation results are compared with the industry test data to confirm the theoretical consideration.

## NOMENCLATURE

$A_\alpha$ Volt-radian area

$A_u$ Current commutation voltage drop area

$\alpha$ AC-DC rectifier section firing angle

$f_1$ (Modulating frequency) is the desired fundamental frequency of the inverter voltage output, which is also the frequency of the control signal.

$f_s$ ( carrier frequency), which establishes the frequency with which the inverter switches are switched.

$i_{LO}$ Induction coil current.

$i_{SE}$ Series inductance current (HFPS system output).

$\boldsymbol{K(\infty)}$ Steady state feed backward gain (1×3 vector).

$\boldsymbol{K_k}$ Discrete time feed backward gain (1×3 vector).

$\boldsymbol{K^v(\infty)}$ Steady state feed forward gain (1×3 vector).

$\boldsymbol{K^v_k}$ Discrete time feed forward gain (1×3 vector).

$\boldsymbol{K(t)}$ Continuous time feed backward gain (1×3 vector).

$\boldsymbol{K^v(t)}$ Continuous time feed forward gain (1×3 vector).

$CDC$ DC filtering capacitor

$LDC$ DC filtering reactor

$L_s$ Input line inductance

$L_{SE}$ Load series inductance

$M_a$ Amplitude modulation ratio $m_a = \dfrac{\hat{V}_{control}}{\hat{V}_{tri}}$

$M_f$ Frequency modulation ratio $m_f = \dfrac{f_s}{f_1}$

$\phi$ DC-AC inverter section firing angle

$r_k$ Discrete time desired reference signal.

r(t) Continuous time desired reference signal.

$\boldsymbol{S(\infty)}$ Steady state auxiliary matrix (3×3 matrix).

$u_k$ Ideal control input.

$v$ Auxiliary vector (3×1 vector)

$V_C$ Tank capacitors voltage.

$V_{control}$ Control signal to modulate the switch duty ratio and has a frequency $f_1$.

$\hat{V}_{control}$ The peak amplitude of the control signal.

$V_d$ Inverter output voltage (HFPS system input).

$V_{LL}$ Input line to line voltage

$V_{tri}$ Triangular waveform is at a frequency $f_s$.

$\hat{V}_{tri}$ The amplitude of the triangular signal, usually kept as a constant.

$Z_{load}$ Load section impedance

# Chapter 1

## Introduction

In high frequency induction heating applications, the desired waveform of High Frequency Power Supply output current is a pure sinusoidal waveform with fixed frequency. This research proposes a LQT optimum controller model, to achieve an optimum closed loop control, and minimize the error between the desired output and the actual system output.

The HFPS system with discrete time LQT optimum controller is shown in Fig. 1. The LQT optimum controller has two independent inputs: the desired reference signal and the system feedback state variables. The desired reference signal is a pure sinusoidal waveform with desired frequency and magnitude. An A/D converter is used to convert the system feedback state variables into discrete time domain. Based on these inputs, the LQT optimum controller generates the optimum control signal ($u_k$). The control signal converter produces inverter section firing angle and switching frequency, to make the rms value and the frequency of the inverter section output voltage ($V_d$) equal to those of the control signal ($u_k$).

The electrical schematic of the HFPS system is shown in Fig. 2. The power input is a three phases, *480 V, 60 Hz* line. The AC-DC rectifier section converts the AC line into

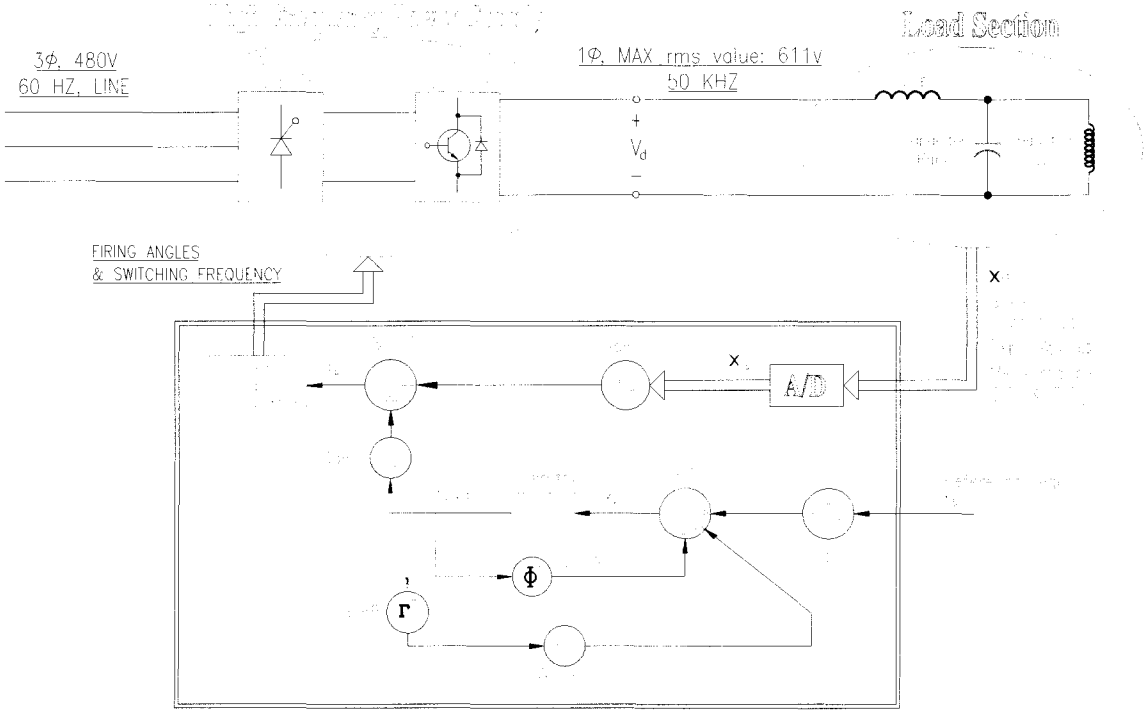


**Fig. 1 HFPS System w/ LQT Controller**

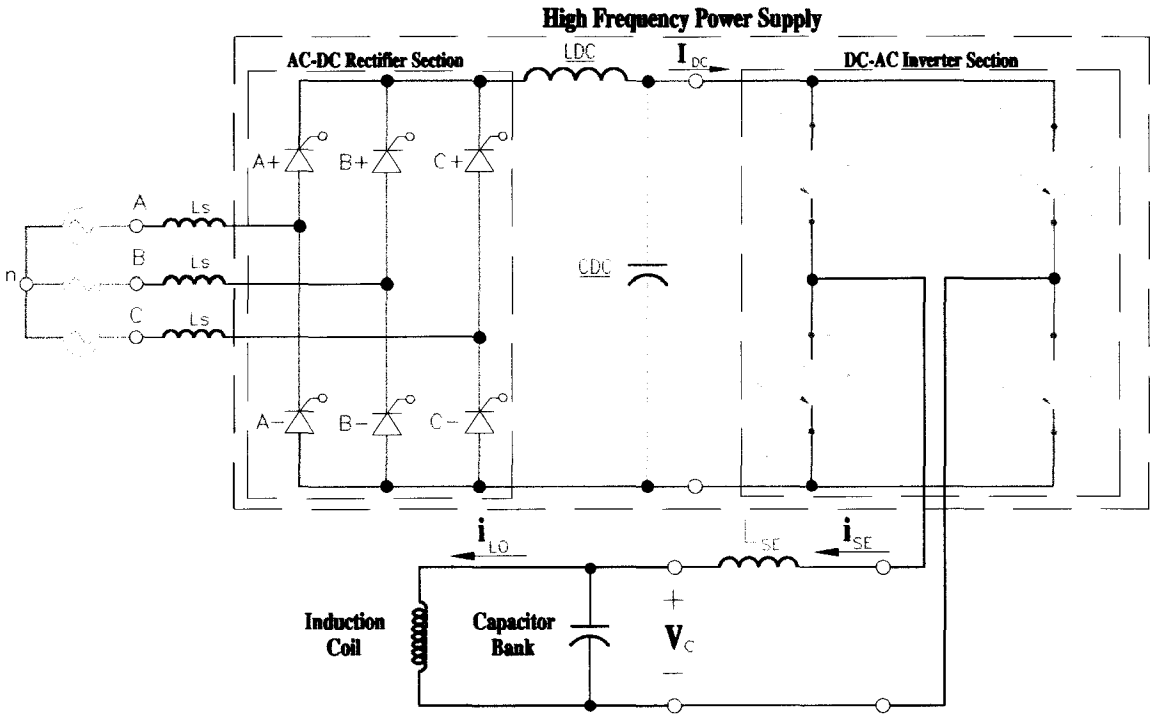


**Fig. 2 HFPS System Electrical Schematic**

DC supply, by switching phase controlled thyristors (*A+*, *B+*, *C+*, *A-*, *B-*, *C-*). The reactor *LDC* and filter capacitor *CDC*, purify the rectified DC output, to produce better DC supply. The DC-AC inverter section uses IGBT modules (*P+*, *P-*, *N+*, *N-*), that converts the DC supply into single phase, *50 kHz* output voltage ($V_d$) with forced commutation. The $L_{SE}$, capacitor bank and induction coil form a series-parallel resonant circuit, where the high resonant induction current and voltage are generated to satisfy the induction-heating requirements.

The HFPS induction heating system is controlled: (a) by controlling the switching device's firing angle $\alpha$ of the rectifier section to adjust the DC output voltage, (b) by controlling the firing angle $\phi$ for the inverter section switching devices, and (c) by controlling the inverter section output frequency to tune the resonant-load section.

The optimum controller produces the firing angle and switching frequency for the DC-AC inverter section based on the system feedback signals ($i_{SE}$), ($V_C$), and ($i_{LO}$), such that the system output ($i_{SE}$) tracks the desired reference signal closely. Due to the requirements for the induction depth of penetration [3] on the heating parts, and the desire to minimizing switching loss and system harmonics, the desired system output ($i_{SE}$) has to be a pure sinusoidal waveform with fixed load resonant frequency *50 kHz* for this case.

# Chapter 2

# Characteristics of High Frequency Power Supply

In this chapter, the basic structure and operation of HFPS, along with the process of AC to DC rectifying and DC to AC converting will be discussed. Also, all the switching devices are assumed to be ideal switches.

## 2.1 AC-DC Rectifier Sections

The AC-DC rectifier section is composed of three positive legs A+, B+, C+, and three negative legs A-, B-, and C-. Each leg has one or more thyristors in parallel. The output voltage of the converter is controlled by the firing angle $\alpha$ of each thyristor. The following subsection will describe the concept of signal phase rectifying and three phases rectifying.

### 2.1.1 Concept of Signal Phase Rectifying

In this section, it is assumed that all the thyristors are perfect switches with zero turn on/off time, also it is assumed that the AC line voltage is a pure sinusoidal waveform with a fixed frequency of 60 Hz. When the firing angles for the thyristors are $0^{\circ}$ and $60^{\circ}$, the waveforms of the input line voltage, current, rectifier bridge (*A+*, *A-*, *B+*, *B-*) output voltage and current for phase A are shown in Fig. 3.

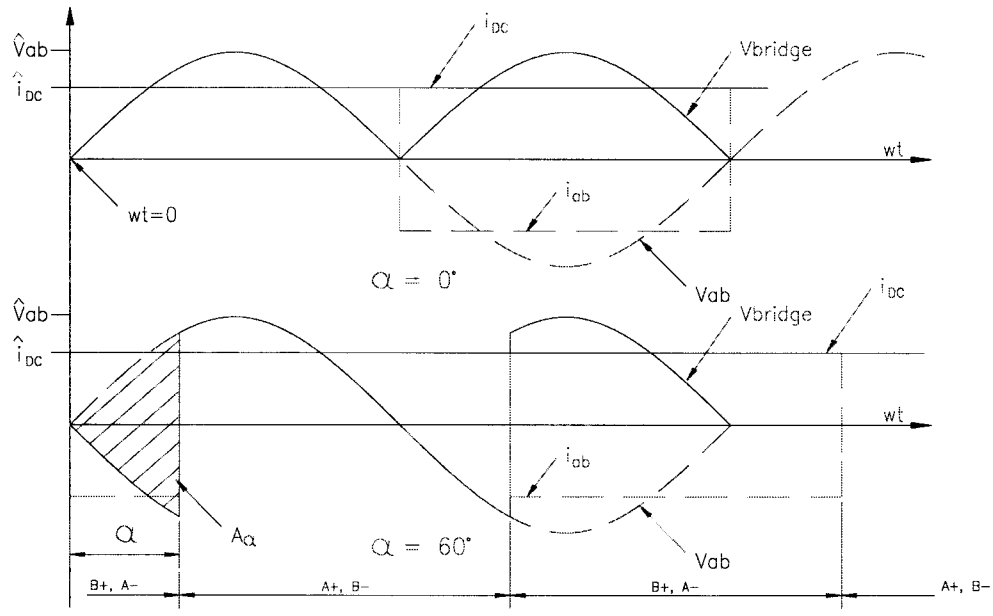


**Fig. 3 Single Phase Rectified Waveforms**

When $\alpha = 0^o$, the rectifier section acts like a diode DC bridge. Also, before $t = 0$, it is assumed that all thyristors have been turned off. At $\omega t = 0^o$ turn on thyristors $A+$ and $B-$. Then the rectifier ouput voltage is the line voltage ($V_{ab}$), and the rectifier bridge output current is equal to the line current ($i_{ab}$).

At $\omega t = 180^o$, turn on thyristors $A-$, $B+$, and the same time turn off thyristors $A+$and $B-$, then the rectifier ouput voltage and current are expected to be the mirror of those of the line voltage ($V_{ab}$). The rectifier bridge output voltage is a periodcal function with a period of $1/120$ sec.

When $\alpha = 60^o$, thyristors $A+$ and $B-$ begin to conduct at $\omega t = 60^o$, and at the same time thyristors $A-$ and $B+$ will be turned off. Then, at $\omega t = 240^o$, $B+$ and $A-$ begin to conduct, $A+$ and $B-$ will turn off and the waveforms repeat every $1/120$ sec.

When $\alpha = 90^o$, thyristors $A+$ and $B-$ begin to conduct at $\omega t = 90^o$, and at the same time thyristors $A-$ and $B+$ will be turned off. Then, at $\omega t = 270^o$, $B+$ and $A-$ begin to conduct, $A+$ and $B-$ will turn off and the waveforms repeat every $1/120$ sec. Therefore, the average output voltage is zero.

The shaded area $A_\alpha$ is called volt-radian area. This area is the difference between the diode full-rectifier bridge and the thyristor bridge. The expression for the average value for $V_{bridge}'$ is

$$\overline{V}_{bridge}' = \frac{1}{\pi}\int_{\alpha}^{\pi+\alpha} (\sqrt{2}\cdot V_{ab}\sin\omega t)\, d(\omega t) \qquad (2\text{-}1\text{-}1)$$

the solution of the above equation is [1]

$$\overline{V}_{bridge}' = \frac{2\sqrt{2}}{\pi} V_{ab}\cos\alpha \qquad (2\text{-}1\text{-}2)$$

From equation (2-1-2), the average rectifier bridge output is a function of thyristor firing angle $\alpha$. By controlling the thyristor-firing angle, the output of the rectifier bridge can be controlled. When the thyristor firing angle $\alpha$ equals to zero, the bridge output voltage is the maximum. When the thyristor firing angle $\alpha$ equals to $90^o$, the bridge output voltage is zero.

The average input power in one period can be calculated by

$$P = \frac{1}{T}\int_0^T p(t)\,dt = \frac{1}{T}\int_0^T v_s(t) i_s(t)\,dt \qquad (2\text{-}1\text{-}3)$$

where $v_s$, and $i_s$ are the instantaneous voltage and current.

Assuming that the utility voltage is a purely sinusoidal waveform at the line frequency. The input current is the sum of its Fourier (harmonic) components as given by equation (2-1-4),

$$i_s(t) = i_{s1}(t) + \sum_{h \neq 1} i_{sh}(t) \tag{2-1-4}$$

where $i_{s1}$ is the fundamental component, $h$ is the order of the harmonics, and $i_{sh}$ is the component at the $h$th harmonic with frequency of $\omega_h/2\pi = hf_1$ . Also, the rms value of the line current can be calculated by equation (2-1-5)

$$I_S = \left( \frac{1}{T_1} \int_0^{T_1} i_s{}^2(t)\,dt \right)^{1/2} \tag{2-1-5}$$

substitute equation (2-1-4) into equation (2-1-5) to obtain

$$I_S = \left( I_{s1}^2 + \sum_{h \neq 1} I_{sh}^2 \right)^{1/2} \tag{2-1-6}$$

The power factor is defined by equation (2-1-7),

$$PF = \frac{V_s I_{s1} \cos\phi_1}{V_s I_s} = \frac{I_{s1} \cos\phi_1}{I_s} \tag{2-1-7}$$

In the above equation, $I_{s1} = 0.78\, I_{DC}$, $I_{DC}$ = the output current of the rectifier section.

For the single phase, the phase angle equals to zero. Therefore, the power factor for the single phase will be

$$PF = \frac{I_{s1}}{I_s} = \frac{3}{\pi} \approx 0.955 \tag{2-1-8}$$

### 2.1.2 Three-phase Rectification With *Ls=0* and $i_d(t) = i_{DC}$, and α=0

The line voltage and current waveforms are shown in Fig. 4. For zero line inductance (*Ls*), the transition of the line current from a value of $\pm I_{DC}$ to zero will be instantaneous. The rectifier section output current is constant, and the voltage drop across the line inductance (*Ls*) is zero. The input line current is shown in equations (2-1-9), (2-1-10), and (2-1-11)[1],

$$i_a = \begin{cases} I_d & when\ A+\ conducting \\ -I_d & when\ A-\ conducting \\ 0 & when\ neither\ A+, A-\ conducting \end{cases} \quad (2\text{-}1\text{-}9)$$

$$i_b = \begin{cases} I_d & when\ B+\ conducting \\ -I_d & when\ B-\ conducting \\ 0 & when\ neither\ B+, B-\ conducting \end{cases} \quad (2\text{-}1\text{-}10)$$

$$i_c = \begin{cases} I_d & when\ C+\ conducting \\ -I_d & when\ C-\ conducting \\ 0 & when\ neither\ C+, C-\ conducting \end{cases} \quad (2\text{-}1\text{-}11)$$

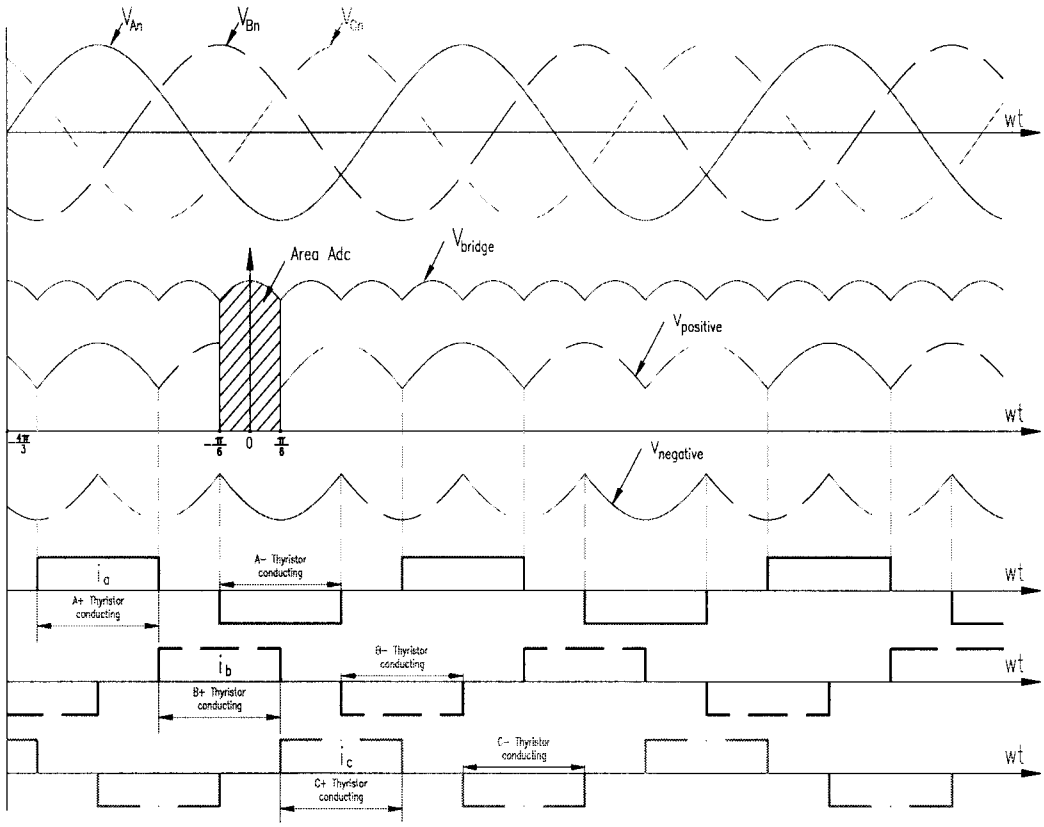


**Fig. 4 Waveforms for Line Voltage and Current**

For three-phase line input at the interval $-\frac{1}{6}\pi < \omega t < \frac{1}{6}\pi$ ,

$$V_{bridge} = v_{An} - v_{Bn} = v_{ab} = \sqrt{2}V_{LL}\cos\omega t \tag{2-1-12}$$

where $V_{LL}$ is the rms value of the line voltage, the output voltage of the AC-DC output voltage is equal to the difference between the phase A voltage and phase B voltage. The average rectifier section output voltage ($V_{DC}$) is show in the following equation.

$$V_{DC} = \frac{1}{\pi/3}\int_{-\pi/6}^{\pi/6}\sqrt{2}V_{LL}\cos\omega t d(\omega t) = \frac{3\sqrt{2}}{\pi}V_{LL} \tag{2-1-13}$$

### 2.1.3 Three-phase Rectification With $Ls \neq 0$, $i_d(t) = i_{DC}$, and $\alpha = 0$

With finite *Ls*, the transition of the line current from a value of $\pm I_{DC}$ to zero, will not be instantaneous, while the sum of the line current is still a constant as $I_{DC}$. Thus there is voltage drop across the *Ls*. During interval u, the output current of the rectifier section is the summation of the current of phase A and phase B. The voltage drop during interval u (area $A_u$) is shown by equation (2-1-14).

$$A_u = \omega L_s I_{DC} \tag{2-1-14}$$

The value of the instantaneous output voltage is shown as the following equation

$$V_{bridge} = \sqrt{2}V_{LL}\cos\omega t - \frac{A_u}{\pi/3} \tag{2-1-15}$$

Therefore, the average output voltage of the rectifier section ($V_{DC}$) is shown as the following equation

$$\begin{aligned} V_{DC} &= \frac{1}{\pi/3}\int_{-\pi/6}^{\pi/6}\left[\sqrt{2}V_{LL}\cos\omega t d(\omega t) - \frac{A_u}{\pi/3}\right] \\ &= \frac{3\sqrt{2}}{\pi}V_{LL} - \frac{3}{\pi}\omega L_s I_{DC} \end{aligned} \tag{2-1-16}$$

Assume both line inductance and line frequency are constants, the average output voltage of the rectifier section ($V_{DC}$) decreases, when the output DC current increases.

### 2.1.4 Three-phase Rectification With $Ls \neq 0$, $i_d(t) = i_{DC}$, and $\alpha \neq 0$

With finite *Ls*, and $\alpha \neq 0$, the transition of the line current from a value of $\pm I_{DC}$ to zero will not be instantaneous. The voltage drop on the AC-DC rectifier section output due to the finite Ls is the area $A_u$. The line voltage and current waveforms are shown in Fig. 5. There are additional voltage drops on the AC-DC rectifier section output, which is represented as $A_\alpha$.

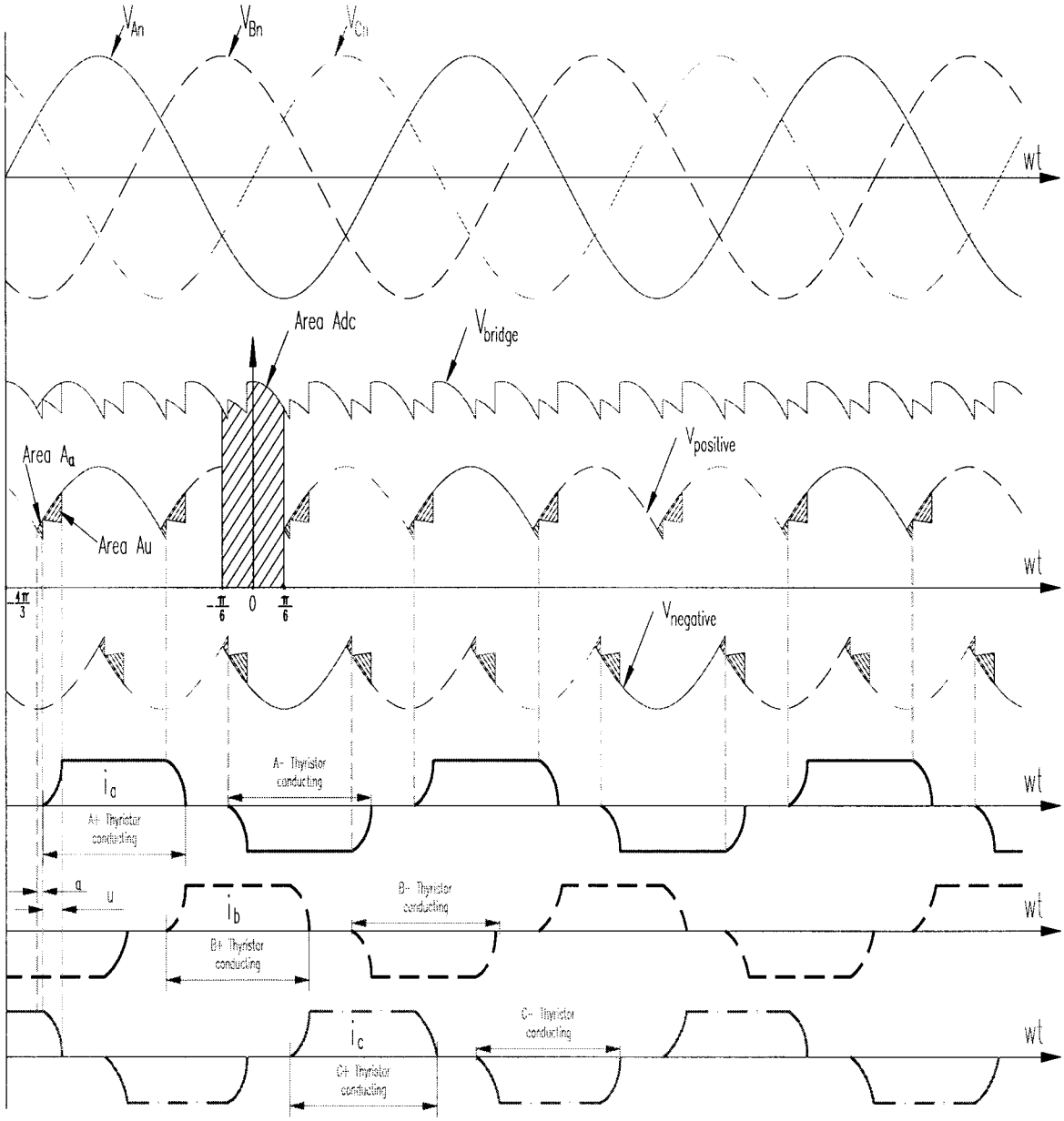


**Fig. 5 Waveforms for Line Voltage and Current**

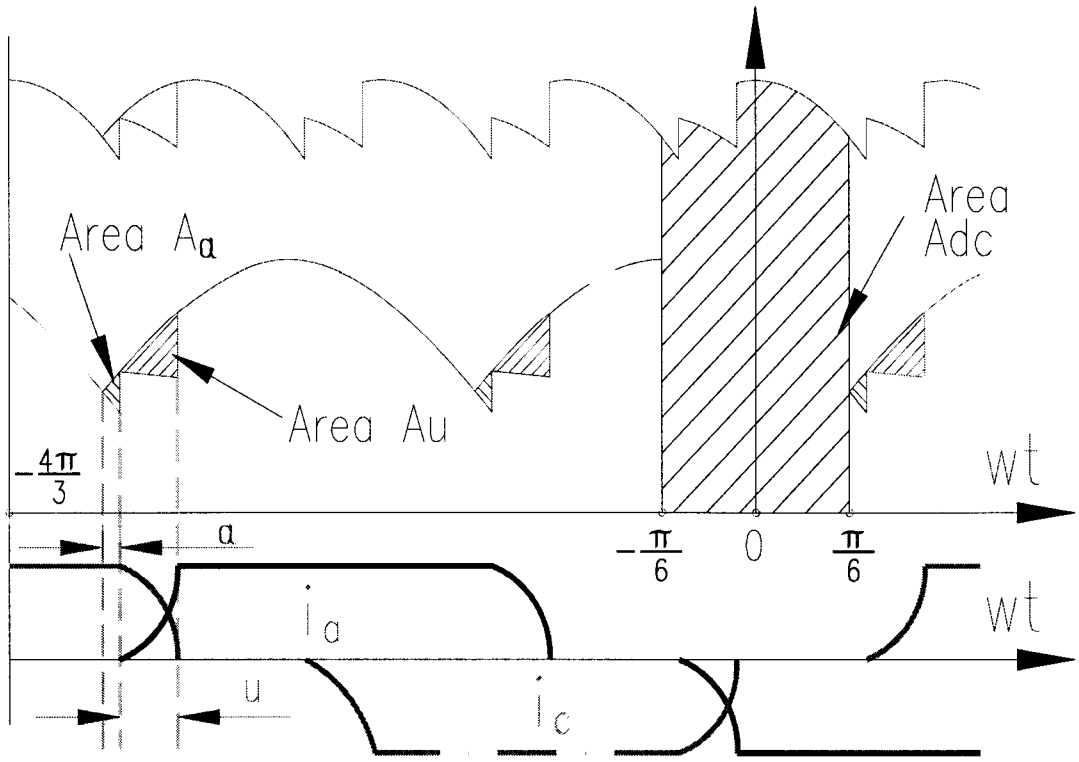


**Fig. 6 Waveforms for Line Voltage and Current (Zoom In)**

When $\alpha \neq 0$, the rectifier section average output voltage is a function of $\alpha$. Therefore, the line current waveform shifts to the right at $\alpha^{o}$. The average output voltage decreases when the firing angle $\alpha$ increases. By considering about one period of operation, as shown in Fig. 6. The voltage drops are areas $A_\alpha$ and $A_u$ [1].

During the interval u, the voltage drop (area $A_u$) is shown in equation (2-1-17).

$$A_u = \int_0^{I_{DC}} \omega L_s di_a = \omega L_s I_{DC} \qquad (2\text{-}1\text{-}17)$$

The voltage drop due to firing angle $\alpha$ (area $A_\alpha$) is shown in equation (2-1-18).

$$A_\alpha = \int_0^{\alpha} \sqrt{2} V_{LL} \sin \omega t d(\omega t) = \sqrt{2} V_{LL} (1 - \cos \alpha) \qquad (2\text{-}1\text{-}18)$$

Therefore, the average output voltage with $Ls \neq 0$ and firing angle $\alpha$ (area $A_{dc}$) is shown in equation (2-1-19).

$$V_{DC} = \frac{3}{\pi}\sqrt{2}V_{LL} - \frac{A_\alpha}{\pi/3} - \frac{A_u}{\pi/3} \qquad (2\text{-}1\text{-}19)$$

substitute equations (2-1-17) and (2-1-18) into equation (2-1-19) to solve $V_{DC}$.

$$V_{DC} = \frac{3}{\pi}\sqrt{2}V_{LL}\cos\alpha - \frac{\omega L_s I_{DC}}{\pi/3} \qquad (2\text{-}1\text{-}20)$$

Therefore, with $\alpha = 0^{\circ}$, 480 V line voltage, the maximum output DC voltage is 610 V and the rated output current $I_{DC}$ is 8000A. Assume ac-side inductance Ls can not be ignored, based on the international standard the line inductance is

$$Ls = 10\% \frac{\sqrt{2}\cdot V_{LL}}{\sqrt{3}\cdot\omega\cdot I_{DC}} = 12.99\mu H \qquad (2\text{-}1\text{-}21)$$

The line current is approximated to be a trapezoidal waveform in interval u, as shown in Fig 7. During the commutation interval u, the summation of the current of phase A and phase C is equal to the output DC current $I_{DC}$. The area $A_u$ and $A_u'$ are approximately equal. The positive leg voltage is defined by equation (2-1-22)

$$v_{postive} = \frac{v_{An} + v_{Cn}}{2} - L_s \frac{di_c}{dt} \qquad (2\text{-}1\text{-}22)$$

Since the line inductance $L_s$ is small, $v_{postive}$ can be approximated by equation (2-1-23)

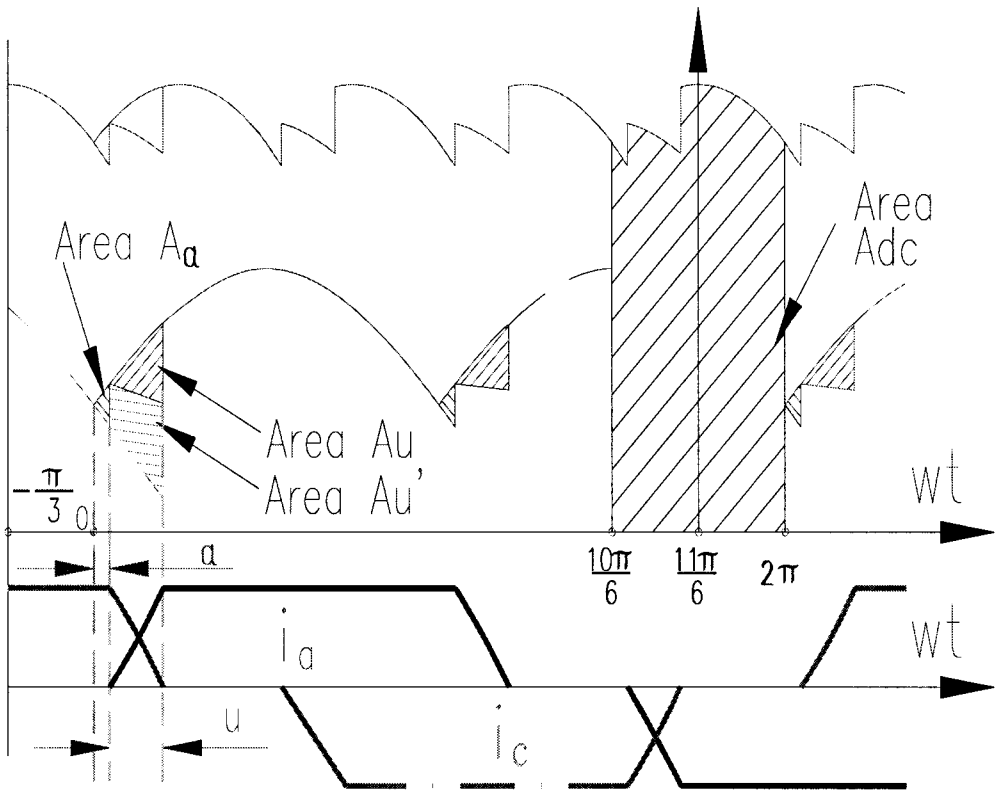


**Fig. 7 Approximation of the Line Current**

$$v_{postive} \approx \frac{v_{An} + v_{Cn}}{2} \tag{2-1-23}$$

By selecting the origin at $\omega t = 0$, the line voltage is $V_{AC} = \sqrt{2}V_{LL}\sin\omega t$, and the line current is shown in equation (2-1-24), the slope of the current of phase A is a function of the frequency, the line voltage, and the line inductance.

$$\frac{di_a}{d(\omega t)} = \frac{\sqrt{2}V_{LL}\sin\omega t}{2\omega L_s} \tag{2-1-24}$$

By changing the variables and integrating equation (2-1-24) in duration from α to α+u, yield

$$\int_0^{I_{DC}} di_a = \frac{\sqrt{2}V_{LL}}{2\omega L_s}\int_\alpha^{\alpha+u} \sin\ \omega d(\omega t) \tag{2-1-25}$$

The displacement power factor (DPF) can be approximated as

$$DPF \approx \cos(\alpha + \frac{1}{2}u) \tag{2-1-26}$$

The rms value $I_a$ and the fundamental frequency component $I_{a1}$ are shown in the following equations

$$I_a = \sqrt{\frac{2}{3}}I_d \text{ and } I_{a1} = \frac{\sqrt{6}}{\pi}I_d \tag{2-1-27}$$

Therefore, the power factor is shown in equation (2-1-28), if the commutation interval for the current is constant, the power factor is a function of the thyristor firing angle α, and the power factor is closest to unity when the firing angle equals to zero. (In this research, the firing angle α for the rectifier section will keep as zero.)

$$PF = \frac{I_{a1}}{I_a}DPF = \frac{3}{\pi}\cos(\alpha + \frac{1}{2}u) \tag{2-1-28}$$

### 2.1.5 Simulation of the Rectifier Section With Ls ≠ 0, $i_d(t) = i_{DC}$, and $\alpha \neq 0$

The Matlab Simulink model for the rectifier section is shown in Fig. 8. The figure represents the line to line voltage $V_{ab}$, $V_{ac}$, and $V_{bc}$ by three pure sinusoidal waveforms with fixed line frequency. By using the Matlab signal generators, to generate and synchronize the line-line voltages ($V_{LL}$). Simulate the rectifier section output voltage, by using the superposition function block, and calculate the voltage drop across line inductance Ls. Then subtract the voltage drop from the rectifier section output voltage. Assume all the switching devices are ideal. Therefore, both turn on or off time and switching losses will not be considered in this simulation. The three sinusoidal signal generators simulate the input voltage $V_{An}$, $V_{Bn}$ and $V_{Cn}$. At each instance, add up the line voltages to get the positive leg and negative voltages. Therefore, the output voltage of the rectifier section is $V_{bridge} = V_{Pn} - V_{Nn}$,

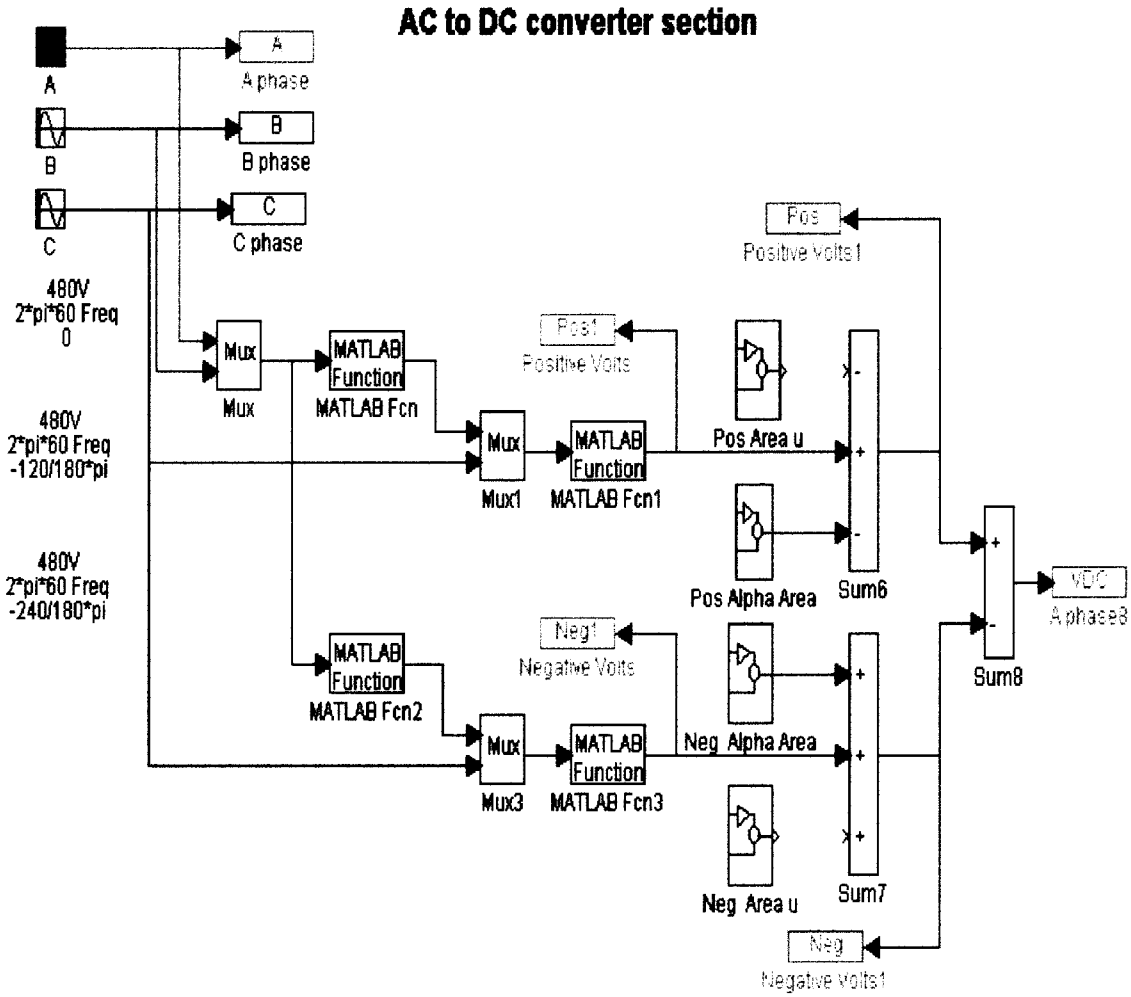


**Fig. 8 Simulink Model for AC-DC Rectifier Section**

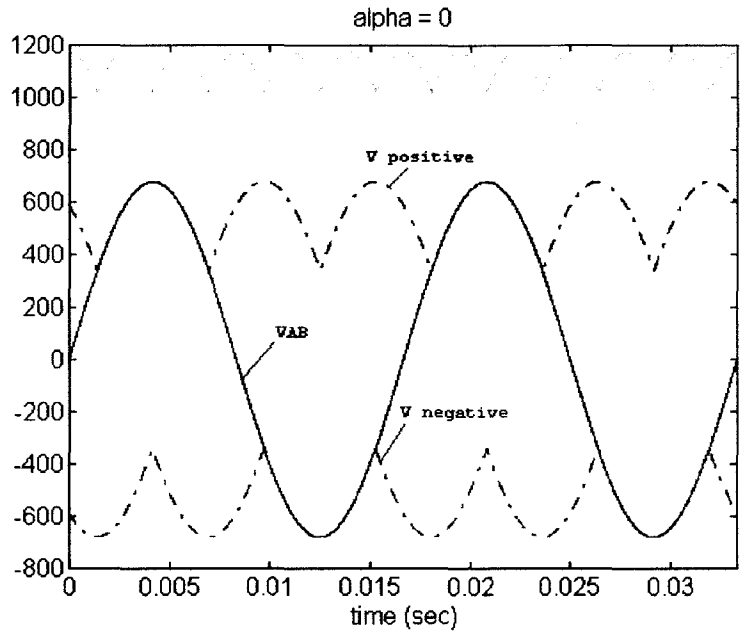


**Fig. 9** **Waveforms for the Voltage Output w/ Ls = 0 and $i_d(t) = i_{DC}$ and $\alpha = 0$**

The voltage waveforms are shown in Fig. 9, in one period, the current commutation of the rectifier section is shown as follows:

when $\frac{\pi}{6} \geq \omega t \geq 0$ Thyristor C+, B- conducting,

$$V_{Pn} = v_{Cn},\ V_{Nn} = v_{Bn},\ \text{and}\ V_{Bridge} = v_{Pn} - v_{Nn} = V_{BC}$$

when $\frac{\pi}{2} \geq \omega t \geq \frac{\pi}{6}$ Thyristor A+, B- conducting,

$$V_{Pn} = v_{An},\ V_{Nn} = v_{Bn},\ \text{and}\ V_{Bridge} = v_{Pn} - v_{Nn} = V_{AB}$$

when $\frac{5\pi}{6} \geq \omega t \geq \frac{\pi}{2}$ Thyristor A+, C- conducting,

$$V_{Pn} = v_{An},\ V_{Nn} = v_{Cn},\ \text{and}\ V_{Bridge} = v_{Pn} - v_{Nn} = V_{AC}$$

when $\frac{7\pi}{6} \geq \omega t \geq \frac{5\pi}{6}$ Thyristor B+, C- conducting,

$$V_{Pn} = v_{Bn},\ V_{Nn} = v_{Cn},\ \text{and}\ V_{Bridge} = v_{Pn} - v_{Nn} = V_{BC}$$

when $\frac{3\pi}{2} \geq \omega t \geq \frac{7\pi}{6}$ Thyristor B+, A- conducting,

$$V_{Pn} = v_{Bn},\ V_{Nn} = v_{An},\ \text{and}\ V_{Bridge} = v_{Pn} - v_{Nn} = V_{BA}$$

when $\frac{11\pi}{6} \geq \omega t \geq \frac{3\pi}{2}$ Thyristor C+, A- conducting,

$$V_{Pn} = v_{Cn},\ V_{Nn} = v_{An},\ \text{and}\ V_{Bridge} = v_{Pn} - v_{Nn} = V_{CA}$$

when $2\pi \geq \omega t \geq \frac{11\pi}{6}$ Thyristor C+, B- conducting,

$$V_{Pn} = v_{Cn},\ V_{Nn} = v_{Bn},\ \text{and}\ V_{Bridge} = v_{Pn} - v_{Nn} = V_{BC}$$

When $\alpha = 0^o$, the average dc output voltage is the maximum, when $\alpha$ gets larger and larger, the voltage drop area $A_\alpha$ gets larger and larger. Therefore, the average output voltage of the rectifier section gets smaller and smaller, the line power factor gets far away from unity. The waveforms of the output voltage for $\alpha = 30^o$ and $\alpha = 60^o$ are shown in Fig. 10 and 11.

From the plots, it is evident that the magnitude of the rectifier section output voltage drops, when the thyristors firing angle increases. Due to the commutation interval (u), there is an additional voltage drop for AC line inductance Ls $\neq$ 0, when the firing angles are equal. When the firing angle continuously increases, the rectifier section averages

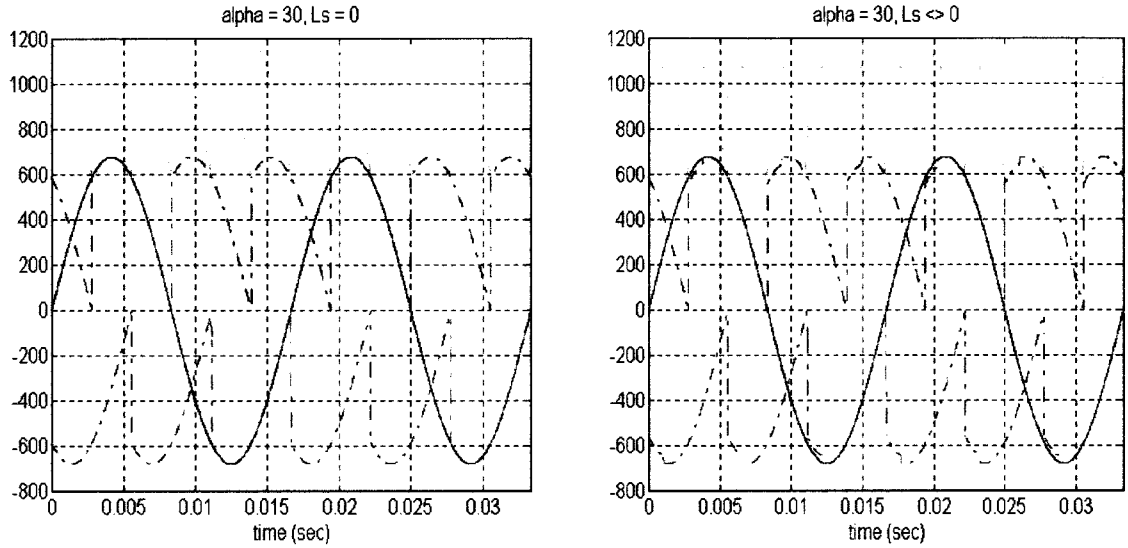


**Fig. 10 Voltage Waveforms When $\alpha = 30^o$**

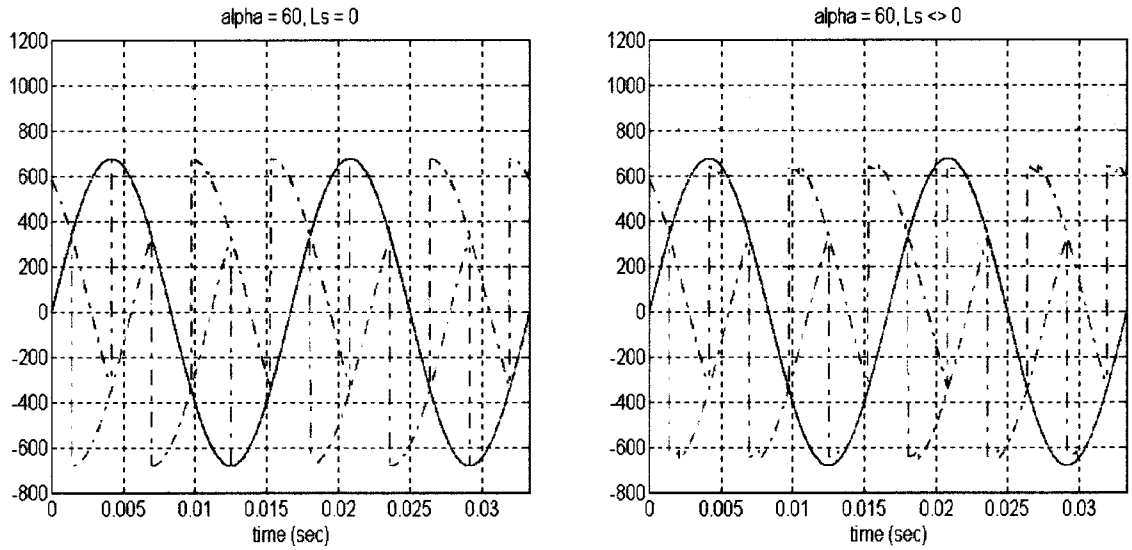


**Fig. 11 Voltage Waveforms When $\alpha = 60^o$**

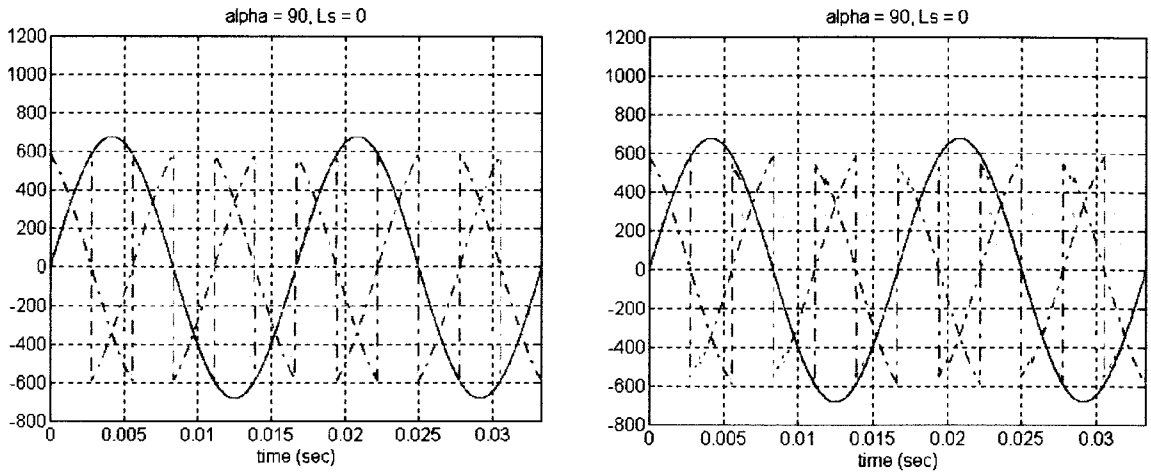


**Fig. 12 Voltage Waveforms When $\alpha = 90^o$**

output voltage approaches to zero. When the firing angle $\alpha = 90^o$, the output voltage for one period is shown in Fig. 12, for one period, the positive area is equal to the negative area. Therefore, the average output of the converter will be zero. When the firing angle $\alpha > 90^o$, the average output of the converter becomes negative. When the firing angle $\alpha = 180^o$, the average output voltage of the converter reaches the minimum negative value.

In this research, the firing angle of the converter is restricted in the range of $90^o \geq \alpha \geq 0^o$, that is the rectifier section only supply positive output voltage. When $\alpha = 0^o$, the PF is closer to one. In this research the constant $\alpha = 0^o$ is selected to get better power factor. With $\alpha = 0^o$, 480 V line voltage, the maximum output DC voltage is 610 V.

## 2.2 DC-AC Inverter Section

Assume the filter reactor and capacitor filter out the ripple voltage from the AC-DC rectifier section. Therefore, the inverter section input voltage ($V_{DC}$) is a pure DC voltage. By using the IGBT technology, the output frequency of the inverter section can easily achieve 50 kHz. One positive leg (P+, P-) and one negative leg (N+, N-) compose the inverter section.

### 2.2.1 The Pulse Width Modulation (PWM) Method

In order to produce a sinusoidal output voltage with desired frequency and magnitude [1], a sinusoidal control signal at a desired frequency is compared with a triangular waveform as in Fig. 13. The frequency of the triangular waveform establishes the inverter switching frequency and keeps constant amplitude $V_{tri}$, .

For the Positive leg (*P+*, *P-*):

If $V_{control} > V_{tri}$, P+ turned on, and $V_{1N} = V_{dc}$
If $-V_{control} < V_{tri}$: P- turned on , and $V_{2N} = 0$

For the Negative leg (*N+*, *N-*):

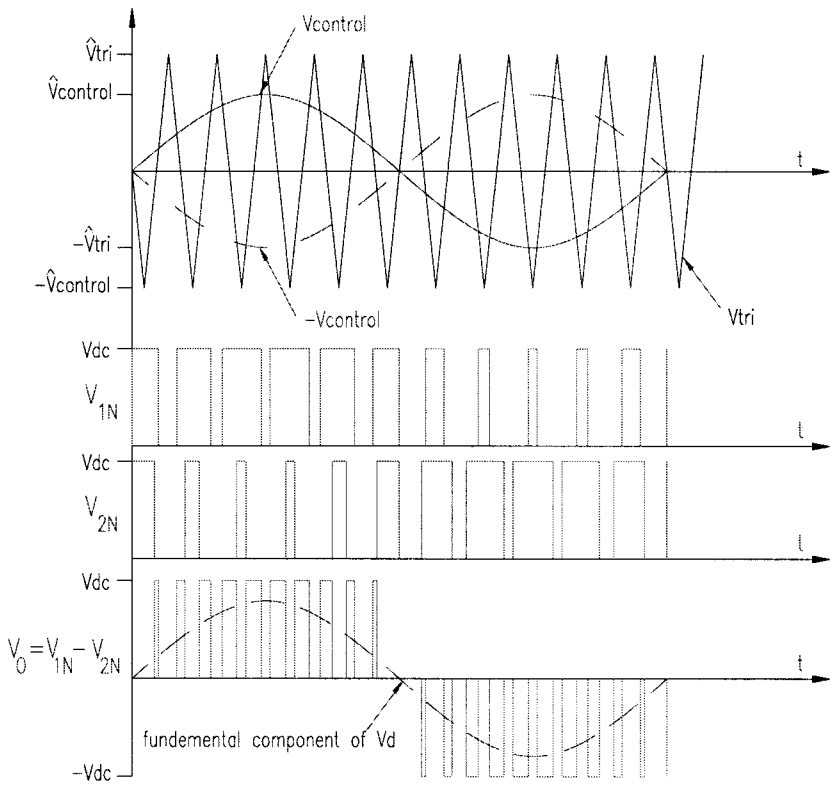


**Fig. 13 PMW Switching**

If $V_{control} < V_{tri.}$ N- turned on, and $V_{1N} = 0$
If $-V_{control} > V_{tri}$, N+ turned on, and $V_{2N} = V_{dc}$

Based on the following six combinations of the status of the switches,

a. P+ turned on, P- turned on, $V_{1N} = V_{dc}$, $V_{2N} = 0$, and the output voltage is $V_{12} = V_{dc}$,
b. N+ turned on, N- turned on, $V_{1N} = -V_{dc}$, $V_{2N} = 0$, and the output voltage is $V_{12} = -V_{dc}$,
c. P+ on, N+ turned on, $V_{1N} = V_{dc}$, $V_{2N} = V_{dc}$, and the output voltage is $V_{12} = 0$,
d. P- on, N- turned on, $V_{1N} = 0$, $V_{2N} = 0$, and the output voltage is $V_{12} = 0$,
e. P+ on, N- turned on, and the inverter section is short circuit,
f. N+ on, P- turned on, and the inverter section is short circuit.

The output voltage is constructed by some square waveforms with different width, the fundamental component of the output voltage ($V_d$) is a sinusoidal waveform with a desired frequency.

### 2.2.2 Square Wave Switching Scheme for Inverter Section

The square wave switching is a special case of the sinusoidal PWM switching when the amplitude modulation ratio $m_a$ becomes so large, the control signal waveform intersect the triangular waveform at the zero crossing point. The waveforms of the output voltage and the control signals are shown in Fig. 14.

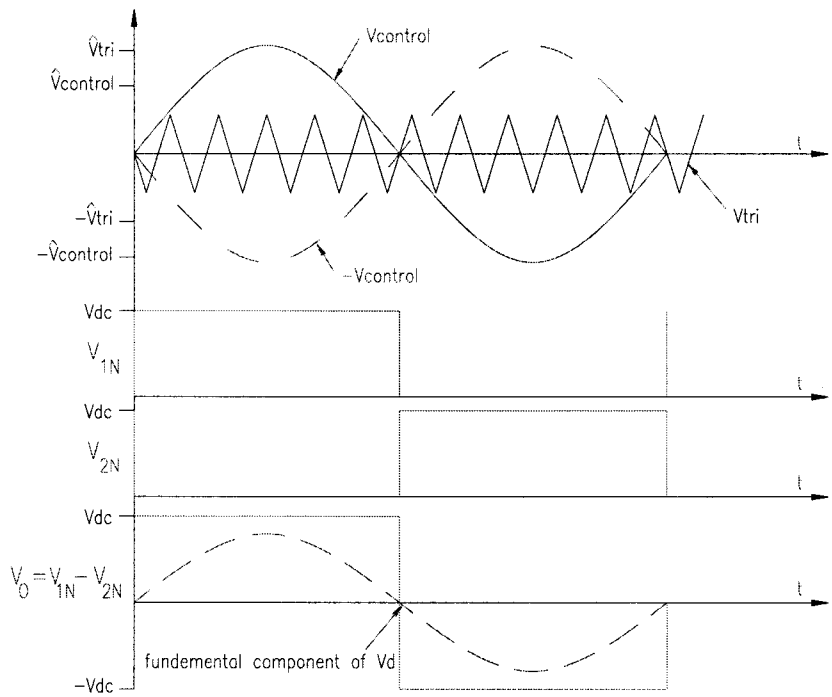


**Fig. 14 Square Wave Switching**

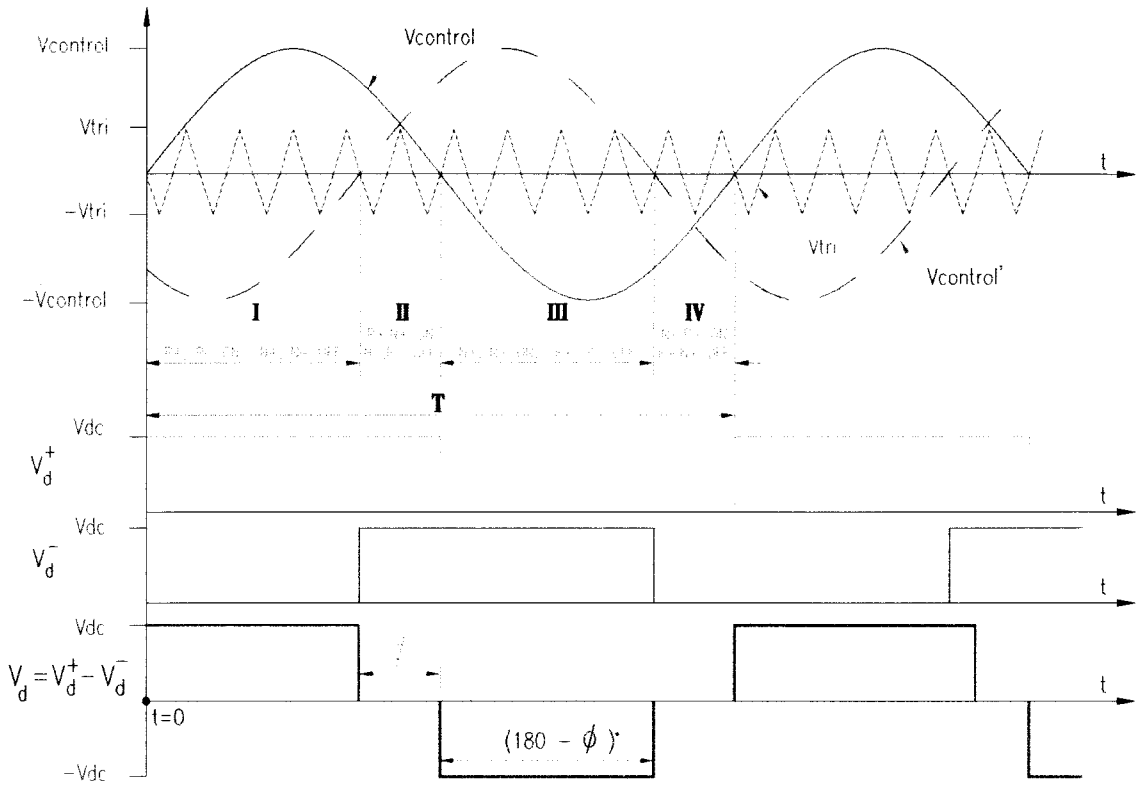


**Fig. 15 Combination of PWM and SW switching**

The implementation of the square wave switching is very easy. By controlling the phase of the $-V_{control}$ and $V_{control}$, each IGBT will turn on for one half cycle of the desired frequency. Therefore, the desired average output voltage can be achieved.

### 2.2.3 Combination of Square Wave Switching and PWM Switching

The control scheme is illustrated in Fig. 15. The control sequence for the inverter section for one period ($T$) is determined by comparing the triangle waveform $V_{tri}$, the sinusoidal waveforms $V_{control}$ and the $V_{control}'$.

The switching sequence for the inverter section in one period is divided into four different sections:

**I.** $V_{control} > V_{tri}$, $V_{control}' < V_{tri}$, $P+$ and $P-$ turned on, $N+$ and $N-$ turned off, the output voltage $V_d$ is $+V_{dc}$.

**II.** $V_{control} > V_{tri}$, $V_{control}' > V_{tri}$, $P+$ and $N+$ turned on, $P-$ and $N-$ turned off, the output voltage $V_d$ is 0.

**III.** $V_{control} < V_{tri}$, $V_{control}' > V_{tri}$, $N+$ and $N-$ turned on, $P+$ and $P-$ turned off, the output voltage $V_d$ is $-V_{dc}$.

**IV.** $V_{control} < V_{tri}$, $V_{control}' < V_{tri}$, $P-$ and $N-$ turned on, $P+$ and $N+$ turned off, the output voltage $V_d$ is $0$.

The desired output frequency can be achieved by controlling the period ($T$). The rms value of the inverter section output voltage is defined by Equation (2-2-1). Therefore, by adjusting the firing angle $\phi$, $V_{drms}$ can be controlled in the range from zero to ($V_{dc}$).

$$V_{drms} = \sqrt{\frac{1}{T}\int_0^T (V_d)^2 dt} = \sqrt{\frac{180 - \phi}{180}} V_{dc} \qquad (2\text{-}2\text{-}1)$$

### 2.2.4 Simulate the Square Wave Control Scheme by Using Matlab

As shown in Fig. 16, by using two square wave signal generators to simulate the positive and negative legs. When the inverter section firing angle ($\phi$) is equal to zero, the output voltage waveforms are shown in Fig. 17, when the result is actually the square wave switching scheme result.

When the firing angle increases from zero, the positive node voltage ($V_{1N}$) and the negative node voltage ($V_{2N}$) starts to overlap each other, this results show the average

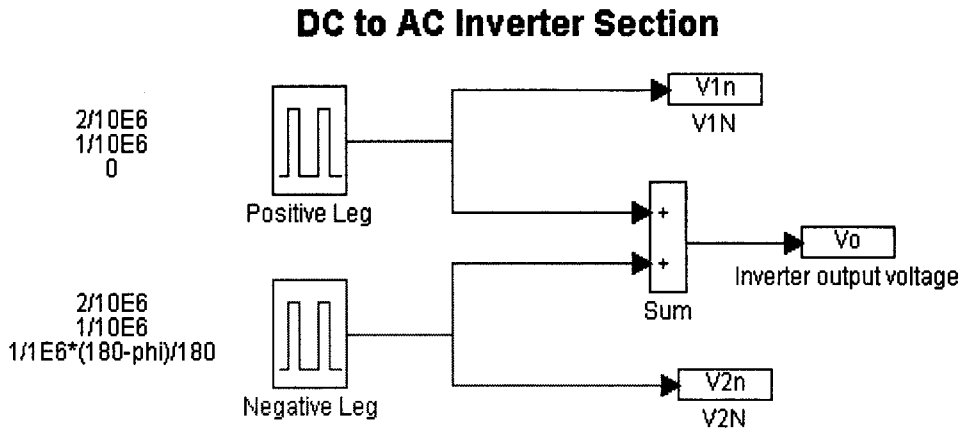


**Fig. 16 Simulink Model for the Inverter**

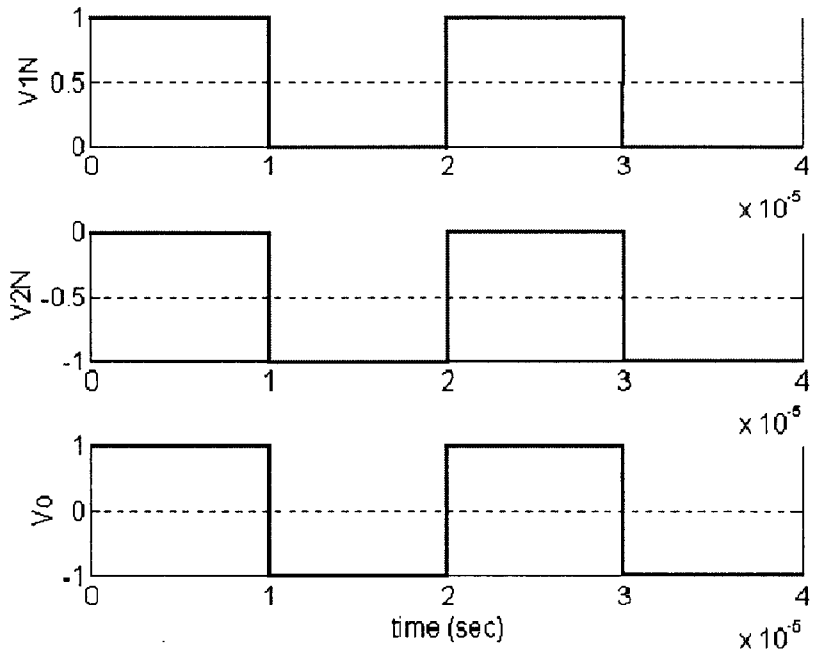


**Fig. 17 Voltage Waveforms at $\phi = 0^o$ (Square Wave Switching)**

output voltage decreases. Also, the voltage waveforms for $\phi = 30^o$ is shown in Fig. 18. Since the simulation results are match the theoretic result, this inverter section output simulate model can be used as an input to the load section in later discussion. When the firing angle $\phi = 90^o$, the average output voltage is exactly half of the one when the firing angle equals to zero. The voltage waveforms for $\phi = 90^o$, is shown in Fig. 19.

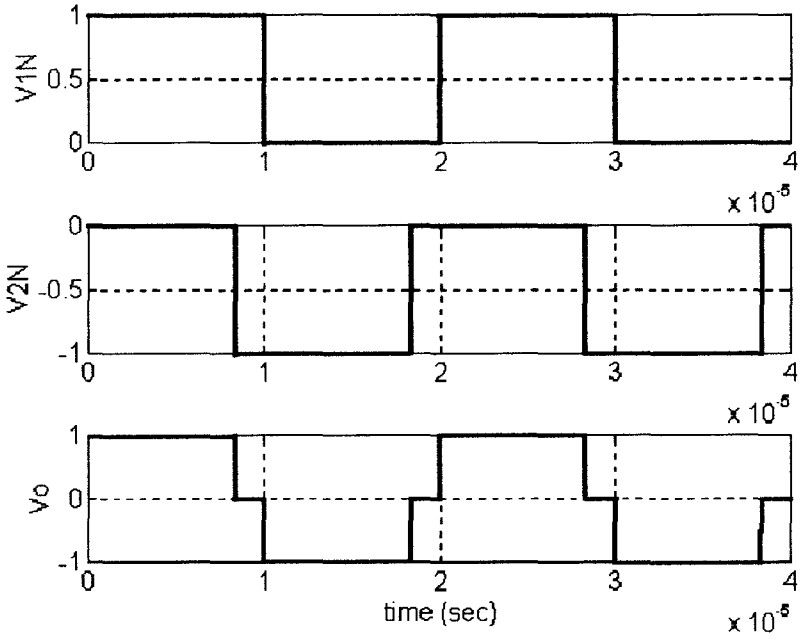


**Fig. 18 Voltage Waveforms at $\phi = 30^o$**

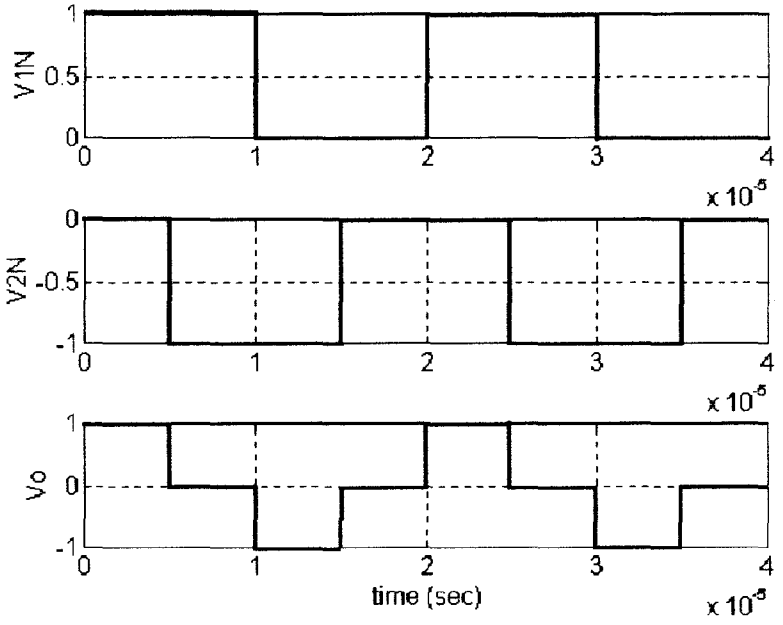


**Fig. 19 Voltage Waveforms at $\phi = 90^o$**

The rms value of the output voltage is decreasing when the firing angle $\phi$ is getting larger. When the firing angle $\phi = 180^o$, the average output voltage equals to zero, the voltage waveforms for $\phi = 180^o$.

### 2.2.5 Fourier Analysis for the Inverter Output Voltage

The output voltage of the inverter is a periodic function with T = $2 \times 10^{-6}$ sec. Therefore, the output voltage can be written as equation (2-2-2).

$$f(x) = \frac{1}{2}a_0 + a_1 \cos x + b_1 \sin x + \cdots + a_n \cos nx + b_n \sin nx + \cdots \quad (2\text{-}2\text{-}2)$$

Since the magnitudes of the positive leg voltage and the negative leg voltage are equal, the DC component of the output voltage waveform is 0 as shown in equation (2-2-3),

$$a_0 = \frac{1}{\pi}\int_{-\pi}^{\pi} f(x)dx = 0 \quad (2\text{-}2\text{-}3)$$

The output voltage waveform is an even function. Therefore, the coefficient $b_n$ is equal to 0, as shown in equation (2-2-4), and the coefficient $a_n$ is shown in equation (2-2-5),

$$b_n = \frac{1}{\pi}\int_{-\pi}^{\pi} [f(x)\sin nx]dx = 0 \quad (2\text{-}2\text{-}4)$$

$$\begin{aligned} a_n &= \frac{2}{\pi}\int_{-\pi/2}^{\pi/2} [f(x)\cos nx)dx \\ &= \frac{2}{\pi}\int_{-\beta}^{\beta} [V_{dc}\cos nx)dx \\ &= \frac{2V_{dc}}{\pi}\int_{-\beta}^{\beta} \cos nxdx \\ &= \frac{2V_{dc}}{\pi \cdot n}[\sin n\beta - \sin(-n\beta)] \\ &= \frac{4V_{dc}}{\pi \cdot n}\sin n\beta \end{aligned} \quad (2\text{-}2\text{-}5)$$

Notice that if n is an even number, $a_n = 0$, so the output voltage of the inverter is shown in equation (2-2-6),

$$\begin{aligned} V_d = &\frac{4V_{dc}}{\pi}\sin\beta \sin x + \frac{4V_{dc}}{3\pi}\sin 3\beta \sin 3x + \cdots + \\ &\frac{4V_{dc}}{n\pi}\sin n\beta \sin nx + \cdots \end{aligned} \quad (2\text{-}2\text{-}6)$$

where n is an odd number.

# Chapter 3

# Induction Load Section

In this chapter, the first two sections introduce the characteristics of series resonant circuit and parallel resonant circuit of the load section as background study. Then, the characteristics of the load section and a series-parallel circuit will be discussed.

## 3.1 Frequency Characteristic of the Series Resonant Circuit

The electrical circuit for the series resonant load is shown in Fig. 20. The circuit is composed of resistor R, capacitor C and inductor L.

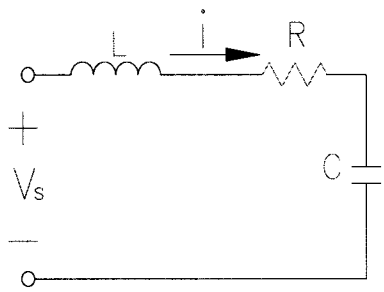


**Fig. 20 Damped Series-Resonant Circuit**

The impedance of the circuit in frequency domain can be written as

$$Z = R + j\omega L + \frac{1}{j\omega C} = R + j(\omega L - \frac{1}{\omega C}) \qquad (3\text{-}1\text{-}1)$$

The phase angle of the impedance is equal to zero, due to the input resonant frequency. For the desired resonant frequency $f_o$ = *50kHz*, the angular frequency will be $2\pi f_o$. The relationship between the angular frequency and the circuit components *L* and *C*, is show in equation (3-1-2).

$$\omega_o = 2\pi f_o = \frac{1}{\sqrt{LC}} \qquad (3\text{-}1\text{-}2)$$

The series resonant load impedance is a pure resistance (*R*), when the frequency is the resonant frequency. In order to measure ratio of the load inductance and load resistance, a quality factor is defined as equation (3-1-3).

$$Q = \frac{\omega_o L}{R} = \frac{1}{\omega_o CR} = \frac{Z_o}{R} \qquad (3\text{-}1\text{-}3)$$

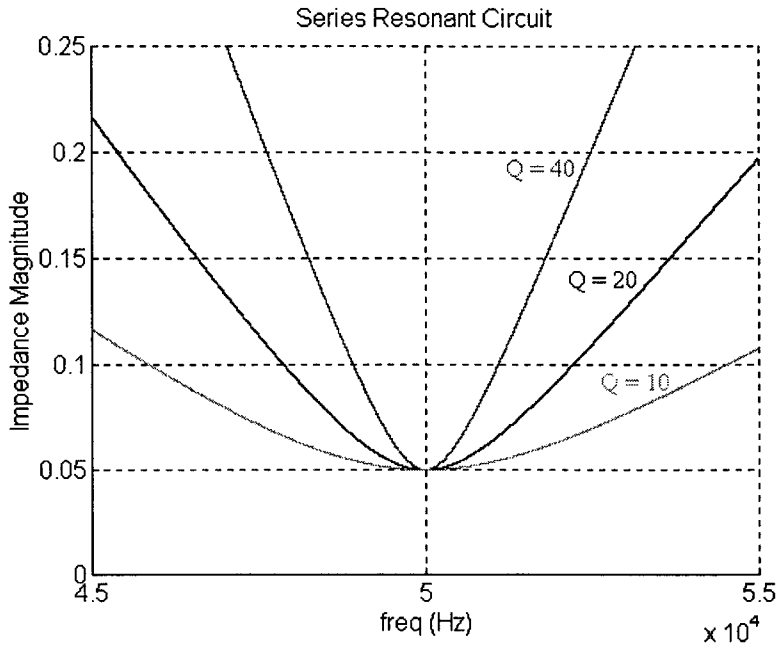


**Fig. 21 The Magnitude of the Circuit Impedance for Different Quality Factor**

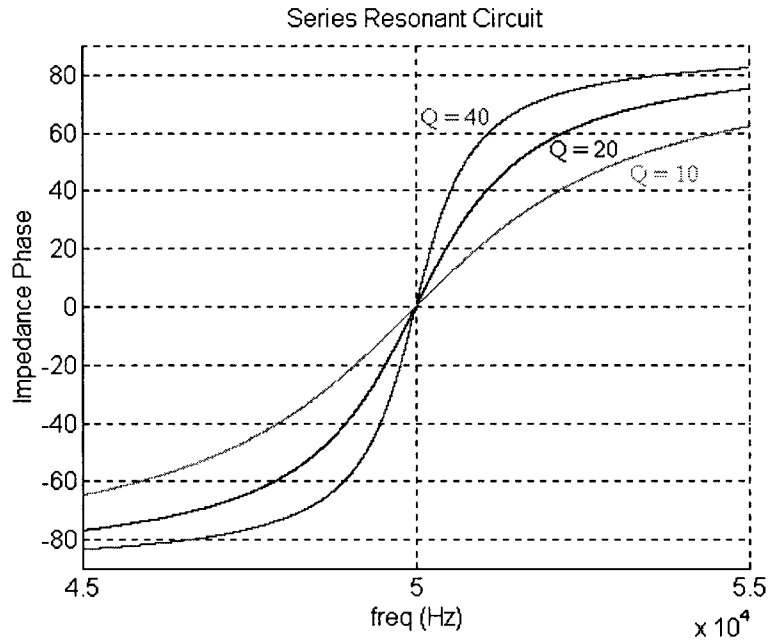


**Fig. 22 The Phase of the Circuit Impedance for Different Quality Factor**

Let R = 50mΩ, and the resonant frequency equal to 50 kHz, for Q= 10, 20, 40 the frequency responses are shown in Fig. 21 and Fig. 22. The capacitance of the series capacitor can be calculated by using equation (3-1-2). For different Q, the load impedance magnitudes at the resonant frequency are equal. The load impedance is more sensitive at Q = 40, compare to Q = 20. Therefore, when the quality factor Q gets bigger, the load impedance will change more dramatically with the frequency.

## 3.2 Frequency Characteristic of the Parallel Resonant Circuit

The electrical equivalent circuit for the parallel resonant load is shown in Fig. 23, which is composed of resistor R, capacitor C and inductor L.

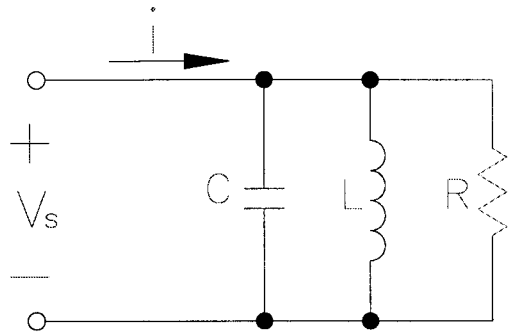


**Fig. 23 Parallel Resonant Circuit**

The impedance of the circuit in frequency domain is shown in equation (3-2-1).

$$Z = \frac{1}{\frac{1}{R} + j\omega C + \frac{1}{j\omega L}} \tag{3-2-1}$$

Impedance $Z$ is a complex number, at the resonant frequency $f_o$=*500kHz*, impedance $Z$ becomes a real number, the angular resonance frequency is defined by

$$\omega_o = 2\pi f_o = \frac{1}{\sqrt{LC}} \tag{3-2-2}$$

The Quality Factor for parallel resonant circuit is defined as

$$Q = \frac{R}{\omega_o L} = \omega_o CR = \frac{R}{Z_o} \tag{3-2-3}$$

The quality factor is a measurement of the ratio of the resistance to the inductance of the circuit. The larger the quality factor is, the least inductive of the circuit is. Let R = 20 Ω, and for Q= 10, 20, 40 the frequency responses are shown in Fig. 24 and Fig. 25. The quality factor has same effect on the parallel resonant circuit as the series resonant circuit, when the quality factor Q gets bigger, the load impedance will change more dramatically with the frequency.

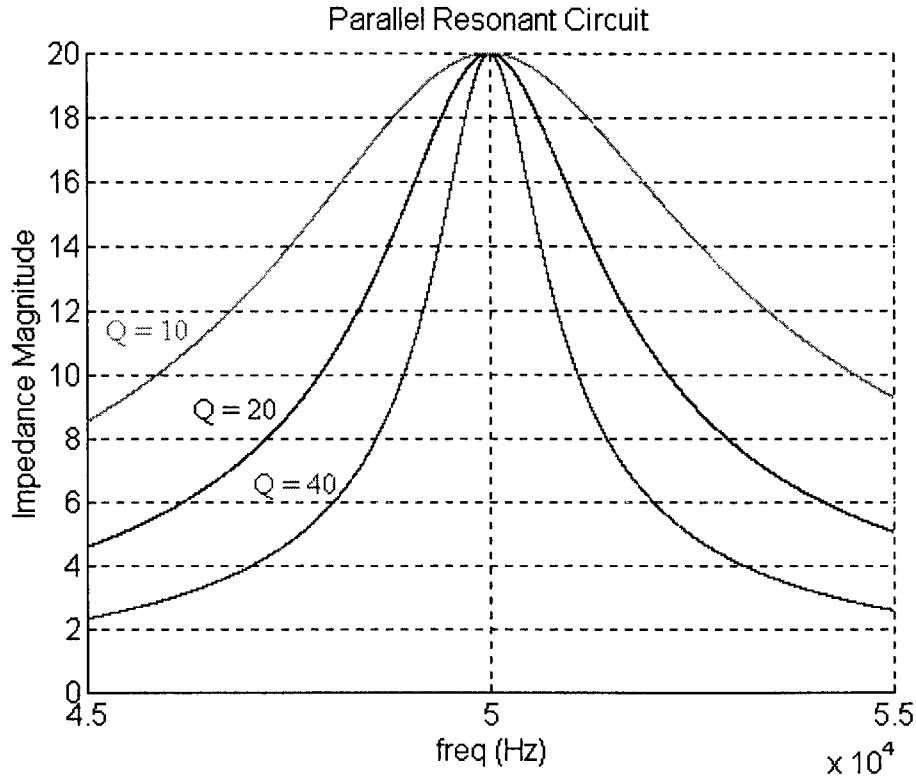


**Fig. 24** **Impedance Magnitude plot for Different Quality Factor Q**

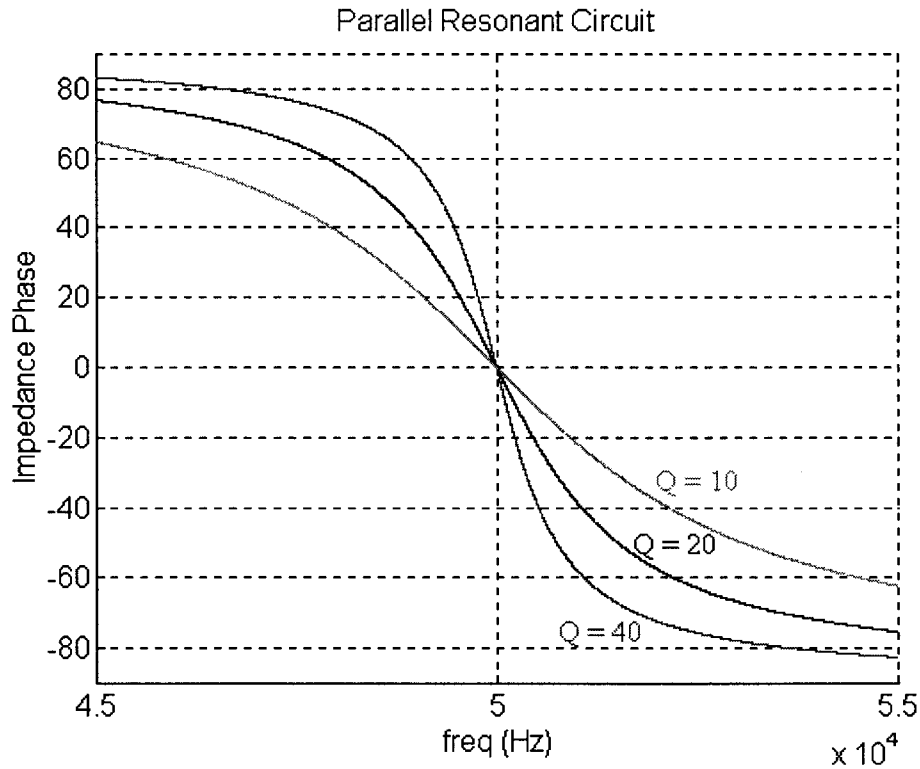


**Fig. 25** **Phase Plots of the Circuit Impedance for Different Quality Factor Q**

## 3.3 Frequency Characteristic of the Resonant Load Section

The load is a series-parallel resonant circuit, one of the natural resonant frequency of the load section is around 50 kHz. Some of the small parameters have been ignored, like the capacitance in the load, the resistance in the series inductor, etc. The equivalent circuit for the load section is shown in Fig. 26.

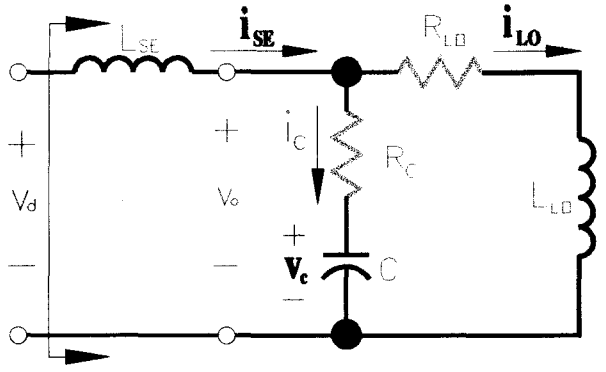


**Fig. 26 Equivalent Circuit for Load Section**

### 3.3.1 Load Impedance Calculation

The load impedance in frequency domain is shown in equation (3-3-1).

$$Z_{LOAD} = j\omega L_{SE} + \frac{1}{\frac{1}{R_{LO} + j\omega L_{LO}} + \frac{1}{R_C + \frac{1}{j\omega C}}} \tag{3-3-1}$$

Let $A = R_l^{\,2} + \omega^2 L_l^{\,2}$ and $B = R_c^{\,2} + \frac{1}{\omega^2 C^2}$, and substitute A, B into equation (3-3-1),

$$Z_{LOAD} = j\omega L_{se} + \frac{AB}{R_l B + R_c A - j(\omega B L_l - A\frac{1}{\omega C})} \tag{3-3-2}$$

Rewrite equation (3-3-2) can be written as equation (3-4-3).

$$Z_{LOAD} = j\omega L_{se} + \frac{AB(E + jF)}{E^2 + F^2} \tag{3-3-3}$$

where $E = R_l B + R_c A$, $F = \omega B L_l - A\frac{1}{\omega C}$, rearrange equation (3-3-3), yield

$$Z_{LOAD} = \frac{ABE + j((E^2 + F^2)\omega L_{se} + ABF)}{E^2 + F^2} \tag{3-3-4}$$

The resonant angular frequency should satisfy the equation (3-4-5), where the phase of the load impedance is equal to zero.

$$(E^2 + F^2)\omega L_{se} + ABF = 0 \tag{3-3-5}$$

Assume the induction coil parameters are shown in Table 1.

**Table 1 Induction Load Parameters**

| $L_{LO}$ (μH) | $R_{LO}$ (mΩ) |
|---|---|
| 0.339 | 10.0 |

Let the frequency of the parallel section of the Resonant Load be

$$f_{o1} = \frac{\omega_{o1}}{2\pi} = \frac{1}{2\pi\sqrt{L_{LO}C}} = 30,\ \ 41,\ \ 45kHz \tag{3-3-6}$$

then the capacitor value can be calculated:

For 30 kHz, C = 83.02 μF.

For 41 kHz, C1 = 44.45 μF.

For 45 kHz, C2 = 36.89 μF.

The desired operating frequency is $f_{o2} = 50kHz$, therefore, the series inductance can be calculated by using equation (3-3-7)

$$L_{SE} = -\frac{ABD}{(E^2 + F^2)\omega} \tag{3-3-7}$$

For different parallel capacitance, the series inductance,

$L_{SE}$ = 0.1891 μH
$L_{SE}1$ = 0.6581 μH
$L_{SE}2$ = 1.2051 μH

### 3.3.2 Load Impedance with the First Resonant Frequency of 30 kHz

When the first resonant frequency is near 30 kHz, the waveforms of the load section impedance, series inductance current $i_{SE}$ and the induction coil current are shown in Fig. 27 and 28. The series inductance current is much larger than the induction coil current. The load section impedance at the second resonant frequency is 3.615 mΩ. The minimum impedance is 3.593 mΩ, when the input frequency is 50.11 kHz.

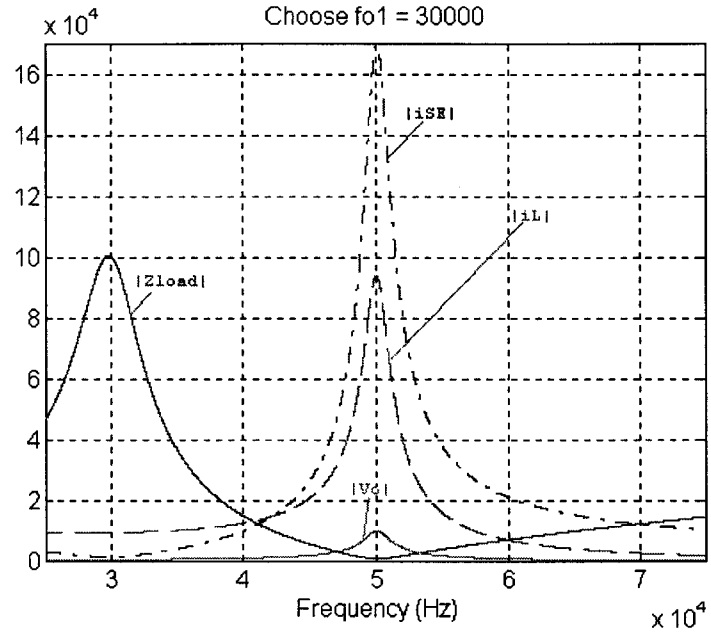


**Fig. 27 Amplitude of $Z_{LOAD}$×250000, $i_{SE}$, $v_o$, and $i_{LO}$**

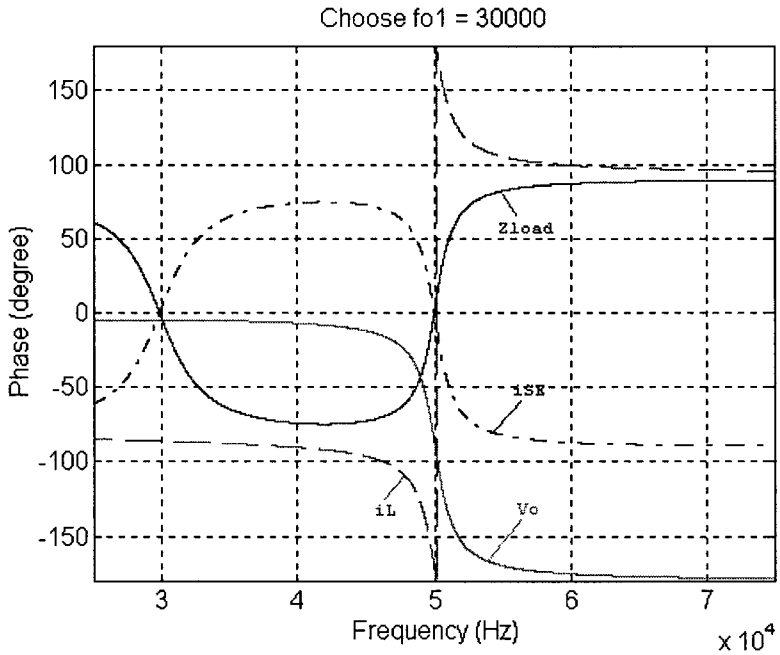


**Fig. 28 Phase of $Z_{LOAD}$×250000, $i_{SE}$, $v_o$, and $i_{LO}$**

### 3.3.3 Load Impedance with the First Resonant Frequency of 37.5 kHz

With the first resonant frequency chose near 37.5 kHz, the magnitude of the induction coil current is greater than the load input current. The load section impedance at the second resonant frequency is 16.86 mΩ. The minimum impedance is 16.45 mΩ, when the input frequency is 50.20 kHz.

### 3.3.4 Load Impedance with the First Resonant Frequency of 41.75 kHz

With the first resonant frequency chosen near 41.75 kHz, the magnitude of the induction coil current is greater than the load input current. The waveforms of load impedance, series inductance current ($i_{SE}$), induction coil voltage and current are show in Fig. 29 (Magnitude) and Fig. 30 (Phase).

The load section impedance at the second resonant frequency is 50.35 mΩ. The minimum impedance is 46.74 mΩ, when the input frequency is 50.45 kHz.

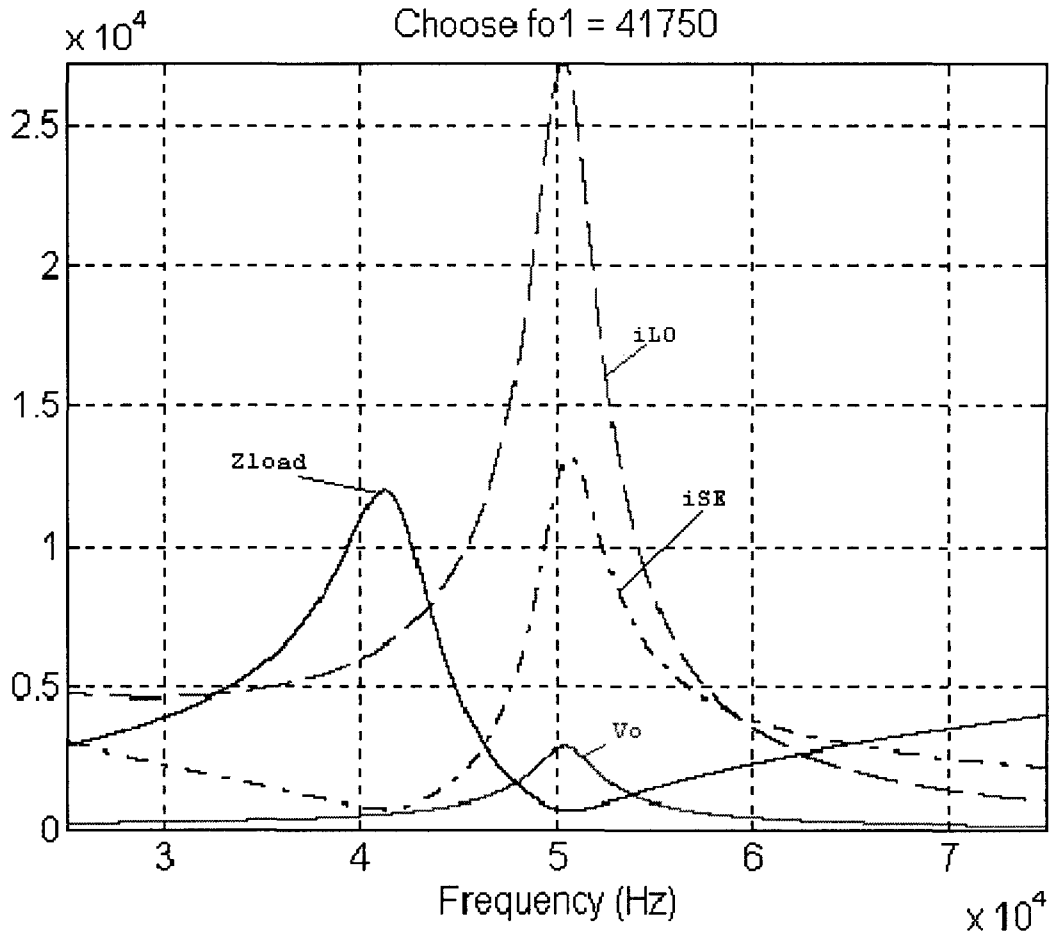


**Fig. 29 Amplitude of $Z_{LOAD}$×100000, $i_{SE}$, Vo and $i_{LO}$**

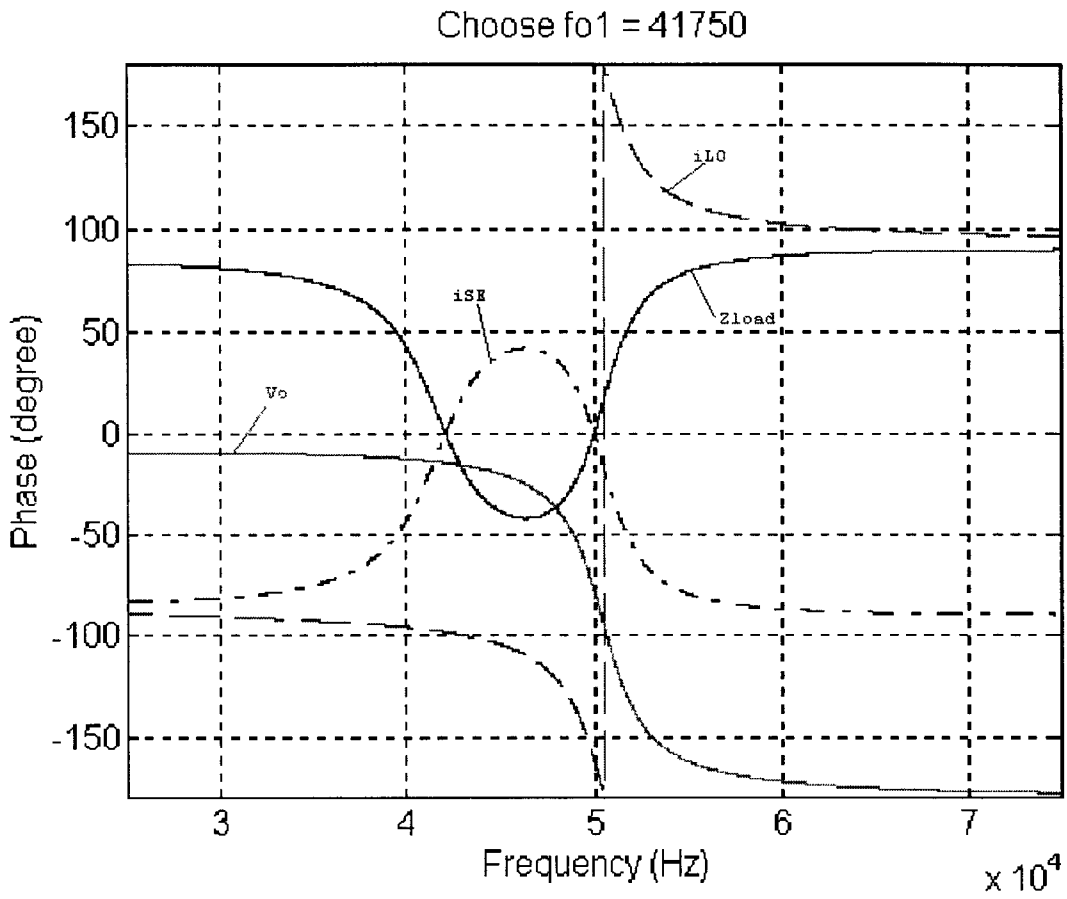


**Fig. 30 Phase of the Load Section Impedance, $i_{SE}$, Vo and $i_{LO}$**

### 3.3.5 Load Impedance with the First Resonant Frequency of 45 kHz

With the first resonant frequency chose near 45 kHz, the magnitude of the induction coil current is greater than the load input current. The load section impedance at the second resonant frequency is 149.64 mΩ. The minimum impedance is 121.96 mΩ, when the input frequency is 50.82 kHz.

The relationship between the first resonant frequency and the ratio of the inverter section output current and induction coil current is shown in Fig. 31.

In order to lower the inverter section switching device loss, the current through the inverter bridge is the smaller the better. In the meaning time the induction application need high current through the induction coil. From the plot, when the first resonant frequency increases from the low (near 30kHz) frequency, the induction coil current increases while the current through the Inverter Bridge decreases. When the first resonant is closing to the second resonant frequency, the load section impedance is getting larger, and the induction coil current is getting smaller. So choose the 41.75 kHz

as the first resonant frequency. At the operating frequency, the induction coil current to inverter section output current ratio is about 2.1:1.0.

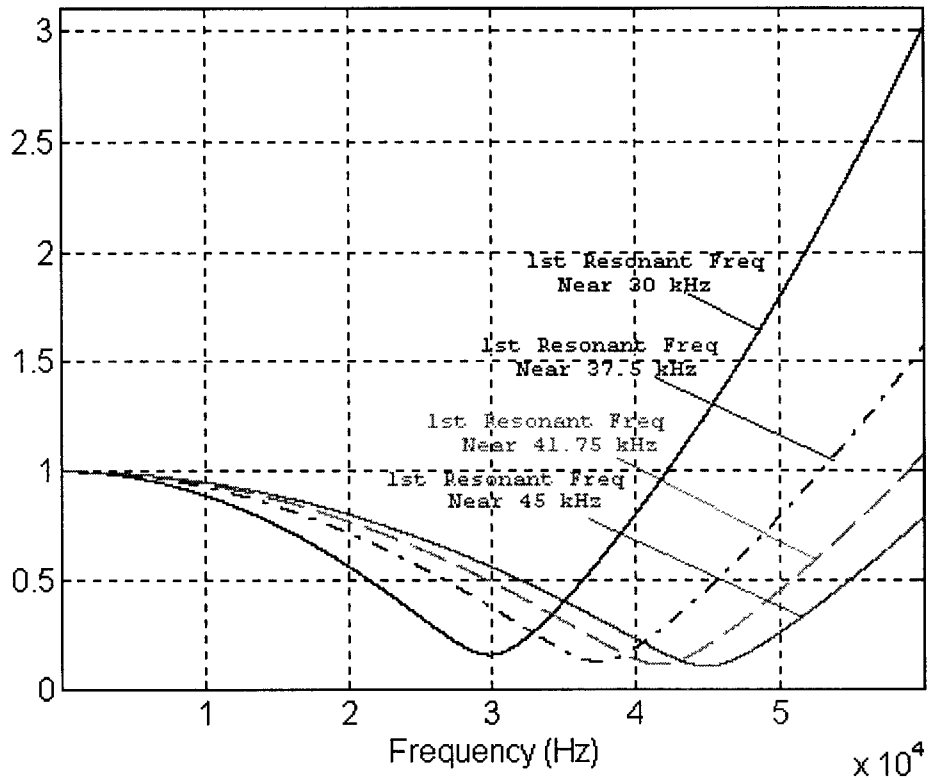


**Fig. 31 The Ratio of the rms value of Load Input Current $i_{SE}$ and Induction Coil Current vs. Frequency**

## 3.4 Frequency Characteristic of Different Resonant Loads

When the load changes the load resistance and inductance changes also. By changing the load resistance and inductance, the following illustrate the effect on the load impedance. At the operating frequency, the load impedance becomes pure resistive, and the resistance is much smaller than the real load resistance $R_{LO}$, this help the system to generate high voltage and current. The minimum absolute value of the load impedance is not occurs at the second resonant frequency.

### 3.4.1 Effects of Different Load Inductance

With different load inductance, the tank capacitance and series inductance must be changed to get exactly the same resonant frequency. The plots of the magnitude and phase of the resonant frequency are shown in Fig. 32 and 33. When the load inductance increases the pure resistance at resonant frequency also increases, and the impedance gets more sensitive to the frequency.

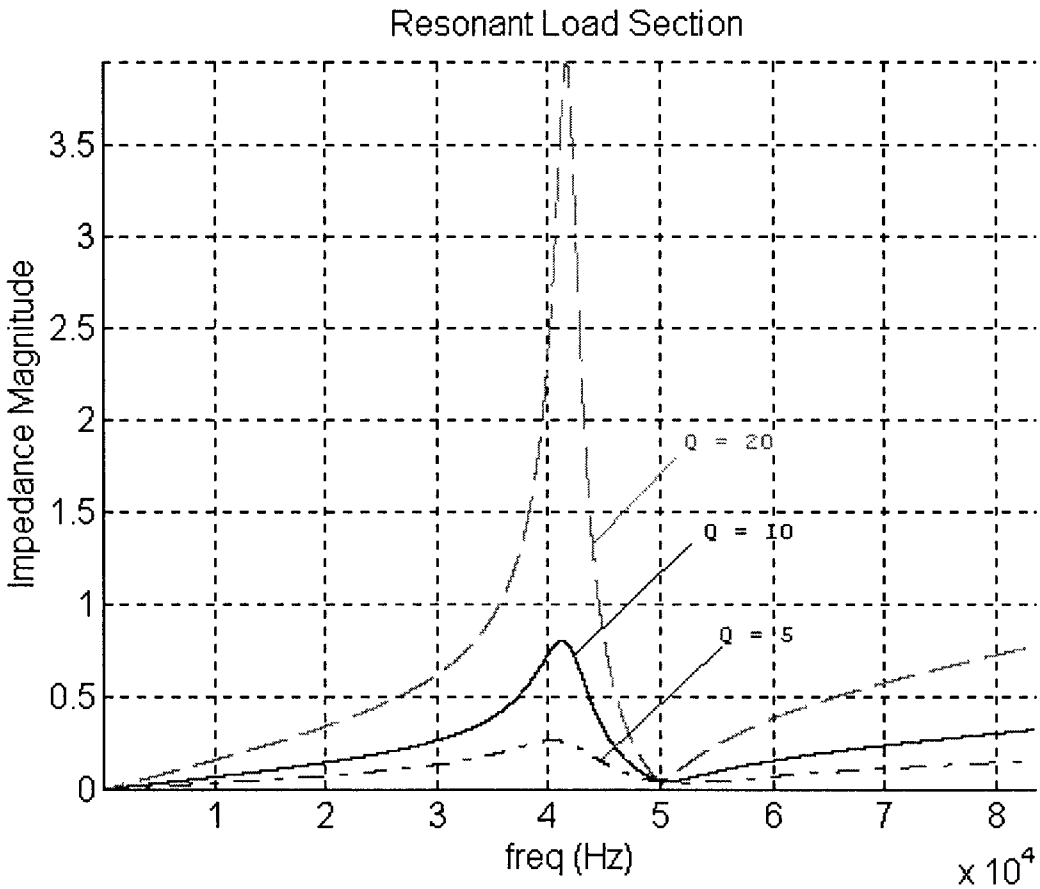


**Fig. 32 Load Impedance Magnitude with Different Load inductance**

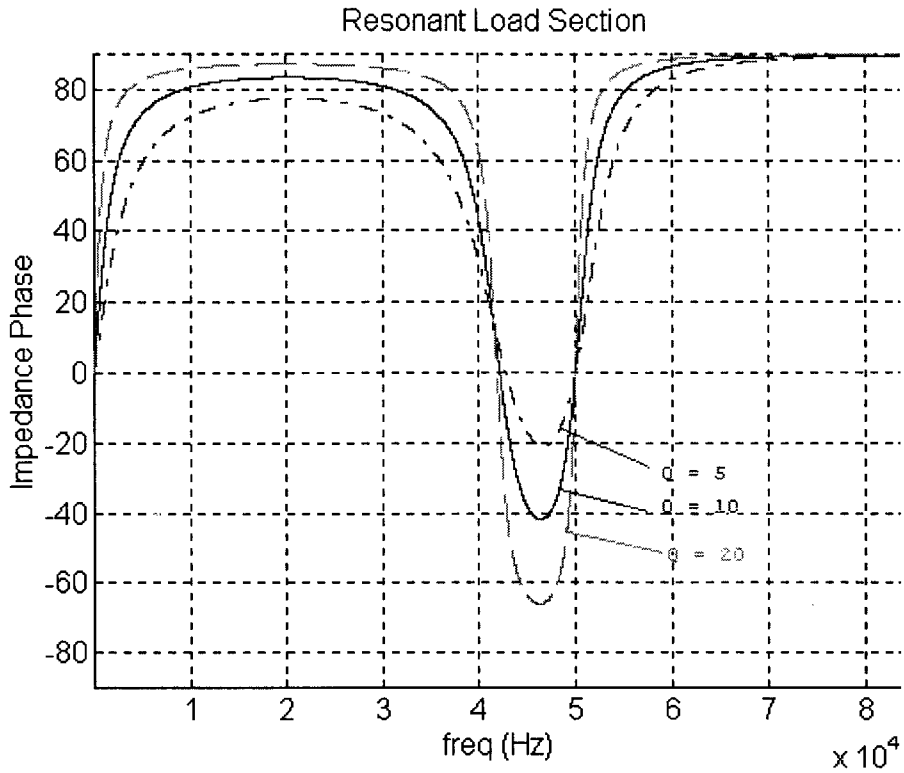


**Fig. 33 Load Impedance Phase with Different Load Inductance**

By using Matlab, the values of the tank capacitance and series inductance are:

| | |
|---|---|
| *L1 =* | *0.3390 μH* |
| *L11 =* | *0.1906 μH* |
| *L12 =* | *0.7624 μH* |
| *Q =* | *10.65* |
| *Q1 =* | *5* |
| *Q2 =* | *20* |
| *R1 = R11 = R12 =* | *0.0100 Ω* |
| *C =* | *42.87 μC* |
| *C1 =* | *76.24 μC* |
| *C2 =* | *19.06 μC* |
| *Lse =* | *0.7301 μH* |
| *Lse1 =* | *0.3638 μH* |
| *Lse2 =* | *0.1731 μH* |

At the resonant frequency, the load impedance is pure resistive. The value of the pure resistance is shown as

$$Z_{LOAD} = \frac{ABE}{E^2 + F^2} \tag{3-4-1}$$

and the pure resistance is not the minimum absolute value of the load impedance.

### 3.4.2 Effects of Different Series Inductance

When keeping the same induction load, change the series inductance by a factor of 2, the effect on the load impedance is shown in Fig. 34, 35. The second resonant frequency is changed while the first resonant frequency remains unchanged, because the first resonant frequency is mainly depending on the tank capacitance C and the load inductance. By using Matlab, the parameters for the load section components are shown as following,

```
L1 = L11 = L12 =        0.3390 μH
Q = Q1 = Q2 =           10.65
R1 = R11 = R12 =        0.0100 Ω
C = C1 = C2 =           42.87 μC
Lse =                   0.7301 μH
Lse1 =                  0.3650 μH
Lse2 =                  1.4602 μH
```

When decreases the series inductance the magnitude of the load impedance decreases and the second resonant frequency increases, vice versa. Also when the series inductance decreases the minimum phase of the load impedance decreases, vice versa.

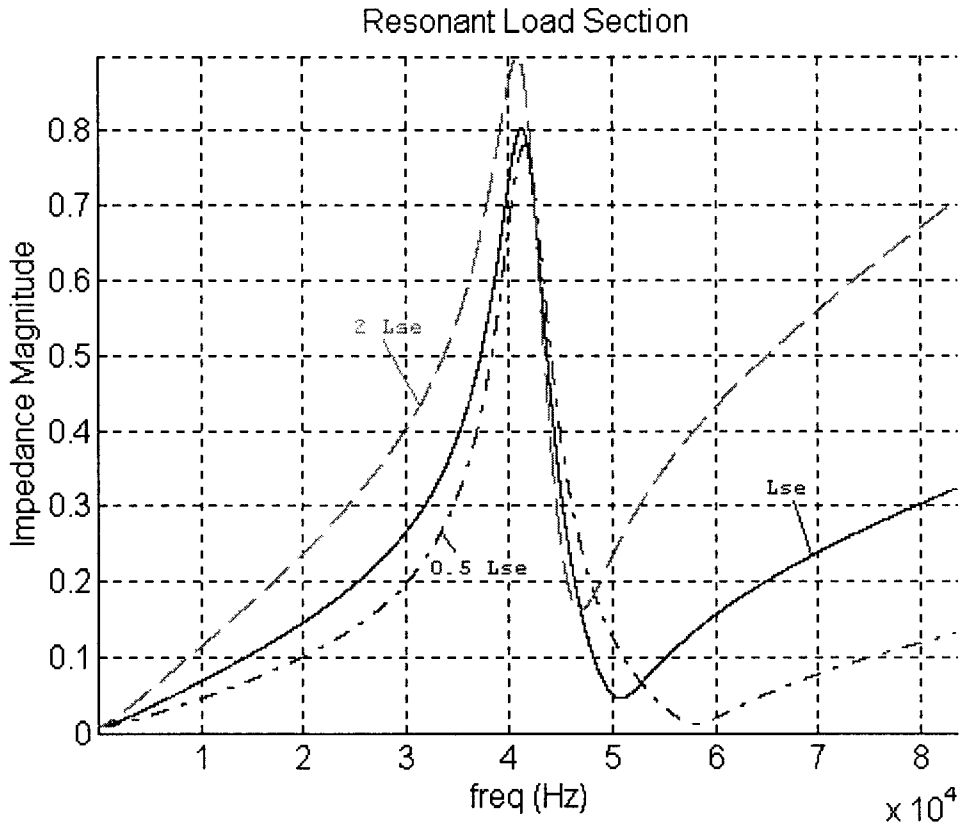


**Fig. 34 Load Impedance Magnitude with Different Series Inductance $L_{SE}$**

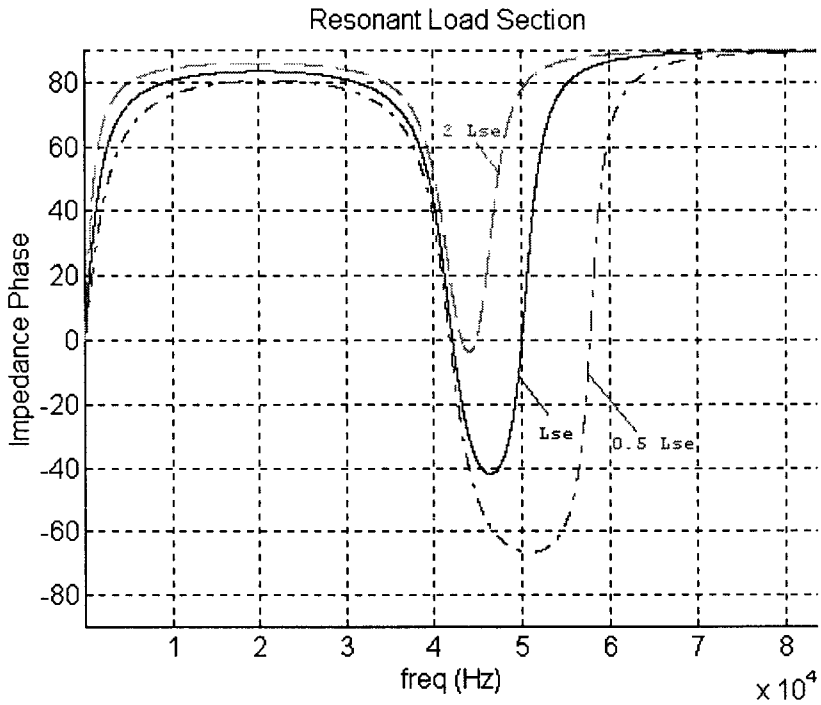


**Fig. 35 Load Impedance Phase with Different Series Inductance $L_{se}$**

### 3.4.3 Effects of Different Tank Capacitance

By changing tank capacitance only, without change the series inductance, the effect on the Load impedance is shown in Fig. 36, 37. When the tank capacitance C decreases, both resonant frequencies increase, also the magnitude of the load impedance increases and the minimum phase angle increases.

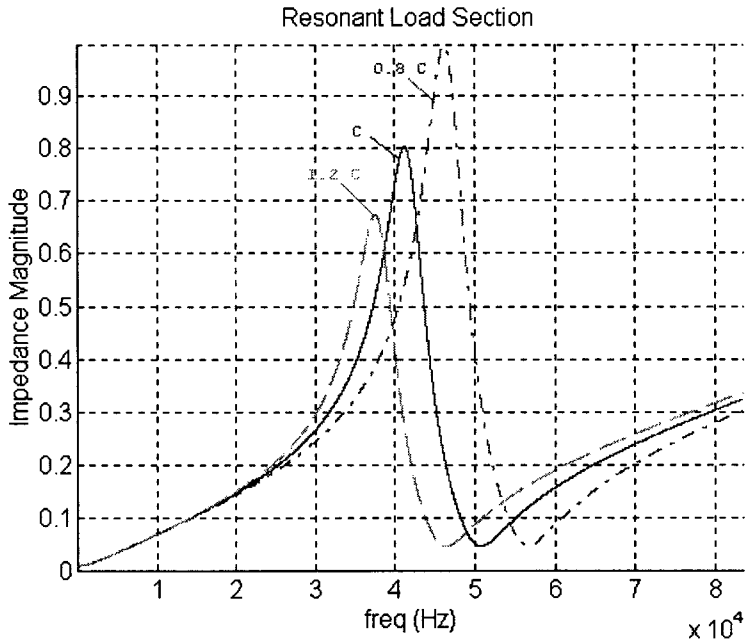


**Fig. 36 Load Impedance Magnitude with Tank Capacitance changing only**

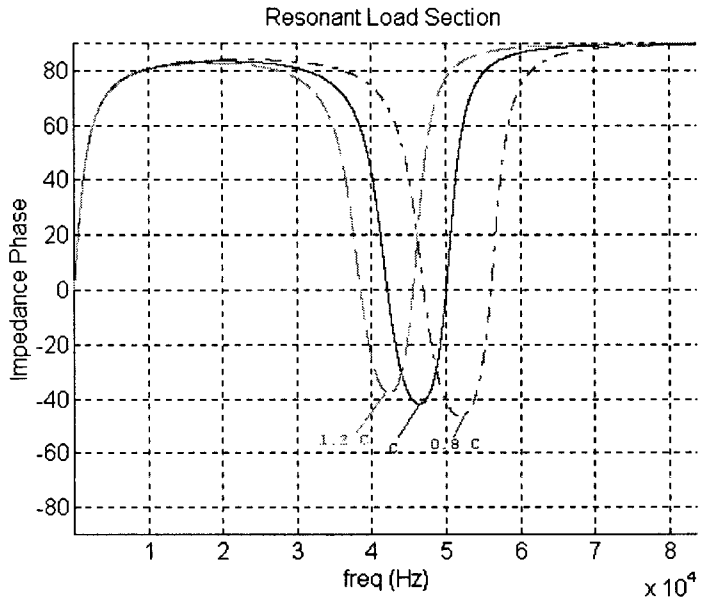


**Fig. 37 Load Impedance Phase with Tank Capacitance changing only**

| | |
|---|---|
| *L1 = L11 = L12 =* | *0.3390 μH* |
| *Q = Q1 = Q2 =* | *10.65* |
| *R1 = R11 = R12 =* | *0.0100 Ω* |
| *C =* | *42.87 μC* |
| *C1 =* | *34.29 μC* |
| *C2 =* | *51.44 μC* |
| *Lse = Lse1 = Lse2 =* | *0.7301 μH* |

By changing the resistance of the tank capacitor only, the series inductance need to be adjusted to keep the resonant frequency the same, but it is really a minor adjustment.

## 3.5 Frequency Response of the Optimum Resonant Load Section

When the first resonant frequency is near 41.75 kHz, and the second resonant frequency is 50 kHz, the parameters of the load section components are shown in Table 2.

**Table 2 Resonant Load Section Parameters**

| $L_{SE}$ | $R_{CA}$ | C | $R_{LO}$ | $L_{LO}$ |
|---|---|---|---|---|
| 0.730 μH | 0.216 mΩ | 42.87 μF | 10.0 mΩ | 0.339 μH |

Let the rectifier section firing angle $\alpha = 0^{o}$, the inverter section firing angle $\phi = 0^{o}$, i.e. with the maximum rms value of the input voltage. Assume that the rms value of the inverter section output voltage equal to the rms value of the rectifier section output voltage.

$$V_d = V_{DC} = \frac{3}{\pi}\sqrt{2}V_{LL}\cos\alpha - \frac{\omega L_s I_{DC}}{\pi/3} = 610\,V \qquad (3\text{-}5\text{-}1)$$

Therefore, the resonant load section input current is $V_d$ divided by the magnitude of the load section impedance. The voltage on the induction load can be written as in the following equation

$$V_o = I_{SE} \cdot \frac{AB(E + jF)}{E^2 + F^2} \qquad (3\text{-}5\text{-}2)$$

The induction load current is $I_{LO} = \dfrac{V_o}{R_l + j\omega L_l}$. The output power on the induction load is $P_{LO} = |I_{LO}|^2 R_l$.

Figures 38 and 39 show that when the frequency of the input voltage ω changes, the input voltage rms value keeps the same, but the magnitude of the series inductance current and induction load current will change.

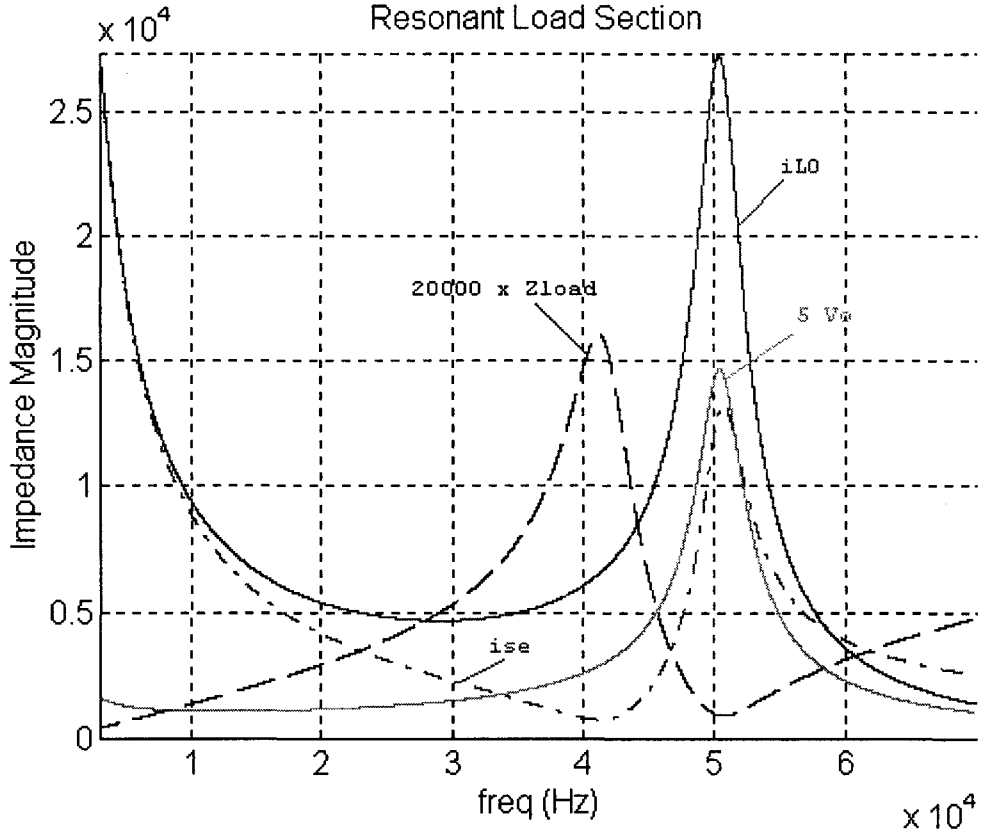


**Fig. 38 Magnitude Waveforms of $i_{SE}$, and $i_{LO}$, $5\times V_O$ and $20000 \times Z_{load}$**

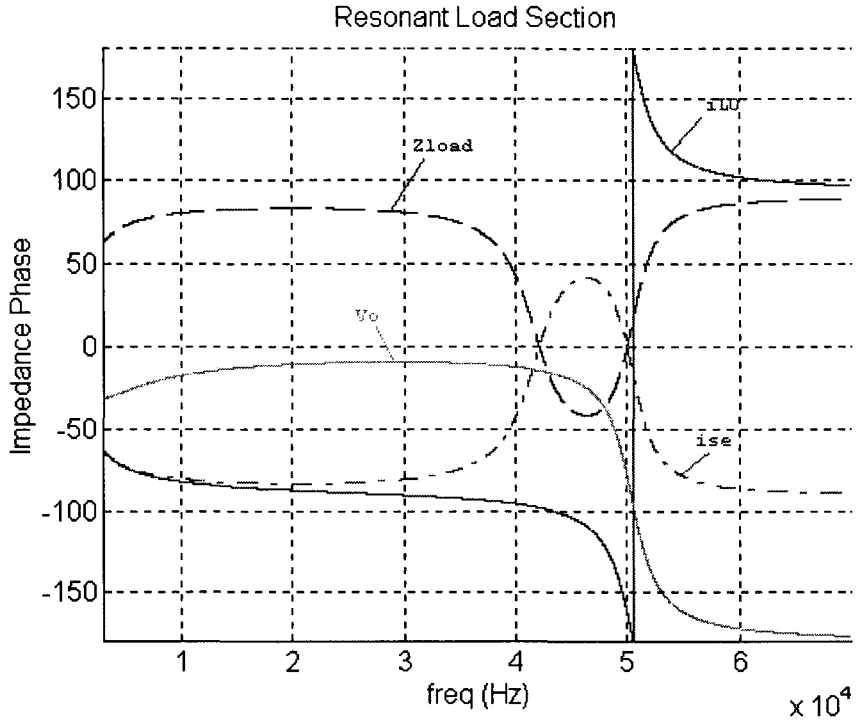


**Fig. 39 Phase Waveforms of $i_{SE}$, and $i_{LO}$, $5\times V_O$ and Load Impedance $Z_{load}$**

From above plots, the maximum power can be achieved near the second resonant frequency, also the voltage and current on the induction load reach to the maximum value. The Power is more sensitive to the frequency changing, compare to the current and voltage.

## 3.6 Using Laplace Transform for the Resonant Load Section

By using Laplace transform,

$$Z_{LOAD} = sL_{se} + \frac{(R_l + sL_l)(R_C + \frac{1}{sC})}{(R_l + sL_l) + (R_C + \frac{1}{sC})} \tag{3-6-1}$$

rearrange equation (3-6-1), yield

$$Z_{LOAD} = \frac{as^3 + bs^2 + cs + d}{s^2 L_l C + s(R_l + R_C)C + 1} \tag{3-6-2}$$

where $a = L_{Se} L_l C$, $\quad b = [L_{Se}(R_l + R_C) + L_l R_C]C$

$c = (L_{se} + R_l R_C C + L_l)$, $\quad d = R_l$

Therefore, the transfer function of the load section is shown as equation (3-6-3).

$$\frac{i_{SE}}{V_d} = \frac{s^2 L_l C + s(R_l + R_C)C + 1}{as^3 + bs^2 + cs + R_l} \tag{3-6-3}$$

Assume the system is operating at 50 kHz frequency. Substitute the load section parameter Table.2 into equation (3-6-3), yields

$$\frac{i_{SE}}{V_d} = \frac{1.45E-11s^2 + 4.38E-7s + 1}{1.06E-17s^3 + 3.23E-13s^2 + 1.07E-6s + 1.0E-2} \tag{3-6-4}$$

By using Matlab command "roots", the poles and zeroes of the above equation are:

$P_{1,2}$ = -1.5030E03 ± i3.1696E05,
$P_3$ = -9.3714E04
$Z_{1,2}$ = -1.5068E04 ± i2.6189E05,

All the poles and zeroes are on the left half plan, so the system is stable. With different input frequency, the response changes to eventually stable the oscillation. The peak value of the load current goes down when the input frequency shifts either low or high from 50 kHz. Therefore, the maximums load current always take place when the frequency of the input voltage is 50 kHz. The peak load current is 228.78 when the input voltage has the value of 1.

# Chapter 4

# Continuous LQT Optimum Controller

This chapter will discuss the analog linear quadratic optimum controller. First the continuous time system equations are developed. Second, the LQT optimum controller equations are derived. Third, the closed loop system with LQT optimum controller is simulated.

## 4.1 Continuous Time Open Loop Plant

The parameters for load section components are shown in Table 3, where the first resonant frequency of the load is about 41.75 kHz and the second resonant frequency of the load is 50 kHz.

**Table 3 Parameters for Load Section Components**

| $L_{SE}$ | $R_{CA}$ | C | $R_{LO}$ | $L_{LO}$ |
|---|---|---|---|---|
| 0.730 μH | 0.216 mΩ | 42.87 μF | 10.0 mΩ | 0.339 μH |

From the electrical schematic of the HFPS,

$$i_C = C\frac{d}{dt}v_C \text{ and } i_C = i_{SE} - i_{LO}$$

KVL equation

$$V_d = L_{SE}\frac{di_{SE}}{dt} + R_C i_C + v_C \tag{4-1-1}$$

$$R_{LO}i_{LO} + L_{LO}\frac{di_{LO}}{dt} = R_C i_C + v_C \tag{4-1-2}$$

KCL equation

$$i_{SE} = C\frac{dv_C}{dt} + i_{LO} \tag{4-1-3}$$

rearrange the above equations, and yield

$$\frac{di_{SE}}{dt} = \frac{V_d}{L_{SE}} - \frac{R_C(i_{SE} - i_{LO})}{L_{SE}} - \frac{v_C}{L_{SE}} \tag{4-1-4}$$

$$\frac{dv_C}{dt} = \frac{i_{SE}}{C} - \frac{i_{LO}}{C} \tag{4-1-5}$$

$$\frac{di_{LO}}{dt} = -\frac{R_{LO} i_{LO}}{L_{LO}} + \frac{R_C (i_{SE} - i_{LO})}{L_{LO}} + \frac{v_C}{L_{LO}} \tag{4-1-6}$$

Define the state-variables, $x_1 = i_{SE}$, $x_2 = v_C$ and $x_3 = i_{LO}$, $u = V_d$

$$\begin{cases} \dot{x}_1 = -\dfrac{R_c (x_1 - x_3)}{L_{SE}} - \dfrac{x_2}{L_{SE}} + \dfrac{u}{L_{SE}} \\ \dot{x}_2 = \dfrac{x_1}{C} - \dfrac{x_3}{C} \\ \dot{x}_3 = -\dfrac{R_{LO} x_3}{L_{LO}} + \dfrac{R_c (x_1 - x_3)}{L_{LO}} + \dfrac{x_2}{L_{LO}} \end{cases} \tag{4-1-7}$$

Write the State-variable equation in Matrix form [5]

$$\begin{aligned} \dot{\mathbf{X}} &= A \cdot \mathbf{X} + B \cdot u \\ y &= C \cdot \mathbf{X} \end{aligned} \tag{4-1-8}$$

where

$$A = \begin{bmatrix} -\dfrac{R_C}{L_{SE}} & -\dfrac{1}{L_{SE}} & \dfrac{R_C}{L_{SE}} \\ \dfrac{1}{C} & 0 & -\dfrac{1}{C} \\ \dfrac{R_C}{L_{LO}} & \dfrac{1}{L_{LO}} & -\dfrac{R_{LO}}{L_{LO}} - \dfrac{R_C}{L_{LO}} \end{bmatrix} \quad B = \begin{bmatrix} \dfrac{1}{L_{SE}} \\ 0 \\ 0 \end{bmatrix} = \begin{bmatrix} 1.37\,E6 \\ 0 \\ 0 \end{bmatrix} \quad C = [1 \quad 0 \quad 0]$$

$$= \begin{bmatrix} -2.96\,E2 & 1.37\,E6 & 2.96\,E2 \\ 2.33\,E4 & 0 & -2.33\,E4 \\ 6.37\,E2 & 2.95\,E6 & -3.01\,E4 \end{bmatrix}$$

## 4.2 Implementation of the LQT Continuous Time Controller

### 4.2.1 The Performance Index Function

$$\begin{aligned} J_o = {} & \frac{1}{2}(y_T - r_T)^T P (y_T - r_T) + \\ & \frac{1}{2}\int_{t_o}^{T} [(Cx(t) - r(t))^T Q (Cx(t) - r(t)) + u(t)^T R u(t)] dt \end{aligned} \tag{4-2-1}$$

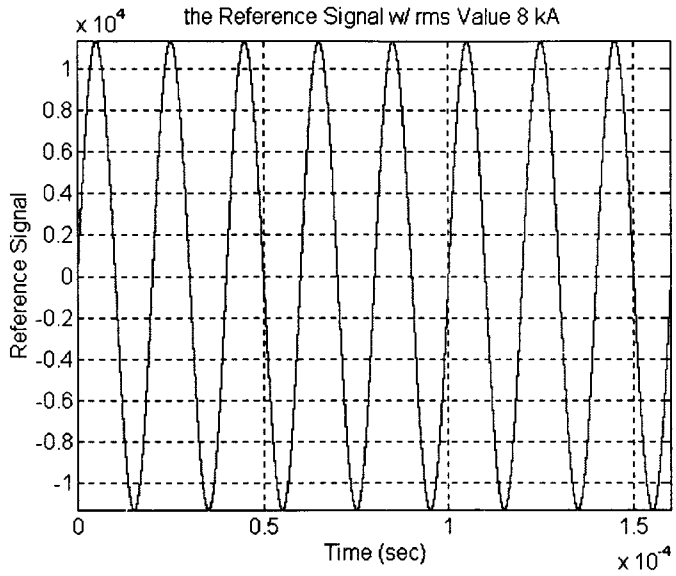


**Fig. 40 The Reference Signal**

Since the system eventually goes to steady state, there is no use for putting much weight on the final state in the cost function, so assume the final state weighing matrix P = 1.

### 4.2.2 Desired Reference Signal

The reference signal is the desired system output. The controller is designed to construct a system input, such that, the system output follows the reference signal exactly with the minimization of the cost function.

The waveform of the reference signal is shown in Fig. 40. There are 8 periods in the plot. To fulfil the induction heating requirements, the desired system output is a sinusoid waveform whose rms value is 8000 A and the natural frequency is 50 kHz, so construct the following reference signal r(t):

$$r(t) = i_{SE}(t) = \sqrt{2} \cdot 8000 \cdot \sin(2 \cdot \pi \cdot 5E4 \cdot t) \qquad (4\text{-}2\text{-}2)$$

### 4.2.3 Derivation of the Optimum Control Equation

The objective of the LQT controller is to minimize the system output error. It is a minimization problem with constraint of the system equation. There is no simple equation to define the solution of minimization problem with constraints. So by using LaGrange Multiplier Method, define $\lambda \in R^3$ as an undetermined LaGrange Multiplier, and the Hamiltonian function is shown as equation (4-2-3) [6].

$$H = L(x(t), u(t)) + \lambda f(x(t), u(t)) \qquad (4\text{-}2\text{-}3)$$

To find the minimum value for the cost function, the following critical conditions need to be satisfied:

state system equation

$$\frac{\partial H}{\partial \lambda} = -\dot{\mathbf{x}}(t) + A\mathbf{x}(t) + Bu(t) = 0 \tag{4-2-4}$$

co-state system equation

$$\frac{\partial H}{\partial x} = -\dot{\lambda} - A^T\lambda - C^T QC \cdot x(t) + C^T Qr(t) = 0 \tag{4-2-5}$$

stationary equation

$$\frac{\partial H}{\partial u} = B^T\lambda + Ru(t) = 0 \tag{4-2-6}$$

with boundary condition

$$\mathbf{x}(t_0) = \begin{bmatrix} 0 \\ 0 \\ 0 \end{bmatrix}, \ \lambda(T) = C^T P(Cx(T) - r(T))$$

From the stationary equation

$$u(t) = -R^{-1}B^T\lambda(t) \tag{4-2-7}$$

By using the sweep method (Bryson and Ho 1975), yield

$$\lambda(t) = \mathbf{S}(t)\mathbf{x}(t) - \mathbf{v}(t) \tag{4-2-8}$$

where *S(t)* is a 3×3 unknown matrix, and *v(t)* is a3×3 unknown vector, take the derivative of the LaGrange multiplier with respect to time,

$$\dot{\lambda}(t) = \dot{\mathbf{S}}(t)\mathbf{x}(t) + \mathbf{S}(t)\dot{\mathbf{x}}(t) - \dot{\mathbf{v}}(t) \tag{4-2-9}$$

Substitute equation (4-2-8) and equation (4-2-9) into the co-state equation yields,

$$\begin{aligned} \dot{\lambda}(t) &= \dot{\mathbf{S}}(t)\mathbf{x}(t) + \mathbf{S}(t)\dot{\mathbf{x}}(t) - \dot{\mathbf{v}}(t) \\ &= -\mathbf{A}^T(S(t)x(t) - v(t)) - \mathbf{C}^T Q\mathbf{C} \cdot \mathbf{x}(t) + \mathbf{C}^T Qr(t) = 0 \end{aligned} \tag{4-2-10}$$

Rearrange equation (4-2-10),

$$\dot{\mathbf{S}}(t) = -A^T\mathbf{S}(t) - \mathbf{S}(t)A + \mathbf{S}(t)BR^{-1}B^T\mathbf{S}(t) - C^TQC \tag{4-2-11}$$

with the boundary condition: $S(T) = C^TPC$.

$$\dot{\mathbf{v}}(t) = -(A - BK(t))^T\mathbf{v} - C^TQr(t) \tag{4-2-12}$$

with the boundary condition: $v(T) = C^TP \cdot r(T)$.

Define the Kalman gain by

$$\mathbf{K}(t) = R^{-1}\mathbf{B}^T\mathbf{S}(t) \tag{4-2-13}$$

The Continuous-Time Linear Quadratic Optimum Tracker equations are: [6]

$$K(t) = R^{-1}B^TS(t)$$

$$\dot{\mathbf{S}} = -A^T\mathbf{S} - \mathbf{S}A + \mathbf{S}BR^{-1}B^T\mathbf{S} - C^TQC, \qquad S(T) = C^TPC$$

$$\dot{\mathbf{v}} = -(A - BK)^T\mathbf{v} - C^TQr(t), \qquad v(T) = C^TP \cdot r(T)$$

$$u(t) = -Kx(t) + R^{-1}B^T\mathbf{v}$$

## 4.3 Solving System Equations With Weighing Matrix R = 1 and Q =1

### 4.3.1 Solving Matrix S

Since the initial value of the S matrix equation is unknown, and only the boundary values are known, a backward integration will be used, where the time is reversed and the initial value for the integration is the boundary conditions. Rewrite S matrix equation,

$$-\dot{\mathbf{S}}(t) = A^T\mathbf{S}(t) + \mathbf{S}(t)A - \mathbf{S}(t)BR^{-1}B^T\mathbf{S}(t) + C^TQC \tag{4-3-1}$$

Let $g = T - t$, where T is the final time, rearrange the equation (4-3-2),

$$\dot{\mathbf{S}}(g) = A^T\mathbf{S}(g) + \mathbf{S}(g)A - \mathbf{S}(g)BR^{-1}B^T\mathbf{S}(g) + C^TQC \tag{4-3-2}$$

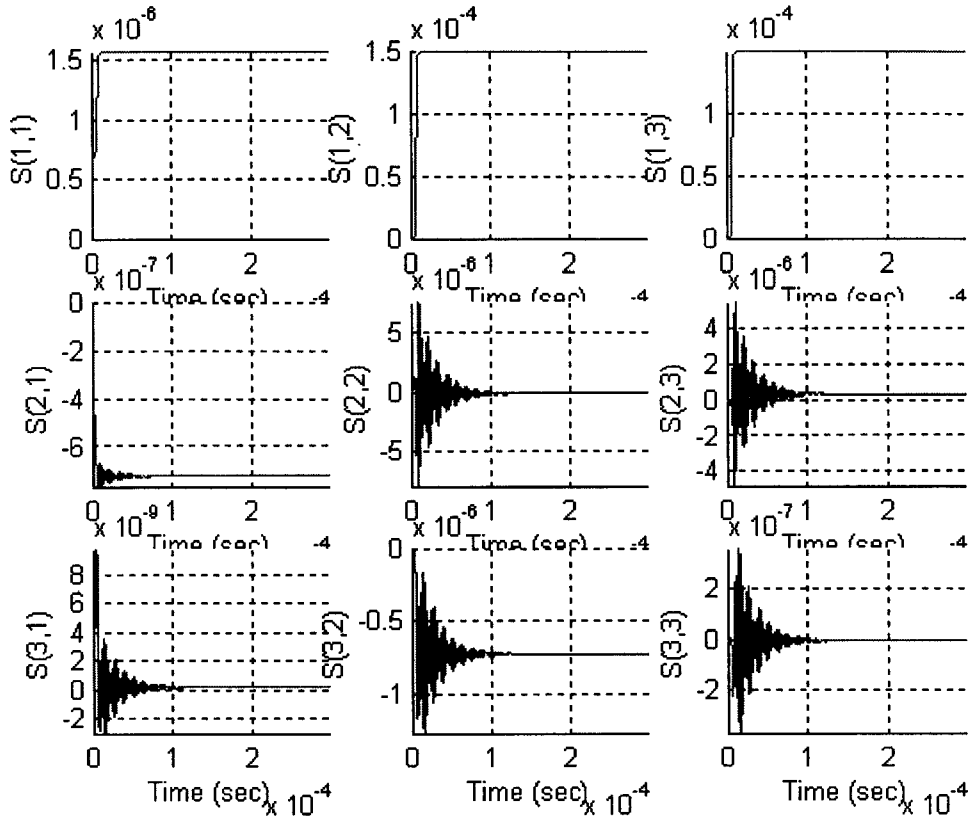


**Fig. 41 The Plot of the S Matrix w/ R = 1 Q = 1 (Time is reversed)**

The plot for the auxiliary S matrix is shown in Fig. 41. Since the plot of S matrix is solved by backward integration, the S matrix is actually starting from a steady state, then when the time approach to the final state, it goes through a transient to go to zero, which has been set as a boundary value. So it is reasonable to use the steady state S matrix to construct the controller, it also simplifies the controller.

```
SS =

   1.564e-6   1.506e-4   1.498e-4
  -7.302e-7   -5.442e-8   3.785e-7
   1.876e-10  -7.260e-7  -4.898e-9
```

Therefore, instead of calculating the K matrix dynamically, the following constant matrix will be used.

$$K(t) = R^{-1}B^{T}SS$$

```
KS =          2.1426e+0   2.0629e+2   2.0524e+2
```

### 4.3.2 Solving Vector v

To solve the system equations, the initial condition of the v vector must be determined. By using the backward integration and solving for vector v, the equation will be changed to

$$-\dot{\mathbf{v}} = (A - BK)^T \mathbf{v} + C^T Q r(t) \tag{4-3-3}$$

Using the changing variable method, and letting $g = T - t$, where $T$ is the final time, yields

$$\dot{\mathbf{v}}(g) = (A - BK)^T \mathbf{v}(g) + C^T Q r(g) \tag{4-3-4}$$

Therefore, the boundary conditions are the initial conditions for equation (4-3-5). By using Matlab Simulink model is shown in Fig. 42.

Solve the v vector in 200 period, i.e. in (0 s, 4 ms) time range. When the vector is in steady state, the rms value of the v vector is as follows:

```
v =
   1.2814e-005
   0.3444
   0.0362
```

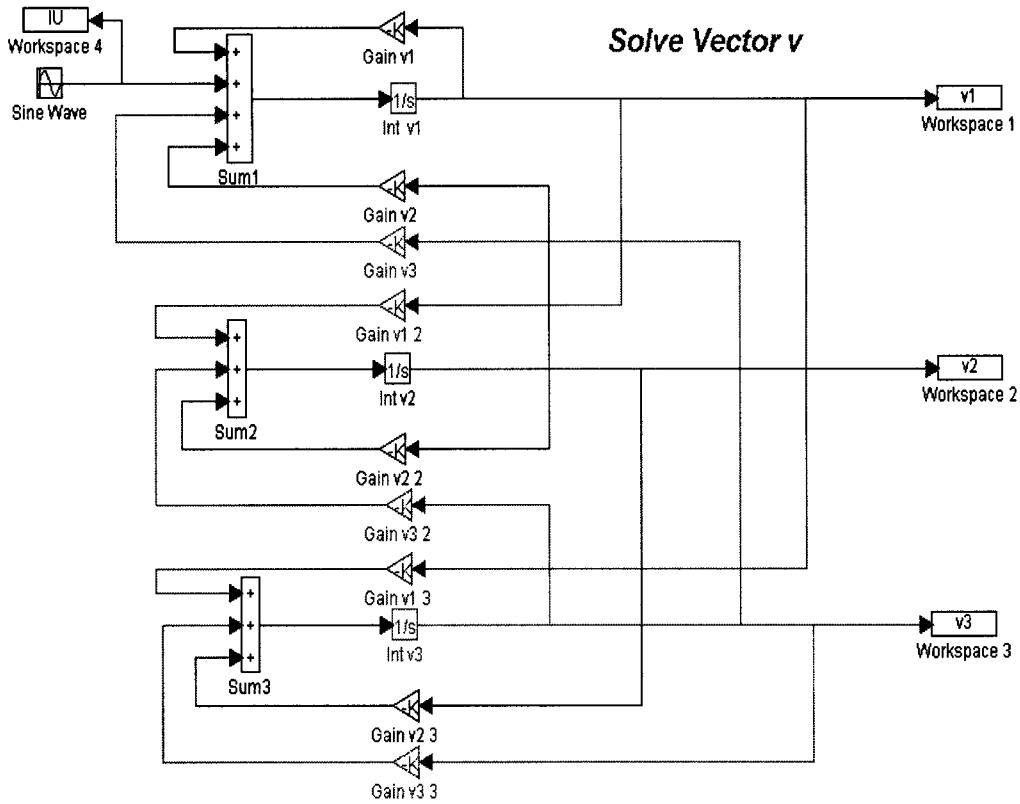


**Fig. 42 Simulink Model to Solve the *v* Vector**

The initial condition for $v(0)$ is:

```
-7.3433e-006
-2.0985e-003
 5.1172e-002
```

Since the results are from the backward integration, the waveforms of the v vector is actually starting from the steady state, then go through a transient to reach the boundary condition.

### 4.3.3 Closed Loop System Response

By using Matlab, the close loop system Simulink model is shown in Fig. 43, the open plant is constructed by the open loop system equations. The continuous time LQT controller has two inputs, one is the reference signal and the other is the system state variable feedback. The simulation period is 4 ms and the simulation step is $10^{-3}$ μs, which is much faster than the resonant frequency. Therefore, the results are close to a real continuous time system.

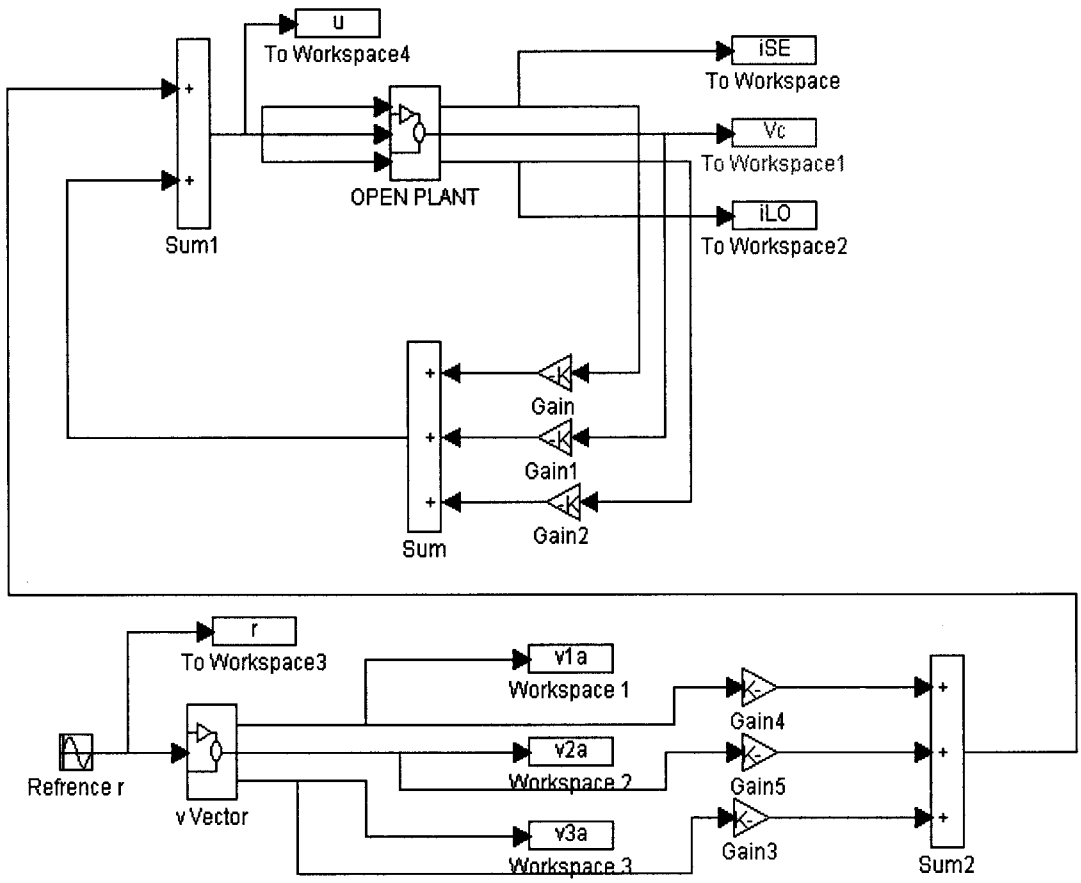


**Fig. 43 Simulink Model of the Closed Loop System**

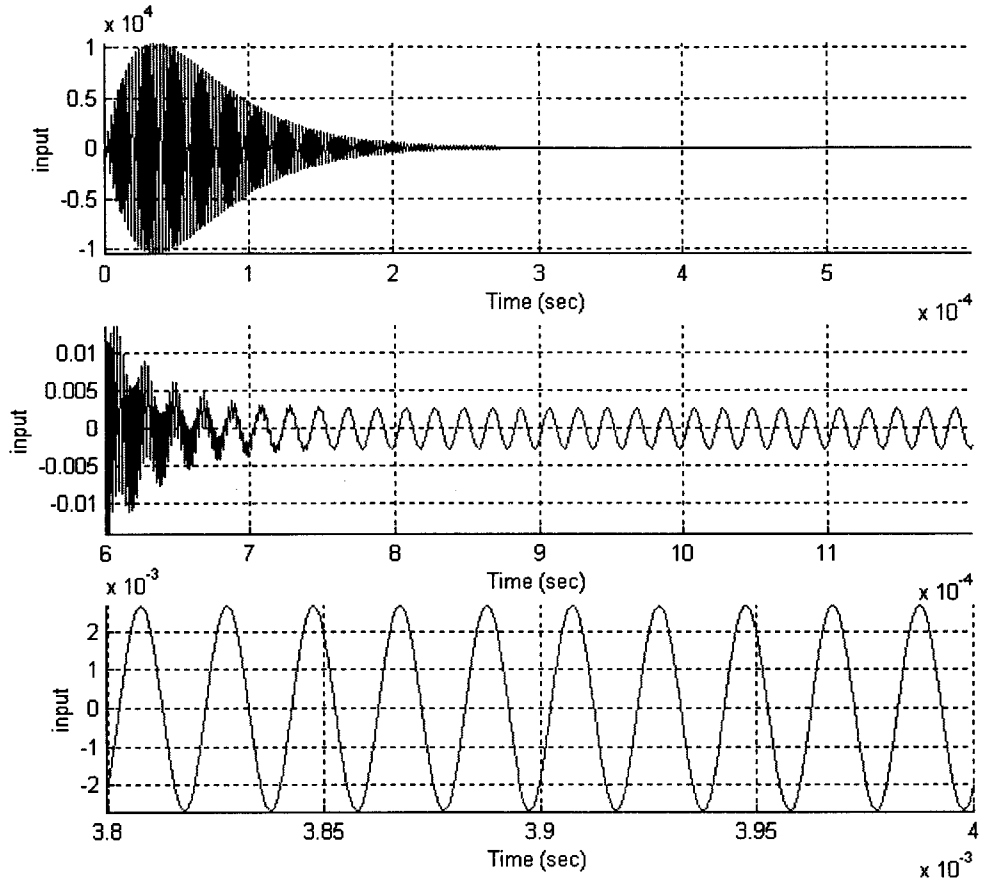


**Fig. 44 Plot of the System Input w/ R = 1 Q = 1**

The waveform of the control input (u(*t*)) is shown in Fig. 44, where the steady-state rms value of the input is as following

$$urms = 1.8993e\text{-}003\ V$$

The rms value of the input is only about two Millie volts, which is unacceptable.

The waveform of the system output ($i_{SE}$) is shown in Fig. 45. The system states all go through a transient then go to a steady state, where the rms values of the system states are:

$$i_{SE}rms = 3.8536e\text{-}002\ A$$

$$V_c rms = 9.0436e\text{-}003\ V$$

$$i_{LO}rms = 8.4545e\text{-}002\ A$$

Which is very small compare to the desired values. So the weigh matrix is not appropriate.

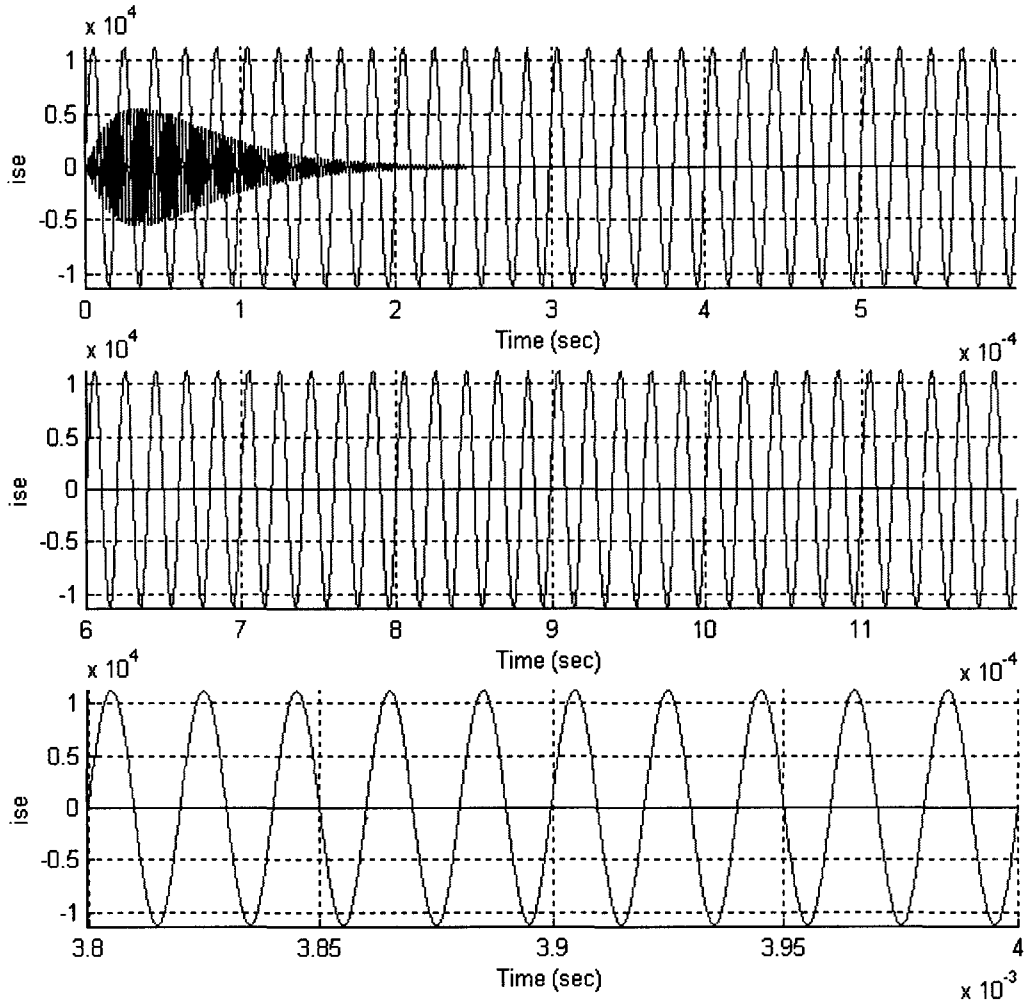


**Fig. 45 Comparison of System Output $i_{SE}$ and Reference Signal w/ R = 1 and Q = 1**

## 4.4 Solving System Equations With R = 0.1 and Q = 0.1

### 4.4.1 Solving Matrix S

By using the same method in section Part (4.3.1), solve the S matrix. The plot of the S matrix is shown in Fig. 46.

The elements in matrix S start with a transient period then go to steady state in a very short period. Since the time is reversed, at the beginning of time, the elements in S matrix are constant, which is the steady state value. By using Matlab, the steady state S matrix is as following

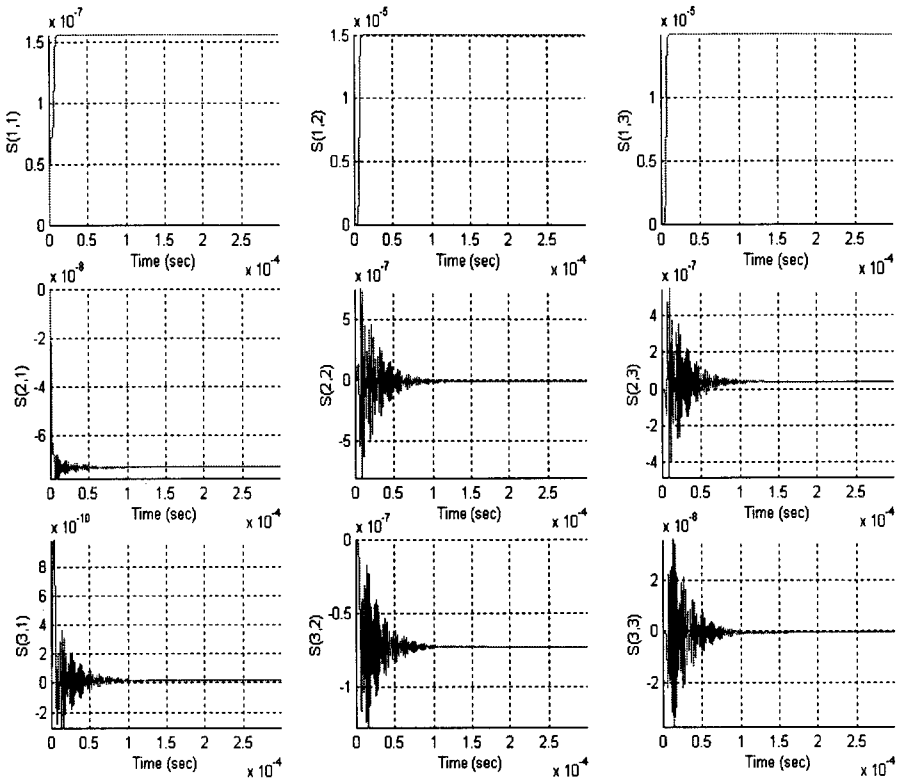


**Fig. 46 Plot of the S Matrix w/ R = 0.1 and Q = 0.1 (Time is reversed)**

```
SS =

   1.564e-7    1.506e-5    1.498e-5
  -7.302e-8    -5.442e-9    3.785e-8
   1.876e011   -7.260e-8   -4.898e-10
```

Therefore, the steady state K matrix is:

$$K(t) = R^{-1}B^{T}SS$$

```
KS =

    2.1426   2.0629e2   2.0524e2
```

### 4.4.2 Solving Vector *v*

Solve the v vector in 200 period, i.e. in (0, 4E-3) time range. When the vector is in steady, the rms value of the v vector is:

```
v =

   1.2814e-005
   3.4445e-001
   3.6206e-002
```

The initial value of the v vector is

```
-7.3433e-006
-2.0985e-003
 5.1172e-002
```

### 4.4.3 Closed Loop System Response

By using the same method in section (4.3.4), the control input ($u(t)$)waveform is shown in Fig. 47, where the steady-state rms value of the input is:

```
urms = 1.9223e-002 V
```

The steady state value of the input voltage is too small, while the rms value of the transient period for control signal is big, and the frequency is too fast. Therefore, the results are not favorable and the weighing matrixes are not appropriate.

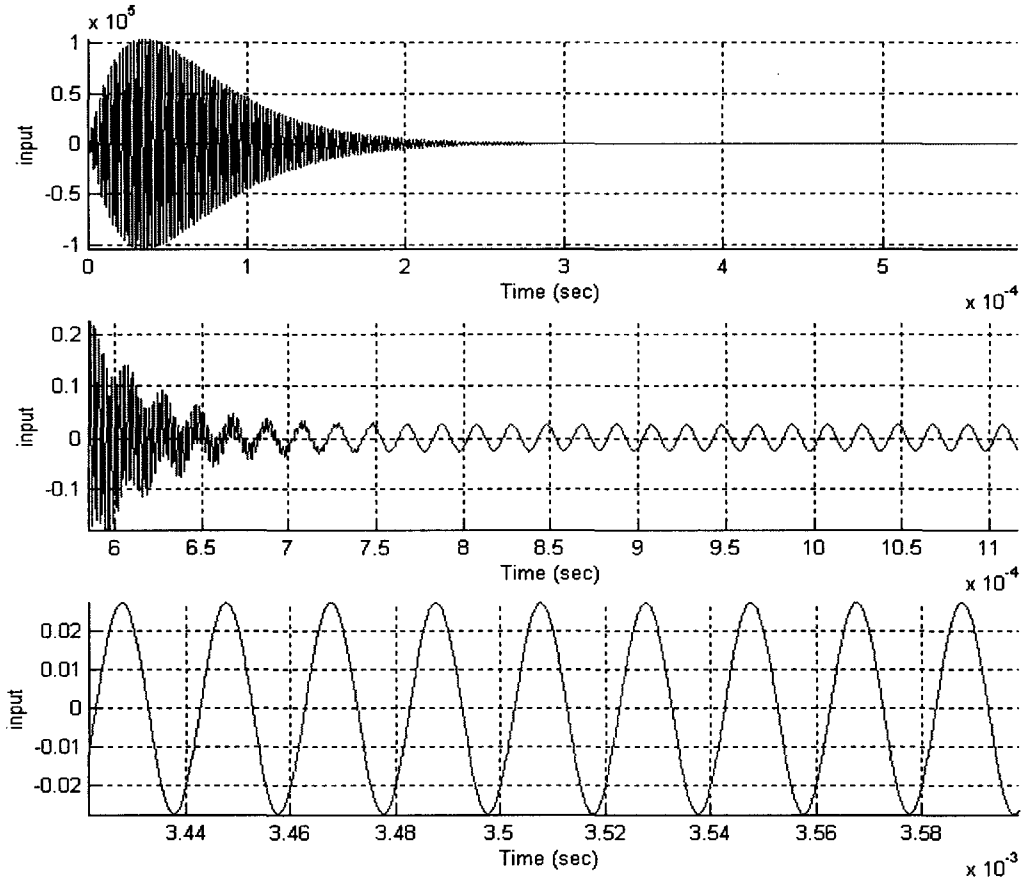


**Fig. 47 Plot of the System Input w/ R = 0.1 and Q = 0.1**

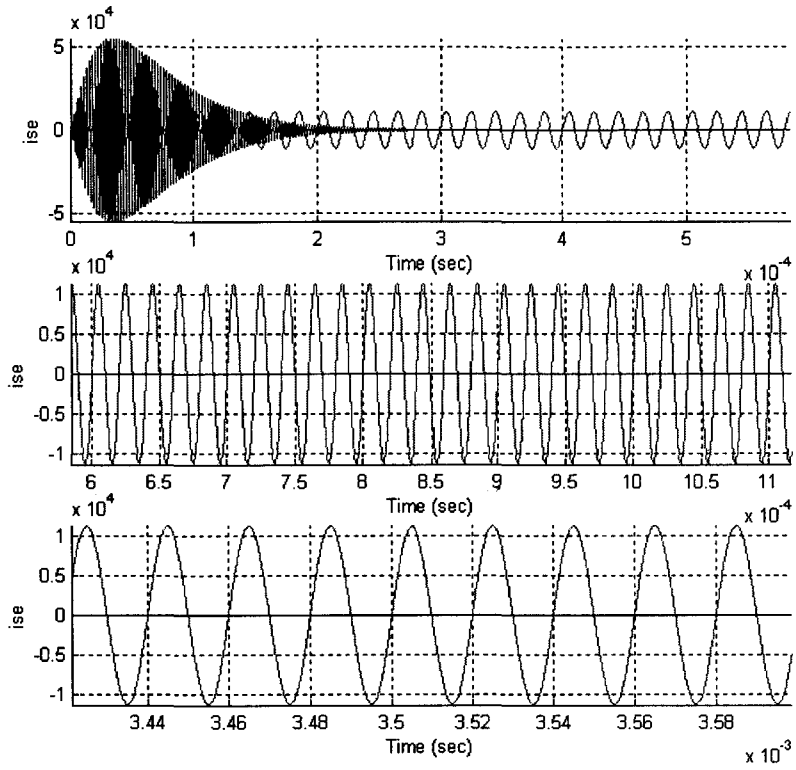


**Fig. 48 Comparison of $i_{SE}$ and the Reference Signal w/ R = 0.1 and Q = 0.1**

The plot of the comparison of the system output ($i_{SE}$) and the desired reference signal is shown in Fig. 48. The system states all go through a transient then go to a steady state, where the rms values of the system states are:

$i_{SE}rms$ = 3.8523e-001 A

$V_c rms$ = 9.0437e-002 V

$i_{LO}rms$ = 8.4545e-001 A

Which is very small compare to the desired values. So the weigh matrix is not appropriate.

## 4.5 Solving System Equations With R = 10 and Q = 10

### 4.5.1 Solving Matrix S

By using the same method in section Part (4.3.1), the plot of the S matrix is shown in Fig. 49. Since the time is reversed, the elements of S matrix are in steady state initially, then go through a transient period, and finally end up with the boundary condition.

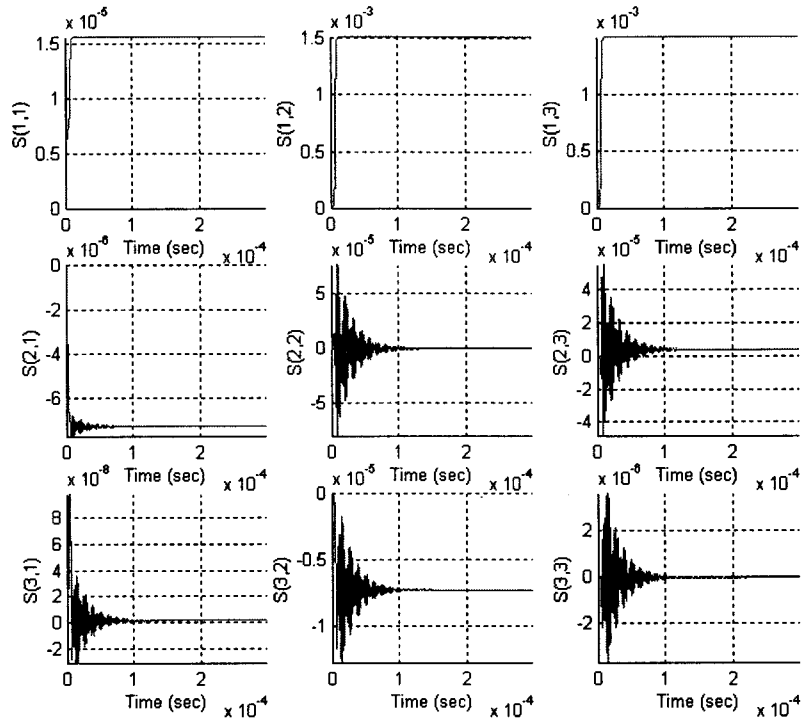


**Fig. 49 Plot of the S Matrix W/ R = 10 and Q = 10 (Time is reversed)**

By using Matlab, the steady state S matrix is:

```
SS =

   1.5643e-5   1.5061e-3   1.4984e-3
  -7.3017e-6  -5.4419e-7   3.7854e-6
   1.8758e-9  -7.2603e-6  -4.8977e-8
```

Therefore, the steady state K matrix is $K(t) = R^{-1}B^{T}SS$

```
KS =        2.1426   2.0629e+2   2.0524e+2
```

### 4.5.2 Solving Vector *v*

Solve the v vector in 200 period, i.e. in (0, 4E-3) time range. When the vector is in steady, the rms value of the v vector is:

```
v =   1.2814e-5
      3.4445e-1
      3.6206e-2
```

The initial value of the v vector is

```
   -7.3433e-6
   -2.0985e-3
    5.1172e-2
```

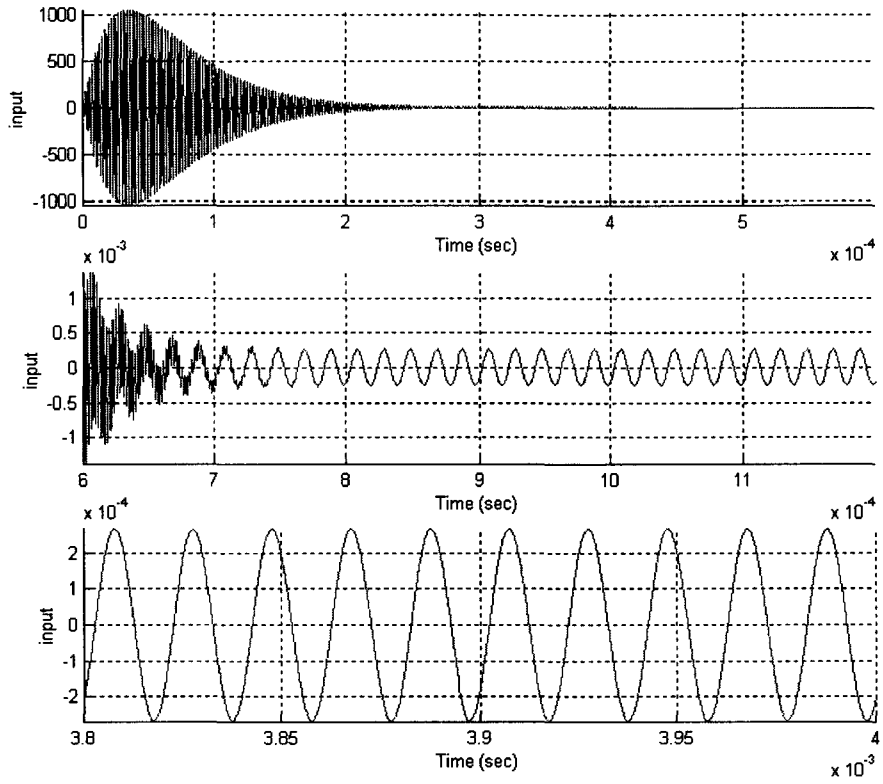


**Fig. 50 Plot of the System Input**

The waveform of the control input is shown in Fig. 50, where the steady-state rms value of the input is

```
urms = 1.8994e-4
```

### 4.5.3 Closed Loop System Response

The plots of the comparison of the system output ($i_{SE}$) and the desired reference signal is shown in Fig. 51. The system states all go through a transient then go to a steady state, where the rms values of the system states are:

$i_{SE}rms$ = 3.8532e-3 A

$V_c rms$ = 9.0435e-4 V

$i_{LO}rms$ = 8.4541e-3 A

The values of state variables are extremely small compare to the desired values. So the weighing matrix is not appropriate.

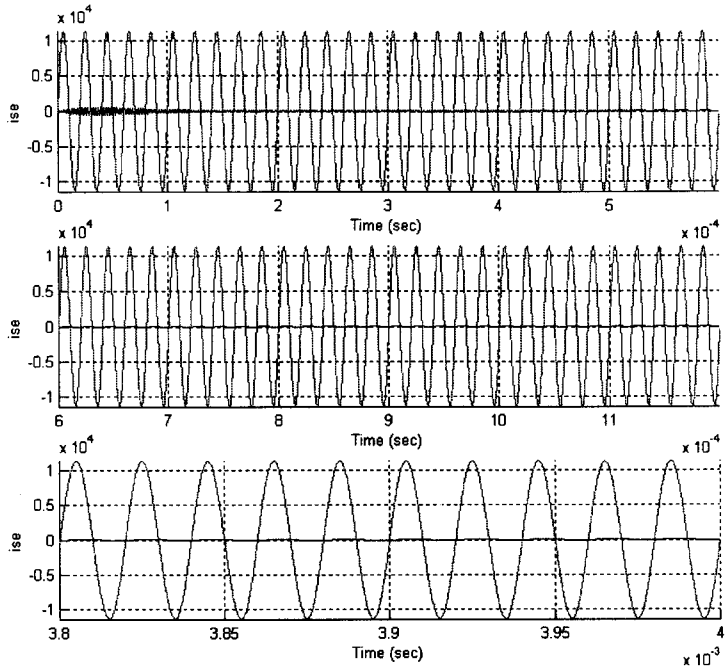


**Fig. 51 Comparison of $i_{SE}$ and the Reference Signal w/R = 10 and Q = 10**

## 4.6 The Best Weighing Matrices

By using different weighing matrices, generates the values of *S* matrix, v vector, *KS* and the rms value of the state variables. The result is shown in Table 4.

**Table 4. Comparison of Different Weighing Matrix**

| | R = 1 | | |
|---|---|---|---|
| | **Q = 0.1** | **Q = 1** | **Q = 10** |
| **SS(1,1)** | 1.56E-6 | 1.56E-6 | 2.31E-6 |
| **SS(1,2)** | 1.88E-4 | 1.51E-4 | 1.63E-7 |
| **SS(1,3)** | 1.87E-6 | 1.50E-4 | 1.21E-9 |
| **SS(2,1)** | -7.30E-7 | -7.30E-7 | -6.59E-7 |
| **SS(2,2)** | -5.15E-8 | -5.44E-8 | 1.26E-5 |
| **SS(2,3)** | 3.79E-9 | 3.79E-7 | -3.14E-7 |
| **SS(3,1)** | 1.82E-10 | 1.88E-10 | 3.78E-9 |
| **SS(3,2)** | -7.27E-7 | -7.26E-7 | 1.50E-8 |
| **SS(3,3)** | -4.89E-11 | -4.90E-9 | 1.02E-9 |
| | | | |
| **KS(1,1)** | 2.14 | 2.14E | 3.16 |
| **KS(1,2)** | 2.58E2 | 2.06E2 | 2.23E-1 |
| **KS(1,3)** | 2.56E4 | 2.05E2 | 1.66E-3 |
| | | | |
| **v(1,1)rms** | 1.02E-5 | 1.28E-5 | 2.03E-3 |

| | | | |
|---|---|---|---|
| v(2,1)rms | 3.44E-1 | 3.44E-1 | 5.76E-2 |
| v(3,1)rms | 3.62E-2 | 3.62E-2 | 5.25E-3 |
| | | | |
| ISErms | 2.47E-2 | 3.85E-2 | 9.64E2 |
| Vcrms | 5.78E-3 | 9.04E-3 | 2.26E2 |
| ILOrms | 5.41E-2 | 8.45E-2 | 2.12E3 |
| Urms | 1.21E-3 | 1.90E-3 | 4.86E1 |

When R = 1 (i.e. keeping the weight on the input the same), increasing the Q, the system input increasing, and the system state variable increases too.

**Table 5. Comparison of Different Weighing Matrix**

| | Q = 1 | | |
|---|---|---|---|
| | R = 0.1 | R = 1 | R = 10 |
| SS(1,1) | 2.31E-7 | 1.56E-6 | 1.56E-5 |
| SS(1,2) | 1.63E-8 | 1.51E-4 | 1.88E-3 |
| SS(1,3) | 1.21E-10 | 1.50E-4 | 1.87E-5 |
| SS(2,1) | -6.59E-8 | -7.30E-7 | -7.30E-6 |
| SS(2,2) | 1.26E-6 | -5.44E-8 | -5.15E-7 |
| SS(2,3) | -3.14E-10 | 3.79E-7 | 3.79E-8 |
| SS(3,1) | 3.78E-10 | 1.88E-10 | 1.82E-9 |
| SS(3,2) | 1.50E-9 | -7.26E-7 | -7.27E-6 |
| SS(3,3) | 1.02E-10 | -4.90E-9 | -4.89E-10 |
| | | | |
| KS(1,1) | 3.16 | 2.14 | 2.14 |
| KS(1,2) | 2.23E-1 | 2.06E2 | 2.58E2 |
| KS(1,3) | 1.66E-3 | 2.05E2 | 2.56E4 |
| | | | |
| V(1,1)rms | 2.03E-3 | 1.28E-5 | 1.02E-5 |
| V(2,1)rms | 5.76E-2 | 3.44E-1 | 3.44E-1 |
| V(3,1)rms | 5.25E-3 | 3.62E-2 | 3.62E-2 |
| | | | |
| ISErms | 9.64E3 | 3.85E-2 | 2.47E-3 |
| Vcrms | 2.26E3 | 9.04E-3 | 5.78E-4 |
| ILOrms | 2.12E4 | 8.45E-2 | 5.41E-3 |
| Urms | 4.86E2 | 1.90E-3 | 1.21E-4 |

When Q = 1, increasing weight on the input in the cost function, i.e. increasing the R, the system input decreases, and the system state variable decreases too.

By trial and error, the weighing matrices are `R = .205; Q = 1.483.` By using these weighing matrices, the system output follows the reference signal closely.

### 4.6.1 Solving Matrix S

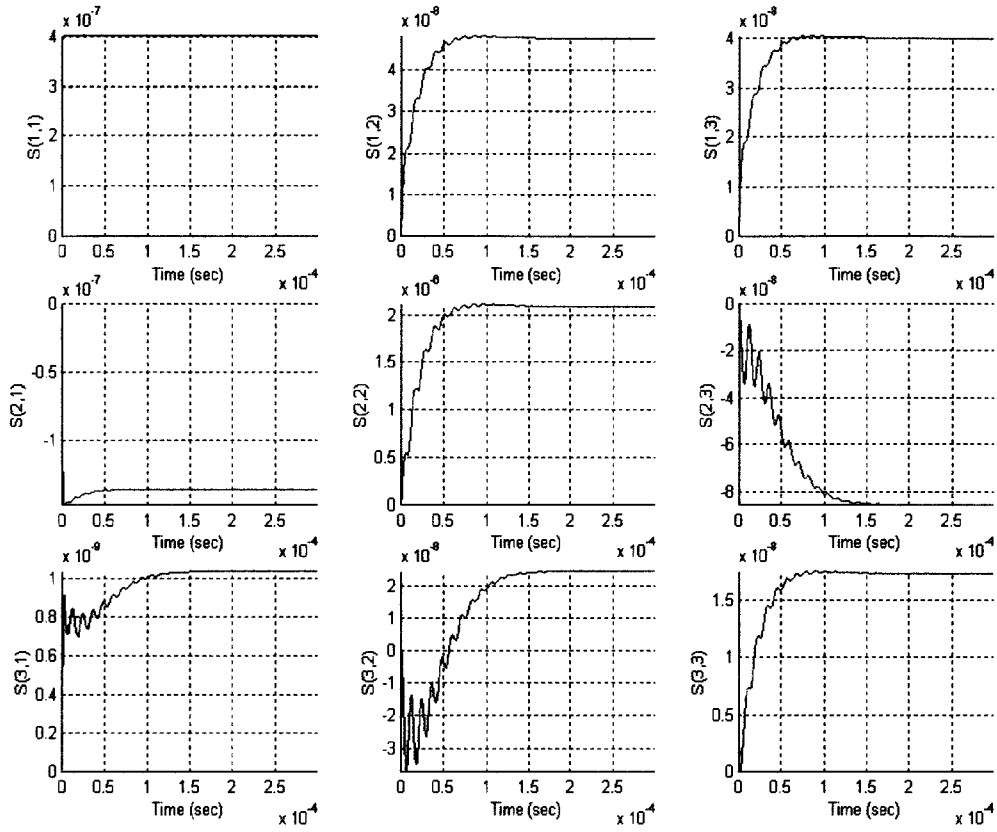


**Fig. 52 Plot of the S Matrix w/ R = 0.205 and Q = 1.483 (Time is reversed)**

By using the same method in section Part (4.3.1), the plot of the S matrix is shown in Fig. 52. The proper weighing matrices make the oscillation of the S matrix is less, and the transient time getting less.

```
SS =

   4.0222e-7   4.7896e-8   4.0060e-8
  -1.3559e-7   2.0899e-6  -8.5664e-8
   1.0431e-9    2.4797e-8   1.7415e-8
```

Therefore, the steady state K matrix is:

$$K(t) = R^{-1}B^{T}SS$$

```
KS =

   2.6875   3.2002e-1   2.6766e-1
```

## 4.6.2 Solving Vector v

Solve the v vector in 200 period, i.e. in (0, 4E-3) time range. When the vector is in steady state, the rms value of the v vector is:

```
v =

   2.6444e-3
   1.0708e-1
   1.0340e-2
```

The initial value of the v vector is

```
  -4.2764e-4
  -1.1724e-1
  -1.0471e-2
```

From the waveform of the v vector, the transient response is getting better, no spike generated.

### 4.6.3 Closed System Response

The waveform of the control input ($V_d(t)$)is shown in Fig. 53.

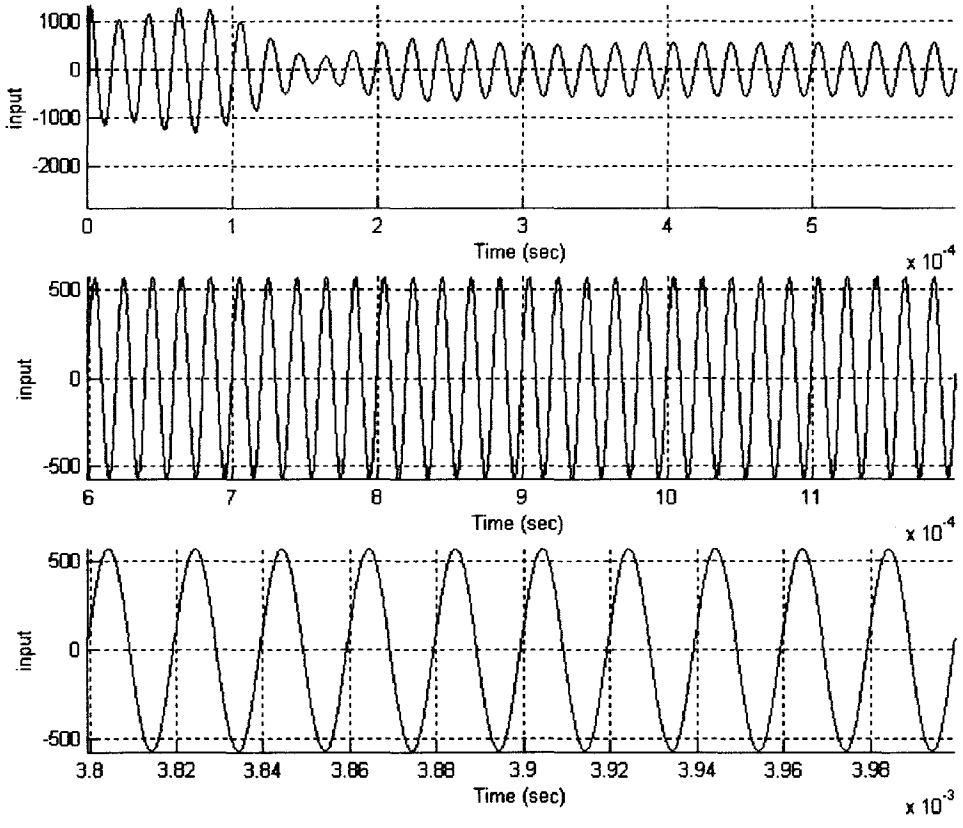


**Fig. 53 Plot of the System Input**

From the plot, the steady-state rms value of the input is

```
urms = 4.196 E2
```

The system states all go through a transient then go to a steady state, where the rms values of the system states are:

$i_{SE}rms$ = 8.0000e3 A

$V_c rms$ = 1.8784e3 V

$i_{LO}rms$ = 1.7561e4 A

The rms value of the system output is equal to the rms value of the reference signal. From Fig. 54, there exists a delay between the system output and the reference signal, but the system follows the reference signal exactly. The plots for other state variables are shown in Fig. 55 and 56. The waveforms for the tank capacitor voltage and induction coil current are sinusoidal waveform also.

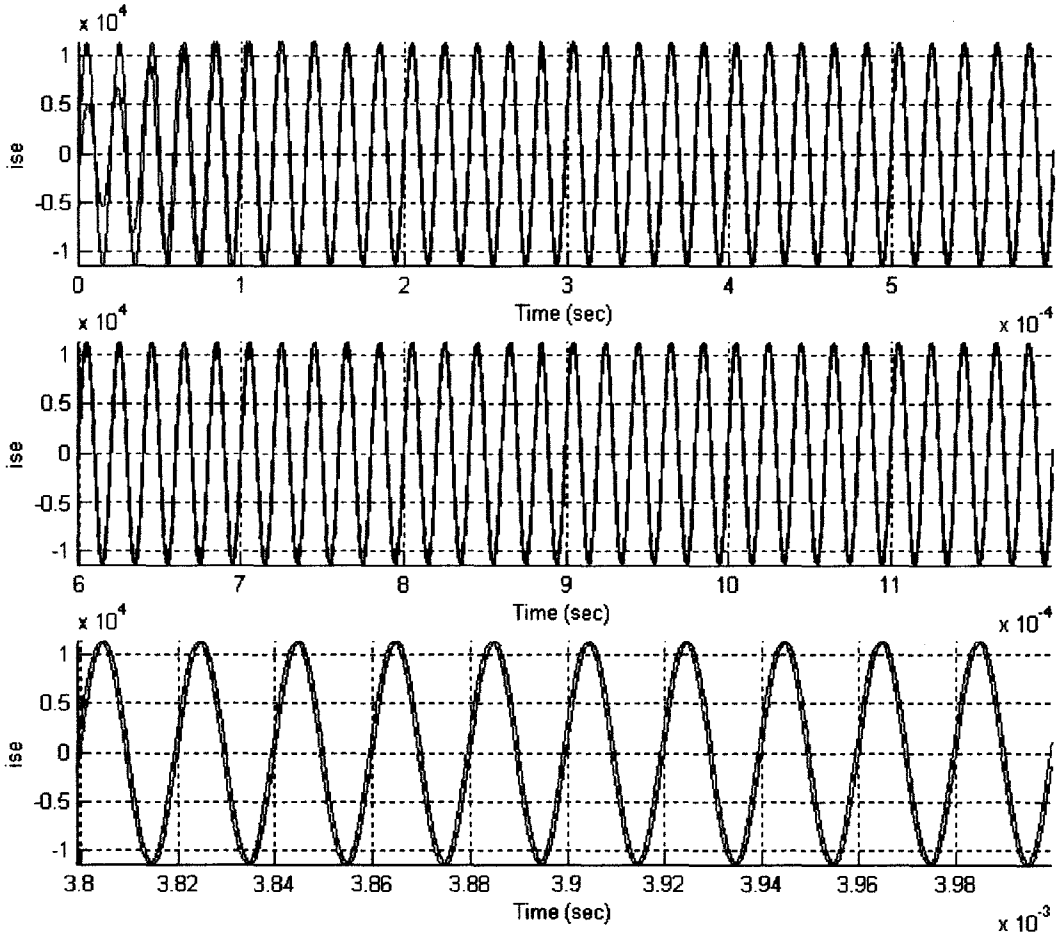


**Fig. 54 Comparison of the State $i_{SE}$ and the Reference Signal**

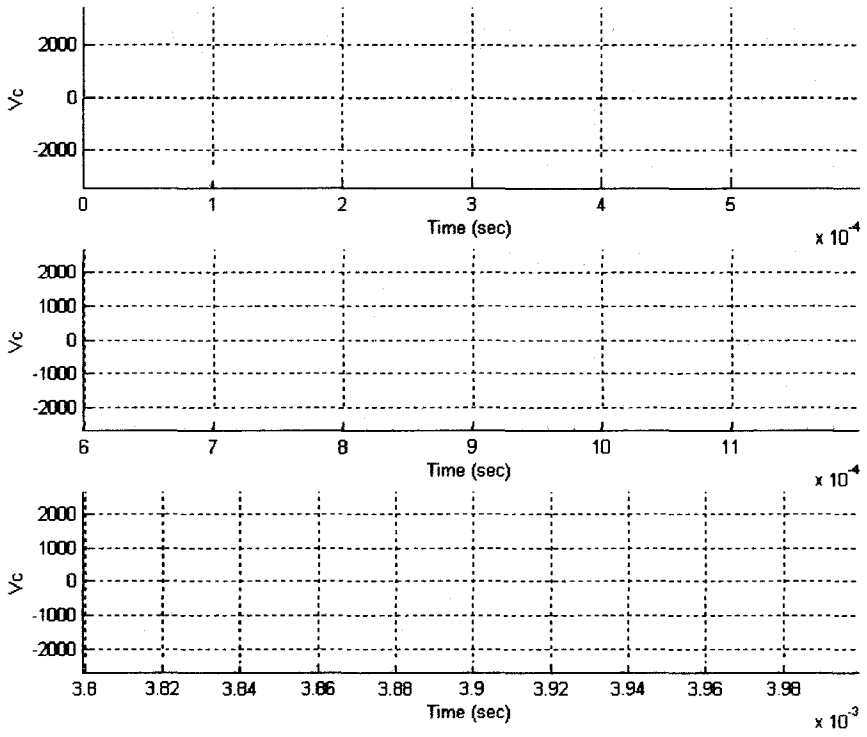


**Fig. 55 Plot of the Tank Voltage (*Vc*)**

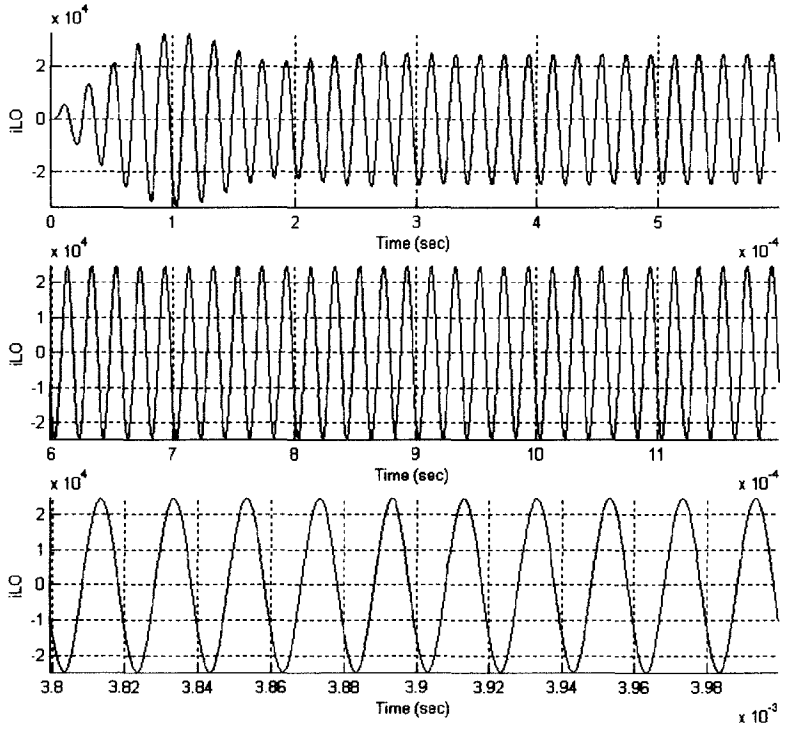


**Fig. 56 Plot of the Induction Coil Current ($i_{LO}$)**

The Continuous Time Linear Quadratic Tracker is hard to implement, since there are many differential equation needs to be solved first.

To get a simpler controller, the following chapter will describe a discrete-time controller, which no differential equations need to be solved.

# Chapter 5

# Discrete-Time LQT Optimum Controller

In this chapter, first convert the continuous time system model into the discrete time model, second pick the appropriate sampling rate by comparing the simulation results of discrete time and continuous time system. Build a discrete time LQT optimum controller with appropriate weighing matrices. Simulate the closed loop system with discrete time LQT optimum controller.

## 5.1 Simulation of Continuous Time System Model

The continuous system state variable equation is shown as equation (5-1-1)

$$\begin{aligned} \dot{\mathbf{x}} &= A \cdot \mathbf{x} + B \cdot u \\ y &= C \cdot \mathbf{x} \end{aligned} \tag{5-1-1}$$

*where,*

```
A =

       -2.9586e2 -1.3697e6  2.9586e2
        2.3328e4  0.0000   -2.3328e4
        6.3717e2  2.9499e6 -3.0136e4

B =
            1.3697e6
                  0
                  0

C =         1     0     0
```

By using Matlab, the system transfer function is:

```
          1.37e6 s^2 + 4.128e10 s + 9.425e16
-----------------------------------------------
s^3 + 3.043e4 s^2 + 1.008e11 s + 9.425e14
```

The open loop system Poles and Zeroes are:

**Poles:**

```
-9.3714e+003
-1.0530e+004+ 3.1696e+005i
-1.0530e+004- 3.1696e+005i
```

**Zeroes:**

```
-1.5068e+004+ 2.6189e+005i
-1.5068e+004- 2.6189e+005i
```

To analyze the system behavior, sinusoid input 560sin(ωt) was added to the open loop system. By using Matlab, investigates twenty periods of the system response with 20,000 sampling points, i.e. 1,000 sampling points per period, so the result is very similar to a continuous time system response.

## 5.2 Converting the Continuous Time Plant to Discrete Time System

### 5.2.1 Zero Order Hold Method With 5 Sampling Points Per Period

By using 5 sampling points per period,

```
>> Ts = 1/fo2/5;
>> [Ad, Bd, Cd, Dd] = c2dm(A,B,C,D,Ts,'zoh');
```

The location of the system Poles and Zeroes is shown in Fig. 57.

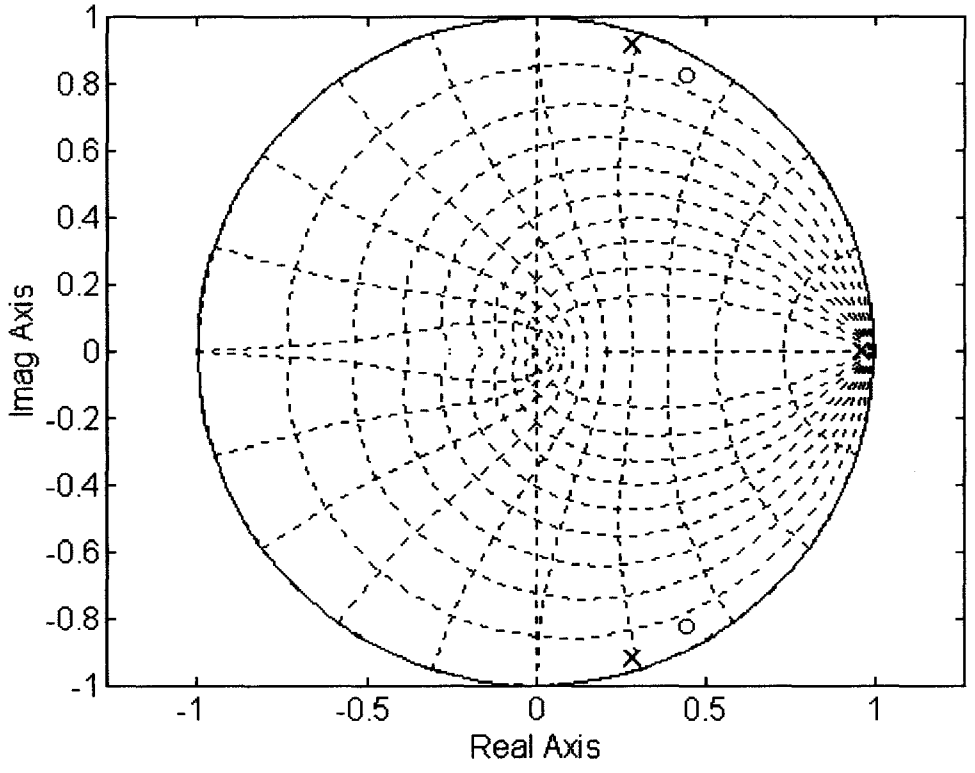


**Fig. 57 Pole-Zero Map w/5 Sampling Points Per Period**

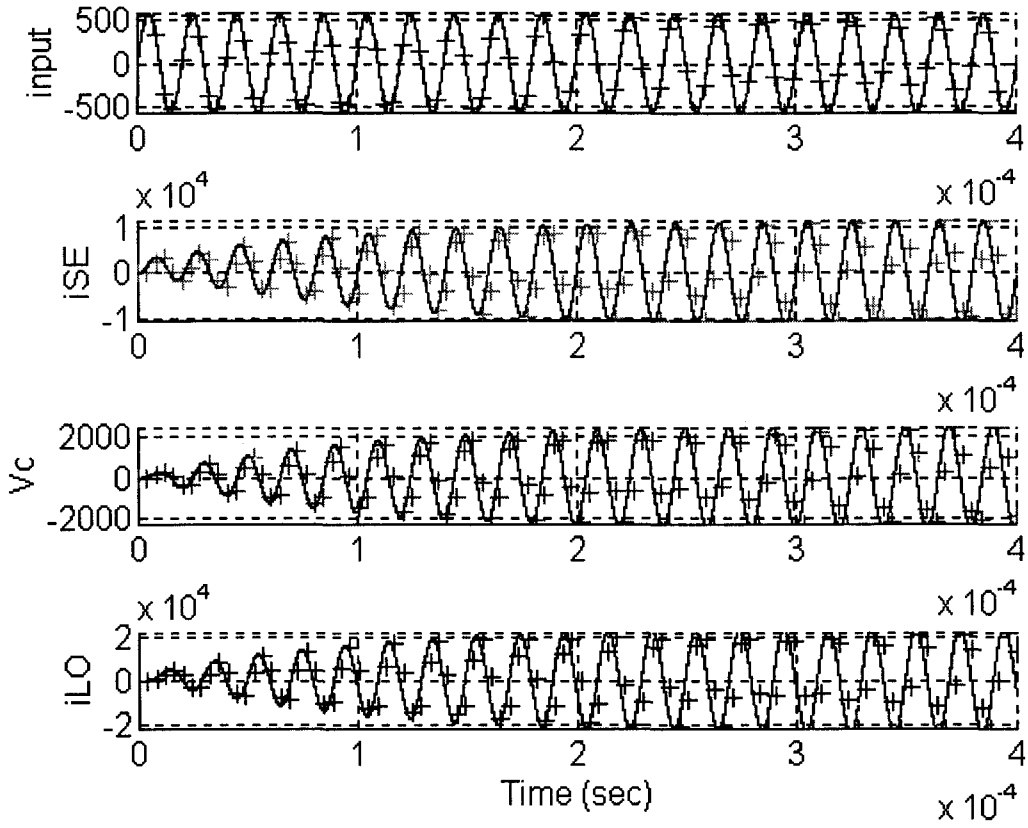


**Fig. 58 Comparison of Discrete-Time with Continuous -Time Response**

**Poles:**

```
0.9632
0.2860 + 0.9151i
0.2860 - 0.9151i
```

**Zeroes:**

```
0.4520 + 0.8259i
0.4520 - 0.8259i
```

Simulating the discrete-time system response by using Matlab, the following are the Matlab command lines,

```
>> Td = linspace(0, 20/fo2,20*5);
>> Ud = 560*sin(wo2.*Td);
>> [Yd,Xd] = dlsim(Ad,Bd,Cd,Dd,Ud);
```

The comparison with the discrete time and continuous time system response is shown in Fig. 58.

### 5.2.2 Zero Order Hold Method With 20 Sampling Points Per Period

By using 20 sampling points per period,

```
>> Ts = 1/fo2/20;
>> [Ad, Bd, Cd, Dd] =   c2dm(A,B,C,D,Ts,'zoh');
```

The location of the system poles and zeroes are

**Poles:**

```
0.9907
0.9402 + 0.3084i
0.9402 - 0.3084i
```

**Zeroes:**

```
0.9514 + 0.2554i
0.9514 - 0.2554i
```

Simulating the discrete-time system response by using Matlab command ***dlsim***:

```
>> Td = linspace(0, 20/fo2,20*20);
>> Ud = 560*sin(wo2.*Td);
>> [Yd,Xd] = dlsim(Ad,Bd,Cd,Dd,Ud);
```

### 5.2.3 Zero Order Hold Method With 40 Sampling Points Per Period

By using 40 sampling points per period,

```
>> Ts = 1/fo2/40;
>> [Ad, Bd, Cd, Dd] =
   c2dm(A,B,C,D,Ts,'zoh');
```

**Poles:**

```
0.9953
0.9823 + 0.1570i
0.9823 - 0.1570i
```

**Zeroes:**

```
0.9840 + 0.1296i
0.9840 - 0.1296i
```

Simulating the discrete-time system response by using Matlab command ***dlsim***:

```
>> Td = linspace(0, 20/fo2,20*40);
>> Ud = 560*sin(wo2.*Td);
>> [Yd,Xd] = dlsim(Ad,Bd,Cd,Dd,Ud);
```

The comparison with the discrete time and continuous time system response is shown in Fig. 59.

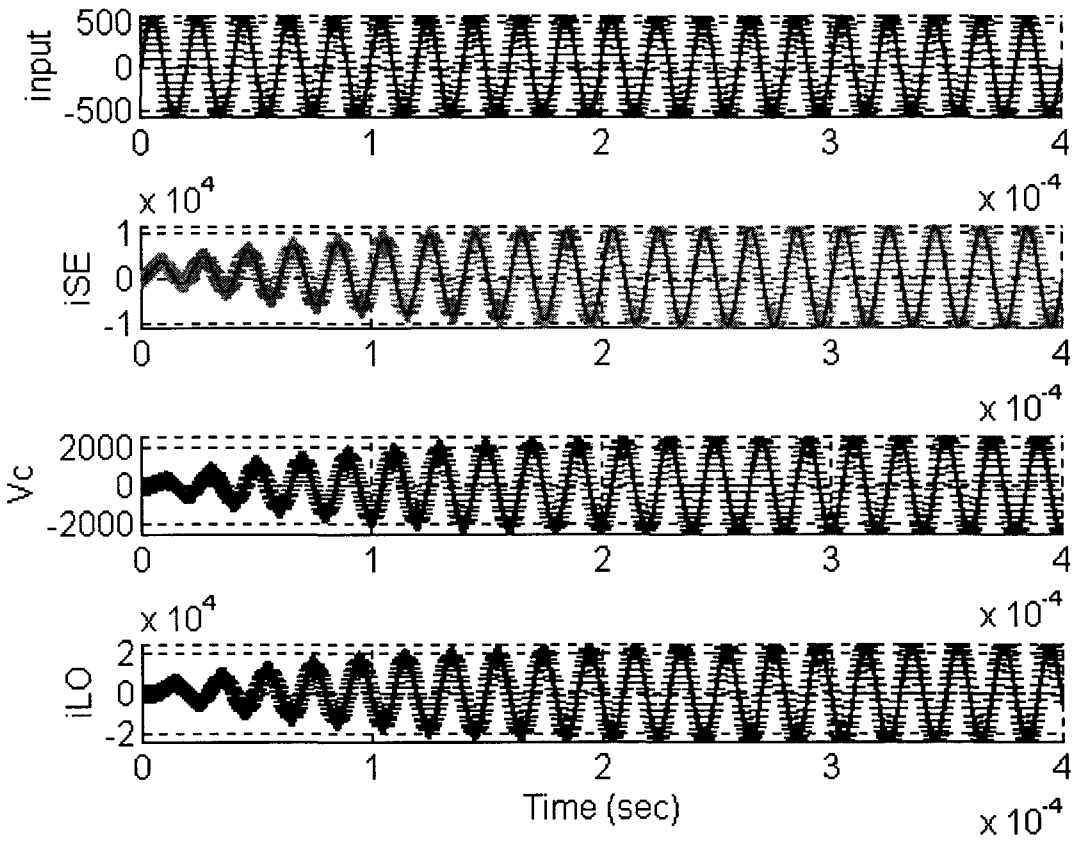


**Fig. 59** **Comparison of Discrete-Time System Response with Continuous - Time System**

### 5.2.4 Discrete-Time System State Variable Equation

$$\begin{aligned} \mathbf{x}(kh+h) &= \Phi \cdot \mathbf{x}(kh) + \Gamma \cdot u(kh) \\ y(kh) &= C \cdot \mathbf{x}(kh) \end{aligned} \tag{5-2-1}$$

where [2],

$$\Phi = e^{A \cdot h} = \begin{bmatrix} 0.9959 & -0.6818 & 0.0041 \\ 0.0116 & 0.9875 & -0.0115 \\ 0.0089 & 1.4576 & 0.9765 \end{bmatrix}, \quad \Gamma = \int_0^h e^{As}\, dsB = \begin{bmatrix} 0.6839 \\ 0.0040 \\ 0.0021 \end{bmatrix}$$

The sampling rate h is equal to `1/fo2/40 = 5.0 e-7` (`40` sampling points per period).

## 5.3 Deriving the Discrete-Time LQT Optimum Controller Equations

The linear quadratic tracking optimization is trying to find the error between the actual system output and the desired system output, the concept is same in the discrete time domain. The following section will find the discrete time LQT optimum controller equations, by taking the same steps as the continuous time system.

### 5.3.1 The Performance Index Function

$$J_o = \frac{1}{2}(y_N - r_N)^T P(y_N - r_N) + \frac{1}{2}\sum_{k=0}^{N-1}[(Cx_k - r_k)^T Q(Cx_k - r_k) + u_k R u_k \quad (5\text{-}3\text{-}1)$$

Since the system goes to steady state, the final time could be infinite, the difference between the final points of the system output and the reference is insignificant. Therefore, let the weighing matrix $P = 0$.

Assume the other weighing matrices are $Q \geq 0$, $R > 0$.

### 5.3.2 The Desired Reference signal

The reference signal is essentially the same as the one in the continuous system, but the signal is no longer continuous signal, it is now a series of sampling points with sampling rate $\boldsymbol{h}$ equal to 40 samples per period.

$$\begin{aligned} r(k) &= i_{SE}(k) \\ &= \sqrt{2} \cdot 8000 \cdot \sin(2 \cdot \pi \cdot 5E4 \cdot kh) \end{aligned} \quad (5\text{-}3\text{-}2)$$

### 5.3.3 Derivation of the Optimum control equation

Let $L(x_k, u_k) = \frac{1}{2}\sum_{k=0}^{N-1}[(Cx_k - r_k)^T Q(Cx_k - r_k) + u_k R u_k$

and $\phi = \frac{1}{2}(y_N - r_N)^T P(y_N - r_N)$, the cost function can be written as equation (5-3-3)

$$J_o = \phi + L(x_k, u_k) \quad (5\text{-}3\text{-}3)$$

By using LaGrange Multiplier Method, define $\lambda \in R^3$ as sequence of undetermined LaGrange Multiplier, and the Hamiltonian function is

$$H = L(x_k, u_k) + \lambda_k{}^T f(x_k, u_k) \tag{5-3-4}$$

To find the minimum value for the cost function, the following critical conditions need to be satisfied:

State System Equation

$$\frac{\partial H}{\partial \lambda_{k+1}} = -x_{k+1} + f(x_k, u_k) = 0 \tag{5-3-5}$$

Co-State System Equation

$$\frac{\partial H}{\partial x_k} = -\lambda_k + \Phi^T \lambda_{k+1} + C^T Q C \cdot x_k - C^T Q r_k = 0 \tag{5-3-6}$$

Stationary Equation

$$\frac{\partial H}{\partial u_k} = \Gamma^T \lambda_{k+1} + R u_k = 0 \tag{5-3-7}$$

with boundary condition

$$\mathbf{x}_0 = \begin{bmatrix} 0 \\ 0 \\ 0 \end{bmatrix}, \ \lambda_N = C^T P(C x_N - r_N) = \begin{bmatrix} 0 \\ 0 \\ 0 \end{bmatrix} \tag{5-3-8}$$

From the stationary equation

$$u_k = -R^{-1}\Gamma^T \lambda_{k+1} \tag{5-3-9}$$

Assume

$$\lambda_k = S_k x_k - v_k \tag{5-3-10}$$

where $S_k$ is an auxiliary $3 \times 3$ matrix and $v_k$ is an auxiliary $3 \times 1$ vector. This assumption is valid only if $S_k$ and $v_k$ can be found, substitute equation (5-3-10) into equation (5-3-5) and (5-3-6).

$$u_k = -R^{-1}\Gamma^T S_{k+1} x_{k+1} + R^{-1}\Gamma^T v_{k+1} \tag{5-3-11}$$

$$\mathbf{x}_{k+1} = \Phi \mathbf{x}_k - \Gamma R^{-1}\Gamma^T S_{k+1} \mathbf{x}_{k+1} + \Gamma R^{-1}\Gamma^T v_{k+1} \tag{5-3-12}$$

rearrange equation (5-3-12),

$$\mathbf{x}_{k+1} = (\mathbf{I} + \Gamma R^{-1}\Gamma^T S_{k+1})^{-1}(\Phi \mathbf{x}_k + \Gamma R^{-1}\Gamma^T v_{k+1}) \tag{5-3-13}$$

substitute equation (5-3-10) in equation (5-3-6)

$$\begin{aligned} S_k x_k - v_k &= \Phi^T (S_{k+1}x_{k+1} - v_{k+1}) + C^T Q C x_k - C^T Q r_k \\ &= \Phi^T S_{k+1}(\mathbf{I} + \Gamma R^{-1}\Gamma^T S_{k+1})^{-1}(\Phi \mathbf{x}_k + \Gamma R^{-1}\Gamma^T v_{k+1}) \\ &\quad - \Phi^T v_{k+1} + C^T Q C x_k - C^T Q r_k \end{aligned} \tag{5-3-14}$$

rearrange Equation (5-3-14), yield

$$\begin{aligned} &\{-S_k + \Phi^T S_{k+1}(\mathbf{I} + \Gamma R^{-1}\Gamma^T S_{k+1})^{-1}\Phi + C^T Q C\} x_k + \\ &\{v_k + \Phi^T S_{k+1}(\mathbf{I} + \Gamma R^{-1}\Gamma^T S_{k+1})^{-1}\Gamma R^{-1}\Gamma^T v_{k+1}) - \Phi^T v_{k+1} - C^T Q r_k\} = 0 \end{aligned} \tag{5-3-15}$$

The above equation must be true for all $x_k$, so the bracketed terms must equal to zero. Therefore, equation (5-3-15) can be written as two independent equations:

$$\{-S_k + \Phi^T S_{k+1}(\mathbf{I} + \Gamma R^{-1}\Gamma^T S_{k+1})^{-1} = 0 \tag{5-3-16}$$

$$\begin{aligned} &v_k - [\Phi^T - \Phi^T S_{k+1}(\mathbf{I} + \Gamma R^{-1}\Gamma^T S_{k+1})^{-1}\Gamma R^{-1}\Gamma^T] v_{k+1} \\ &+ C^T Q r_k = 0 \end{aligned} \tag{5-3-17}$$

rearrange the equation (5-3-16) and (5-3-17), yield

$$S_k = \Phi^T [S_{k+1} - S_{k+1}\Gamma(\Gamma^T S_{k+1}\Gamma^T + R)^{-1}\Gamma^T S_{k+1}]\Phi + C^T Q C \tag{5-3-18}$$

$$\begin{aligned} &v_k - [\Phi^T - \Phi^T S_{k+1}(\mathbf{I} + \Gamma R^{-1}\Gamma^T S_{k+1})^{-1}\Gamma R^{-1}\Gamma^T] v_{k+1} \\ &+ C^T Q r_k = 0 \end{aligned} \tag{5-3-19}$$

The Discrete-Time Linear Quadratic Optimum Tracker is[4]:

$$K_k = (B^T S_{k+1} B + R)^{-1} B^T S_{k+1} A, \; S_N = C^T P C \tag{5-3-20}$$

$$S_k = A^T S_{k+1}(A - B K_k) + C^T Q C \tag{5-3-21}$$

$$v_k = (A - B K_k)^T v_{k+1} + C^T Q r_k, \; v_N = C^T P \cdot r_N \tag{5-3-22}$$

$$K_k^v = (B^T S_{k+1} B + R)^{-1} B^T \tag{5-3-23}$$

$$u_k = -K_k x_k + K_k^v v_{k+1} \tag{5-3-24}$$

## 5.4 The Implementation of the Digital LQT Optimum Controller

### 5.4.1 The LQT Optimum Controller

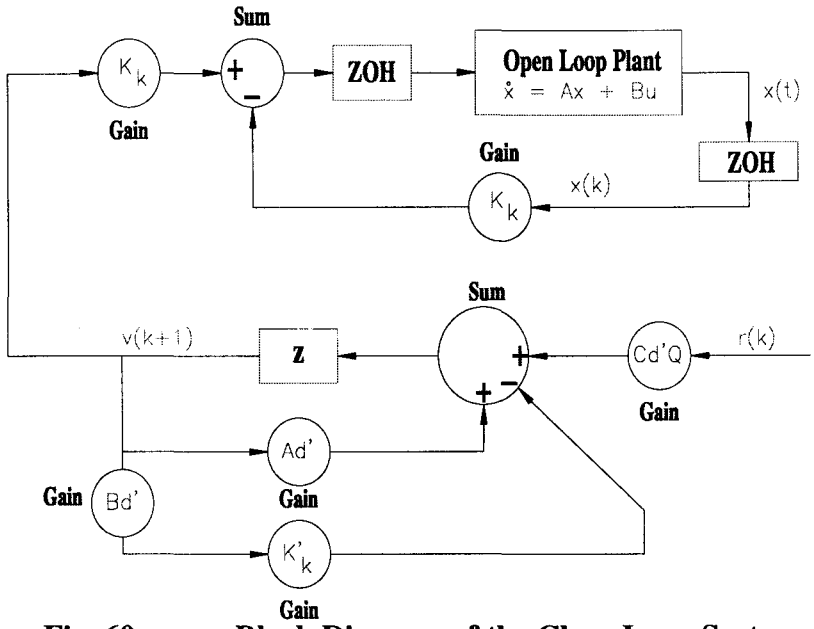


**Fig. 60 Block Diagram of the Close-Loop System**

The block diagram for the LQT controller system is shown in Fig. 60. $K_k$, $K_k^v$, $S_k$ can be calculated and stored offline. Since the reference signal is known, the vector $v_k$ can also be calculated and stored offline.

By using Matlab, choose 400 periods with sampling rate of 40 points per period, to simulate the optimum LQT controller system.

### 5.4.2 Starting with the Weighing Matrices: Q = 1 and R = 1

The S matrix start with a steady state gain as following:

```
Sinf =

   55.5503  -42.6130   18.3808
  -42.6130  908.0339  -19.8132
   18.3808  -19.8132   15.5175
```

and when the time approaches the final time, it goes through a transient then goes to zero. The same characteristic apply to matrices K and $K^v$, only the final value of K and $K^v$ are different, the steady state values are

```
Kinf =   1.0e-006 *

    0.7235   -0.6326    0.2445
```

```
Kvinf =

    0.0255    0.0001    0.0001
```

So when the final time approaches to infinite, instead of using dynamic programming to calculate the S, K and Kv matrices, the steady state value will be used. Therefore, the LQT controller equation can be rewritten as following equations

$$v_k = (A - BK_{\inf})^T v_{k+1} + C^T Q r_k,\ v_N = C^T P \cdot r_N \tag{5-4-1}$$

$$u_k = -K_{\inf} x_k + K_{\inf}^v v_{k+1} \tag{5-4-2}$$

Therefore, the implementation of the LQT controller becomes simpler, only matrix v need to be calculated and stored off line.

The comparison of the system output and the reference signal is shown as Fig. 61, the system goes through a transient, then goes to steady state, where the steady state rms value of the system output is much larger than reference signal, so the weighing matrices are not appropriate.

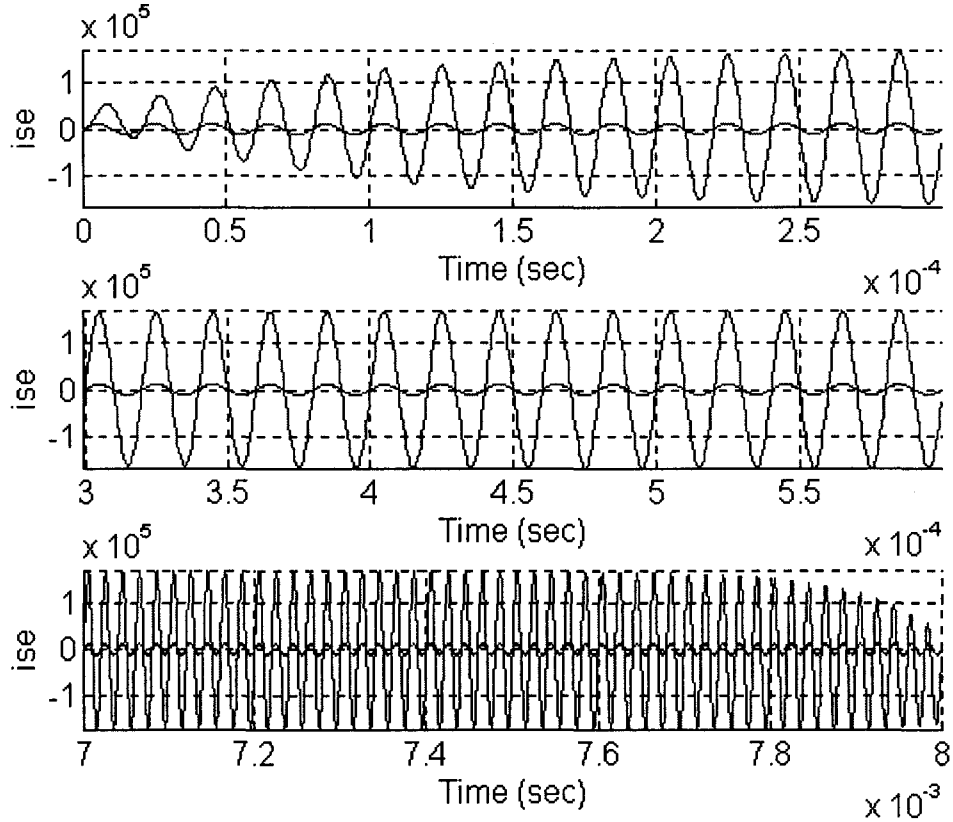


**Fig. 61 Comparison of $i_{SE}$ and the Reference Signal w/ Q = 1 and R=1**

The waveform of the system input is a sinusoidal waveform with rms value of 7,292.53, which exceeds the maximum available input value. Therefore, the values of the other state variable are exceeds the desired values too.

The values of the state variables and the system input are not the desired ones. So in order to get the desired system output, the appropriate weighing matrices must be found.

### 5.4.3 Finding the Appropriate Weighing Matrix

In order to get desired system output, the weighing matrices have to be in the range of $40 \geq Q \geq 0.01$, $40 \geq R \geq 0.01$.

By setting $Q = 0.01$, $R=0.01$, the S matrix start with a steady state gain as following:

```
Sinf =

    0.5555   -0.4261    0.1838
   -0.4261    9.0803   -0.1981
    0.1838   -0.1981    0.1552
```

and when the time approaches the final time, it goes through a transient then goes to zero.

The same characteristic apply to matrices K and $K^v$, only the final value of K and $K^v$ are different, the steady state values are:

```
Kinf =

   7.2348e-7 -6.3260e-7  2.4453e-7

Kvinf =

   2.5504e+0  1.4861e-2  7.6898e-3
```

The vector v goes to steady state immediately, because of the using of steady state values of K, $K^v$ and S matrices. The steady state rms values for v Vector is:

```
vrms =

   2.3002e+003
   3.1371e+004
   2.3065e+003
```

The comparison of the system output and the reference signal is shown in Fig. 62. The system goes through a transient, then goes to steady state, where the rms value of the system output is 117,750 A, compare to the desired system output of 8000 A, the system output is too larger. Therefore, the weighing matrices are not appropriate.

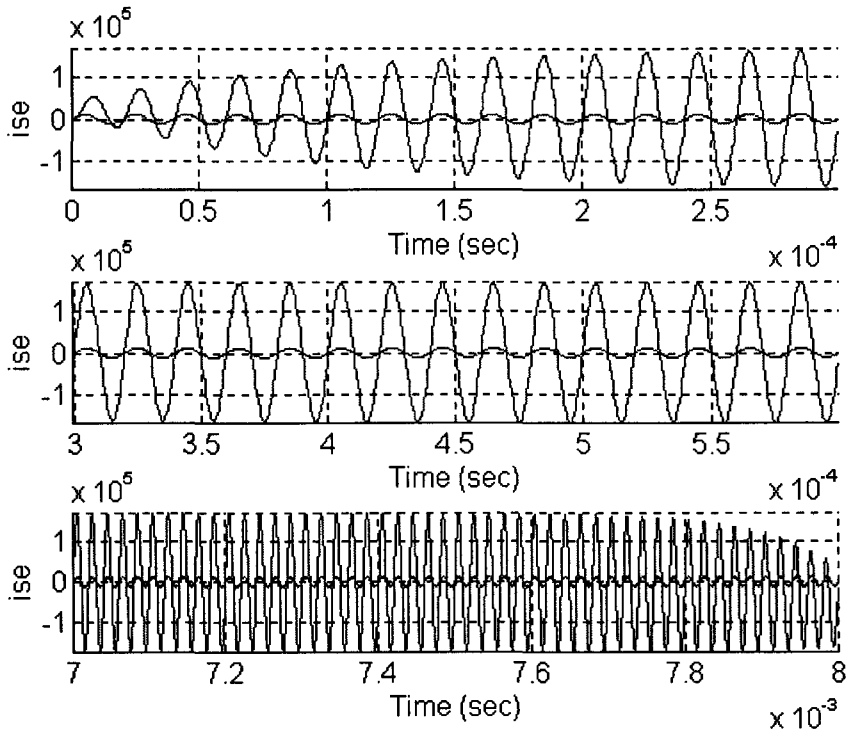


**Fig. 62 Comparison of $i_{SE}$ and the Reference Signal w/ Q = 0.01 and R=0.01**

The system input is a sinusoidal waveform with a steady state rms value of *5923.4 V*, which is much larger than the desired system input range. The enormous system input results the other state variables exceed the desired value, the rms value for the tank voltage Vc is *27, 608* V. The rms value of induction coil current $i_{LO}$ is *258.16* kA.

By setting *Q = 40, R=40,* the S matrix start with a steady state gain as following:

```
Sinf =

    2.2220e3 -1.7045e3  7.3523e2
   -1.7045e3  3.6321e4 -7.9253e2
    7.3523e2 -7.9253e2  6.2070e2
```

and when the time approaches the final time, it goes through a transient then goes to zero, in this paper, the power supply operating time is assumed to be infinite. The same characteristic apply to matrices K and $K^v$, only the final value of K and $K^v$ are different, the steady state values are:

```
Kinf =     7.2348e-7 -6.3260e-7  2.4453e-7

Kvinf =    6.3760e-4  3.7153e-6  1.9224e-6
```

The vector v goes to steady state immediately, because of the using of steady state values of K, $K^v$ and S matrices. The rms values for steady state v Vector is:

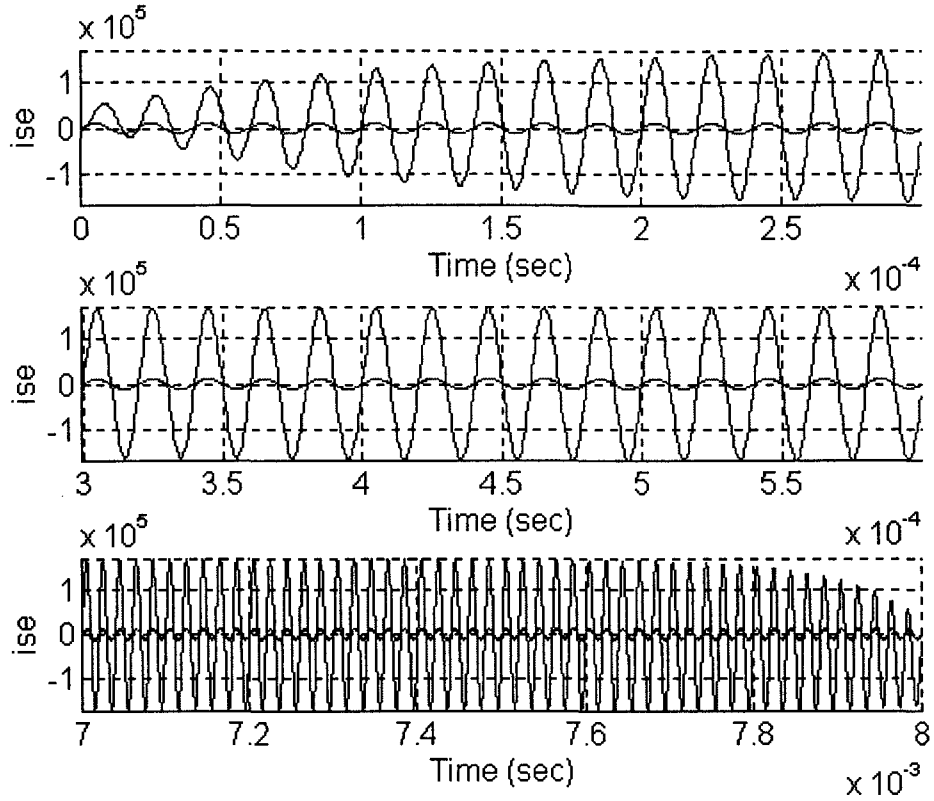


**Fig. 63 Comparison of $i_{SE}$ and Reference Signal w/ Q = 40 and R= 40**

```
vrms =

    9.2008e+006
    1.2548e+008
    9.2259e+006
```

The comparison of the system output and the reference signal is shown as Fig. 63, the system goes through a transient, then goes to steady state, where the rms value of the system output is *117,750 A*.

The waveform of the system input is a sinusoidal waveform with a steady state rms value of *5923.4 V*, which is also much larger than the desired system input range. The enormous system input results the other state variables exceed the desired value, the rms value for the Tank Voltage Vc is *27,608* V. The rms value of Induction Current $i_{LO}$ is *258.16* kA.

## 5.5 The System Response with Appropriate Weighing Matrices

By choosing different weighing matrices and the results are shown in Table 6.

**Table 6 Comparison of Different Weighing Matrix**

| | R =40 | | R = 1 | |
|---|---|---|---|---|
| | Q = 40 | Q = 1 | Q = 40 | Q = 1 |
| S(1,1)inf | 2.22E3 | 5.56E1 | 2.22E3 | 5.56E1 |
| S(1,2)inf | -1.70E3 | -4.26E1 | -1.70E3 | -4.26E1 |
| S(1,3)inf | 7.35E2 | 1.84E1 | 7.35E2 | 1.84E1 |
| S(2,1) | -1.70E3 | -4.26E1 | -1.70E3 | -4.26E1 |
| S(2,2) | 3.63E4 | 9.08E2 | 3.63E4 | 9.08E2 |
| S(2,3)inf | -7.93E2 | -1.98E1 | -7.93E2 | -1.98E1 |
| S(3,1)inf | 7.35E2 | 1.84E1 | 7.35E2 | 1.84E1 |
| S(3,2)inf | -7.93E2 | -1.98E1 | -7.93E2 | -1.98E1 |
| S(3,3)inf | 6.21E2 | 1.55E1 | 6.21E2 | 1.55E1 |
| | | | | |
| K(1,1)inf | 7.23E-7 | 7.23E-7 | 7.23E-7 | 7.23E-7 |
| K(1,2)inf | -6.33E-7 | -6.33E-7 | -6.33E-7 | -6.33E-7 |
| K(1,3)inf | 2.45E-7 | 2.45E-7 | 2.45E-7 | 2.45E-7 |
| | | | | |
| Kv(1,1)inf | 6.38E-4 | 1.04E-2 | 6.62E-4 | 2.55E-2 |
| Kv(1,2)inf | 3.72E-6 | 6.05E-5 | 3.86E-6 | 1.49E-4 |
| Kv(1,3)inf | 1.92E-6 | 3.13E-5 | 2.00E-6 | 7.69E-5 |
| | | | | |
| $i_{SE}$rms | 1.18E5 | 4.79E4 | 1.22E5 | 1.18E5 |
| Vc rms | 2.76E4 | 1.12E4 | 2.86E4 | 2.76E4 |
| $i_{LO}$ rms | 2.58E5 | 1.05E5 | 2.68E5 | 2.58E5 |
| u rms | 5.91E3 | 2.41E3 | 6.14E3 | 5.91E3 |

| | R =1 | R =0.01 | |
|---|---|---|---|
| | Q = 0.01 | Q = 1 | Q = 0.01 |
| S(1,1)inf | 5.56E-1 | 5.56E1 | 5.56E-1 |
| S(1,2)inf | -4.26E-1 | -4.26E1 | -4.26E-1 |
| S(1,3)inf | 1.84E-1 | 1.84E1 | 1.84E-1 |
| S(2,1) | -4.26E-1 | -4.26E1 | -4.26E-1 |
| S(2,2) | 9.08 | 9.08E2 | 9.08 |
| S(2,3)inf | -1.98E-1 | -1.98E1 | -1.98E-1 |
| S(3,1)inf | 1.84E-1 | 1.84E1 | 1.84E-1 |
| S(3,2)inf | -1.98E-1 | -1.98E1 | -1.98E-1 |
| S(3,3)inf | 1.55E-1 | 1.55E1 | 1.55E-1 |
| | | | |
| K(1,1)inf | 7.23E-7 | 7.23E-7 | 7.23E-7 |
| K(1,2)inf | -6.33E-7 | -6.33E-7 | -6.33E-7 |
| K(1,3)inf | 2.45E-7 | 2.45E-7 | 2.45E-7 |
| | | | |
| Kv(1,1)inf | 5.44E-1 | 2.65E-2 | 2.55 |
| Kv(1,2)inf | 3.17E-3 | 1.54E-4 | 1.49E-2 |
| Kv(1,3)inf | 1.64E-3 | 7.98E-5 | 7.69E-3 |
| | | | |

| | | | |
|---|---|---|---|
| ISErms | 2.51E4 | 1.22E5 | 1.18E5 |
| Vc rms | 5.88E3 | 2.86E4 | 2.76E4 |
| iLO rms | 5.50E4 | 2.68E5 | 2.58E5 |
| u rms | 1.26E3 | 6.14E3 | 5.91E3 |

From Table 6, the best weighing matrices should be $40 > R > 1$ and $1 > Q > 0.01$. If keep the weighing matrix R constant, the larger the Q the larger the system output is. On the contrary, if keep the weighing matrix Q constant, the larger the R the smaller the system output is. By trial and error, the best results take place when the weighing matrices are $Q = 0.538$, $R = 20$.

The steady state S matrix is:

```
Sinf =
    2.9997   -2.3011    0.9926
   -2.3011   49.0338   -1.0699
    0.9926   -1.0699    0.8379
```

The plot of the S matrix is shown in Fig. 64.

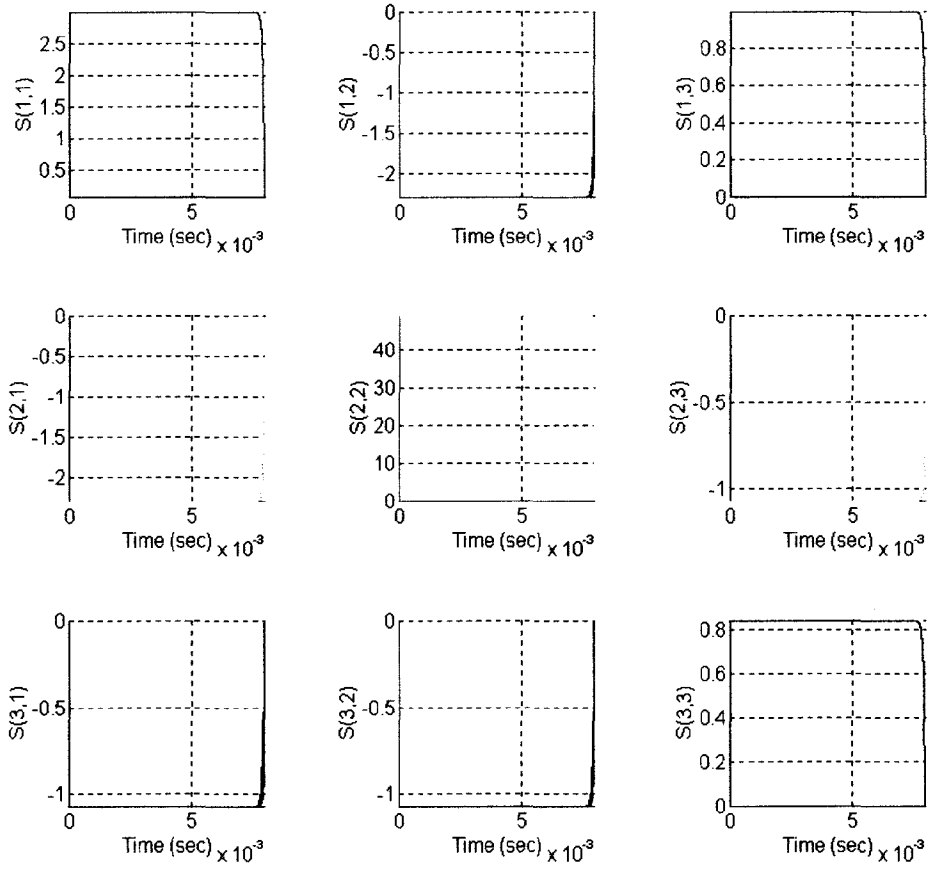


**Fig. 64 Plot of the S Matrix w/ Q = 0.538 and R=20**

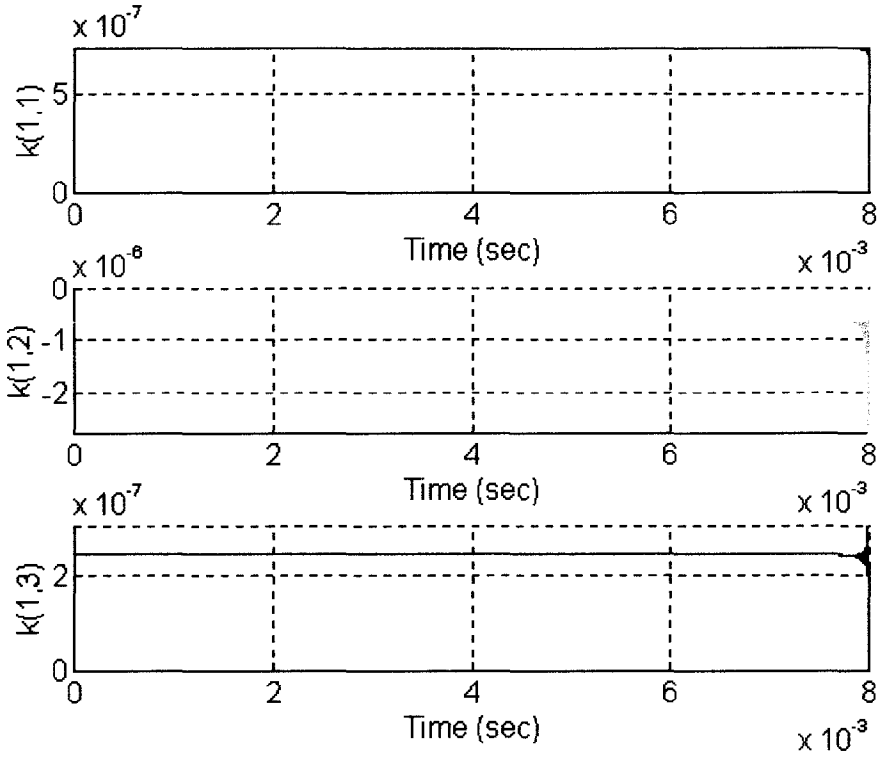


**Fig. 65 Plots of K Matrix**

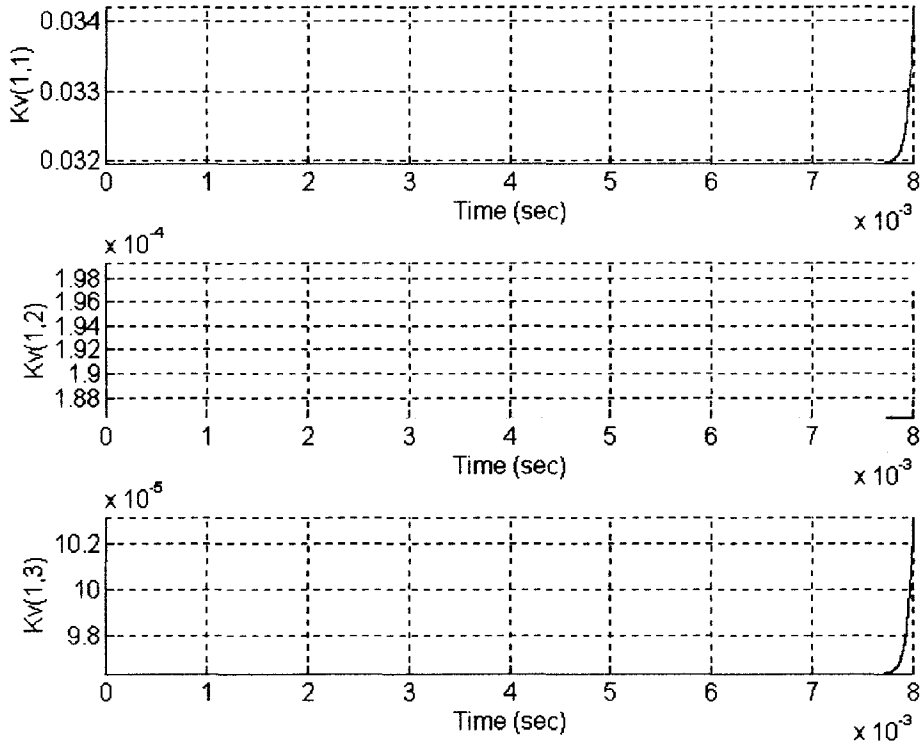


**Fig. 66 Plots of $K^v$ Matrix**

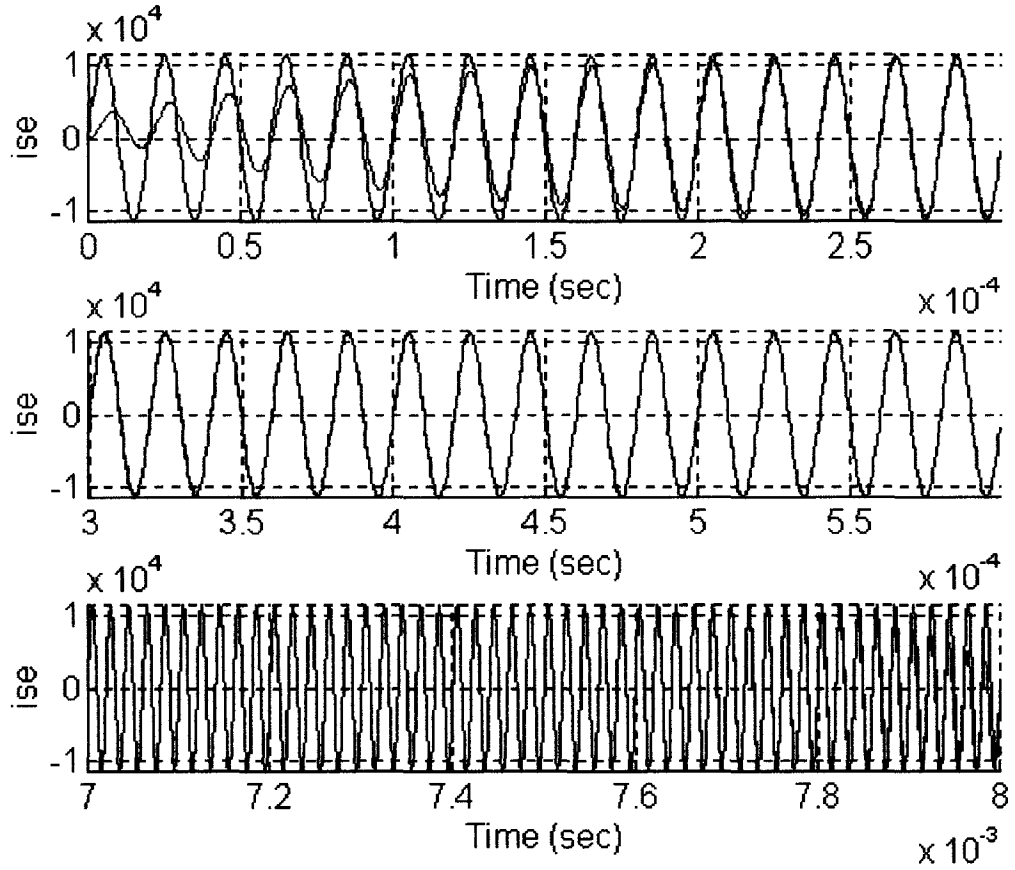


**Fig. 67 Comparison of the System Output $i_{SE}$ and the Reference Signal**

The steady state values of K and $K^v$ are

```
Kinf =          1.0e-006 *      0.7235   -0.6326    0.2445

Kvinf =                         0.0320    0.0002    0.0001
```

The Plots for the elements in K vector is shown in Fig. 65, the plots for the elements in $K^v$ vector are shown in Fig. 66.

The comparison of the system output and the reference signal is shown in Fig. 67, the system goes through a short transient, then goes to steady state, where the system output follows the reference signal exactly. The waveform after 7.6 sec will be ignored, since the system operating time is assumed to be infinity.

The waveforms for the tank voltage and induction coil current are shown in figures 68 and 69. The tank capacitor voltage and the induction coil current are both starting from zero, then go through a smooth transient then go to steady state. The rms value of the capacitor voltage and the induction coil current are at the desired level. Therefore, the weighing matrices are appropriate.

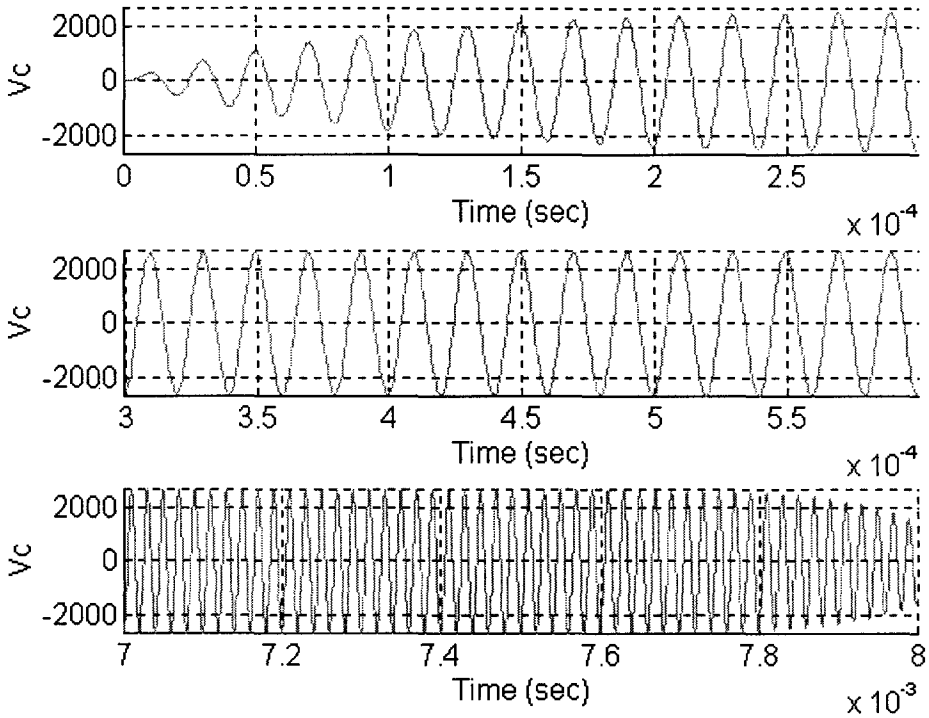


**Fig. 68 Waveform of the Tank Voltage Vc**

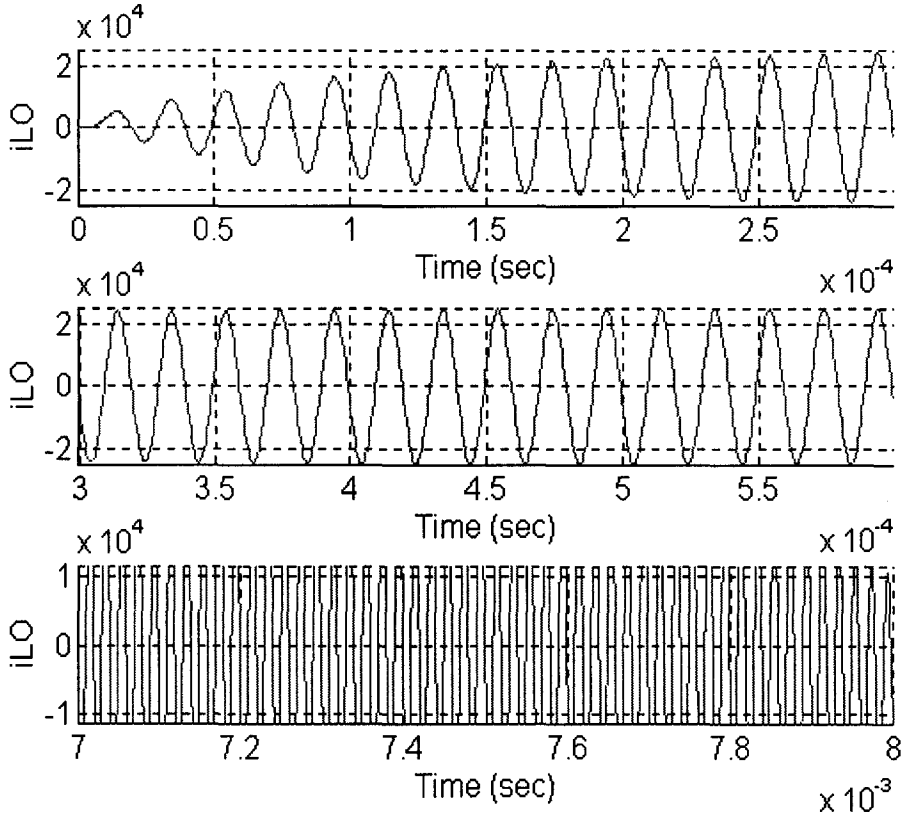


**Fig. 69 Waveform of the Induction Current $i_{LO}$**

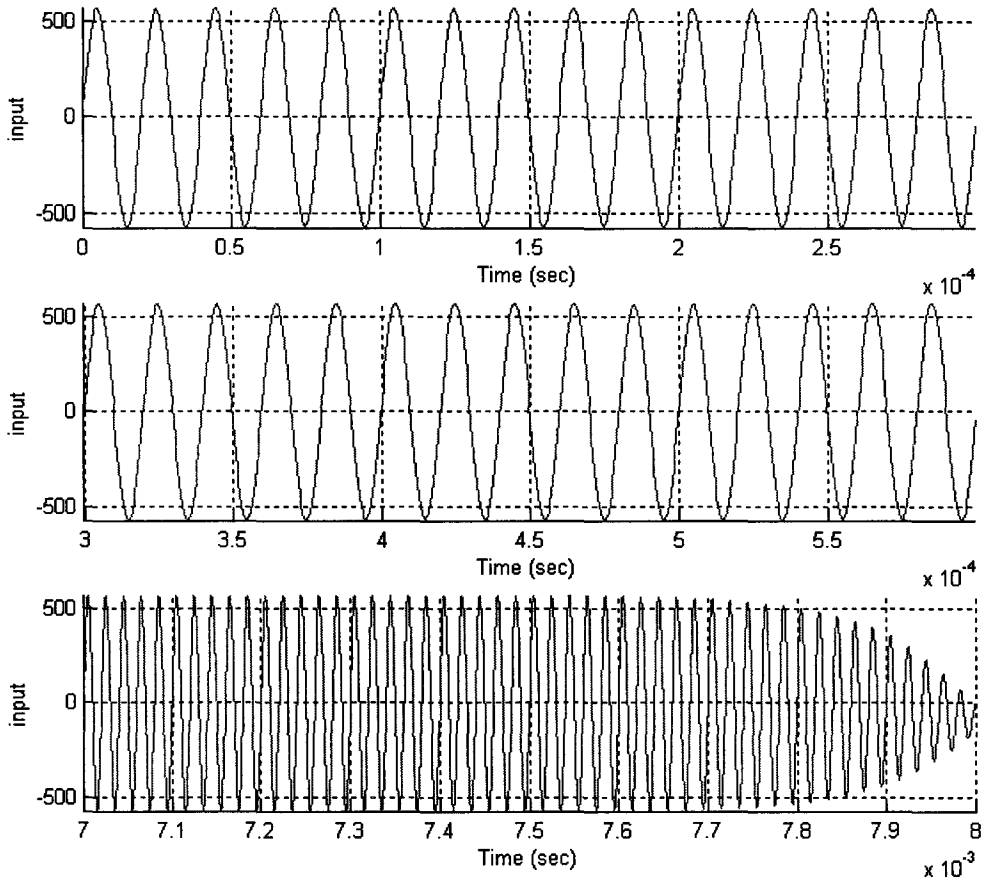


**Fig. 70 System Input Plot**

The input signal is a sinusoid waveform as shown in Fig. 70, with rms value of *400.9 V*.

The discrete time linear quadratic tracker has the following advantages compare to the continuous time LQT optimum controller:

- There is no spike during the starting period.
- The System Output follows the reference signal without any delay.
- The controller is easy to programming, not much memory will be used.
- There is no huge amount induction current feedback, current transformers and prime transformer can be used to get correct feedback information.

# Chapter 6

# Digital LQT Controller With New Reference Signal

In this chapter, a new reference signal has been construct to reduce the losses during the HFPS startup period, by changing the reference signal to a variable frequency and variable rms value signal, then simulate the closed loop system with the same LQT optimum controller in chapter 5.

## 6.1 The Structure of Digital LQT Controller Tracking System

### 6.1.1 Digital Optimum LQT Controller

From the block diagram for Discrete-Time LQT optimum controller, the open loop plant is the High Frequency Power Supply. Since the open loop plant is 3rd order system, the feed back analog state variables $\boldsymbol{x}(t)$ is a 3×1 vector. By using Zero-Order-Hold method, converts $\boldsymbol{x}(t)$ to $\boldsymbol{x}(k)$. The gain matrices are calculated and stored before the system operation.

### 6.1.2 Construct A New Reference Signal

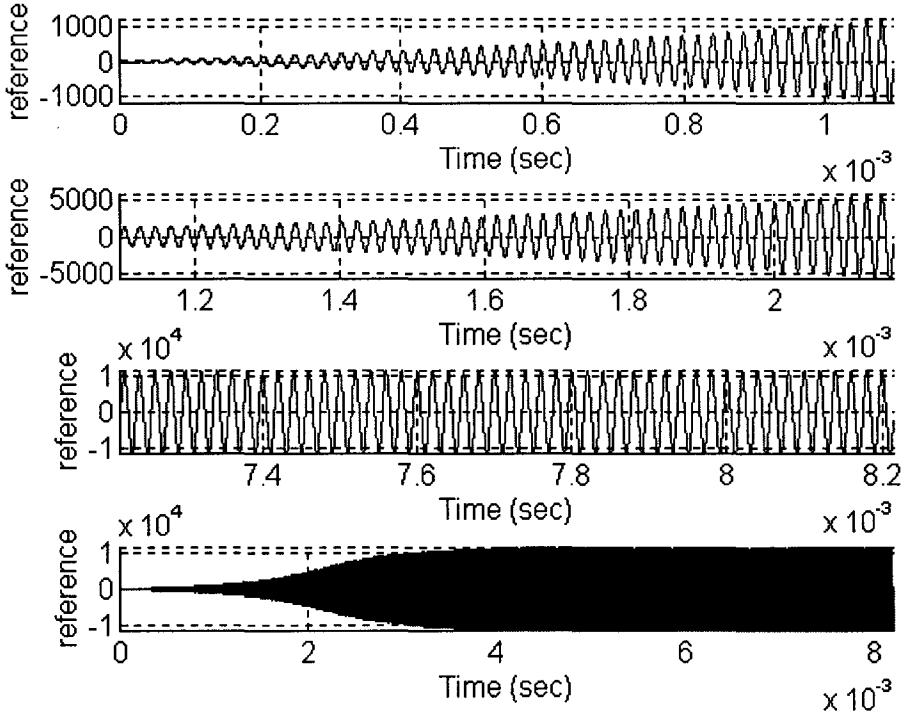


**Fig. 71 New Reference Signal**

Based on the study in section IV, it is more convenient to start the power supply from a lower frequency and lower power, then increase the frequency and the power to reach to the desired values. Such that the system loss is lower. The new reference signal is shown in Fig. 71.

The following reference signal has starting frequency of 45 kHz, and starting rms value of 10 A, after 200 periods, the reference becomes the steady state waveform, where the frequency is 50 kHz, and the rms value is 8000 A. The reason to do this is to keep the values of the system state variable small during the high frequency power supply startup period.

## 6.2 Building LQT Optimum Controller w/ New Reference Signal

By using the same method in Section V, set the weighing matrix to R = 20, Q = 0.05378, which results the rms value of the system output equal to the rms value of reference signal exactly.

The plot of the S matrix is shown in Fig. 72.

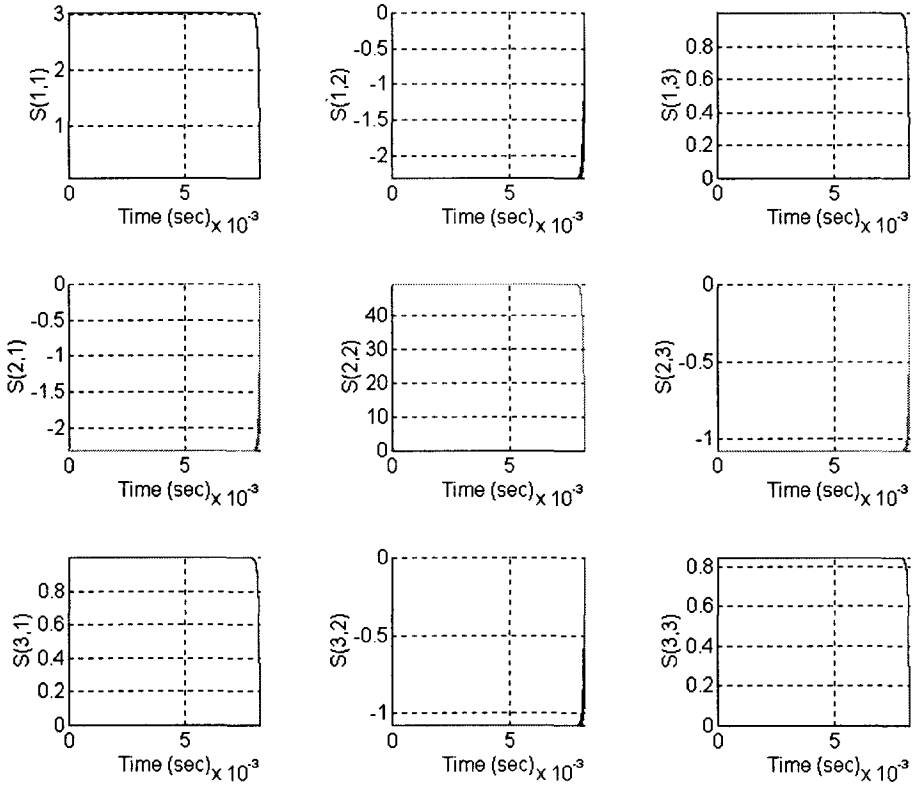


**Fig. 72 S Matrix Plot**

Since the system could be run to infinite time, so only the steady state S matrix is important. The steady state S matrix is

```
Sinf =

    3.0207   -2.3172    0.99950
   -2.3172    49.377   -1.0774
    0.9995   -1.0774    0.84380
```

By using above steady state S matrix, the feed forward and feed backward gains can be calculated as following,

```
Kinf =
              7.2347e-07 -6.3259e-07  2.4453e-07

Kvinf =
              3.1952e-02  1.8619e-04  9.6340e-05
```

The auxiliary matrix v plot is shown in Fig. 73, the waveforms of the elements in v vector are starting from the boundary condition, then smoothly go through a transient, then go to steady state eventually. Since the time is reversed, an initial value for the v vector must be calculated before operating the discrete time LQT optimum controller. Therefore, the initial value need to be calculated off line, then the value for the v vector can be either calculated off line or on line when the HFPS is operating.

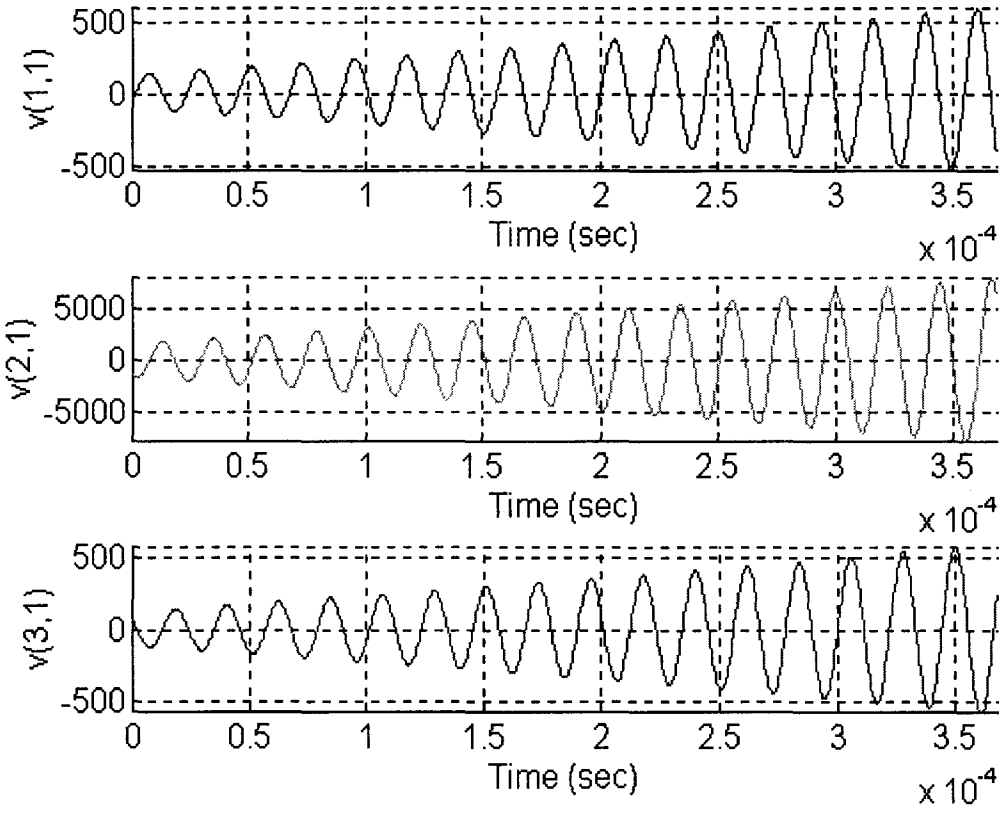


**Fig. 73 *v* Vector Plot (Time is Reversed)**

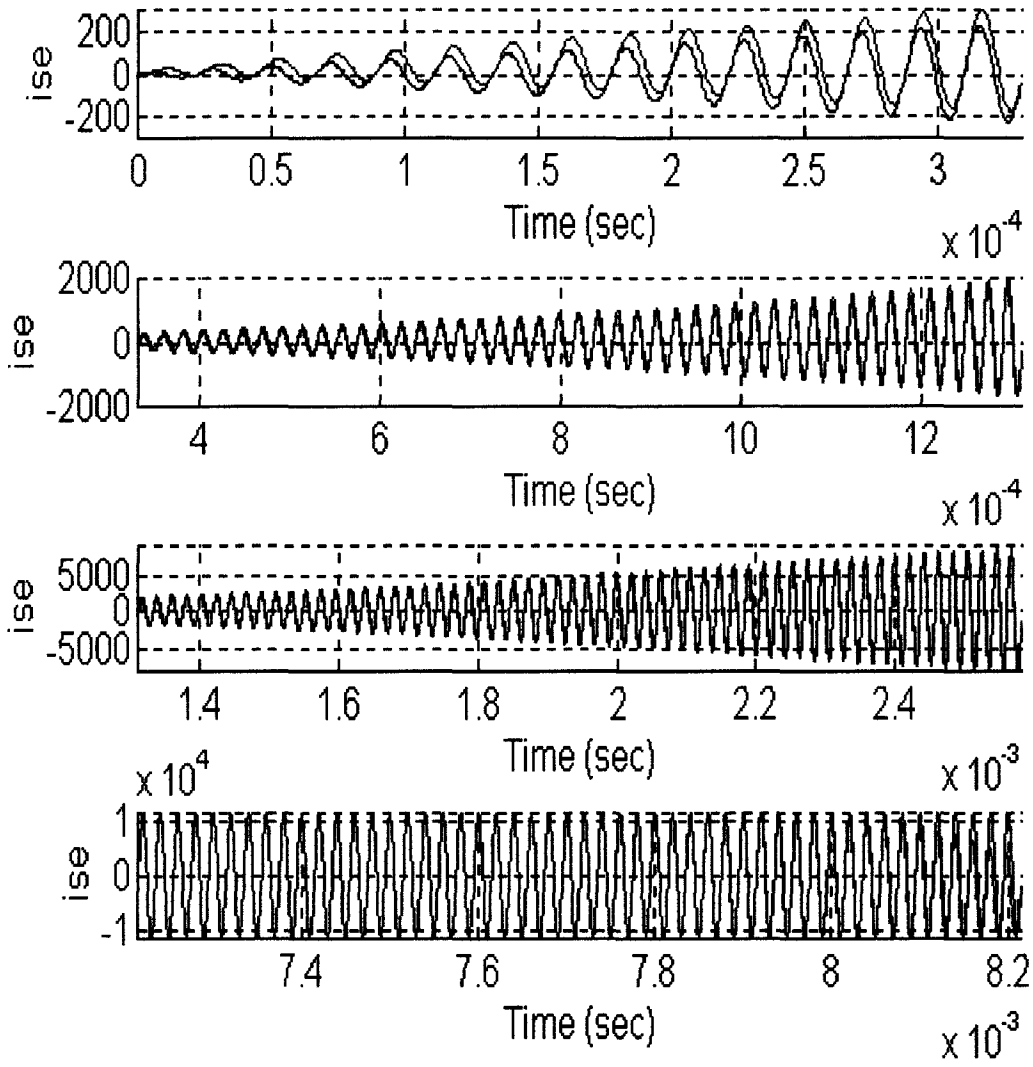


**Fig. 74 Comparison of the Actual System Output $i_{SE}$ and the Reference Signal $i_{SE}^*$**

The comparison of the system output and the reference signal is shown in Fig. 74, the system goes through a transient, then goes to steady state, where the value of the system output is match with the reference signal. From the plot, the error between the actual and the desired system output gets minimized when time continues.

The waveform of system input is shown in Fig. 75, the system input starts with a very small value then increases gradually until reaches to the steady state. No transient spike will harm the switching devices.

From Fig. 76, 77, the values of the other state variable at steady state are the desired values.

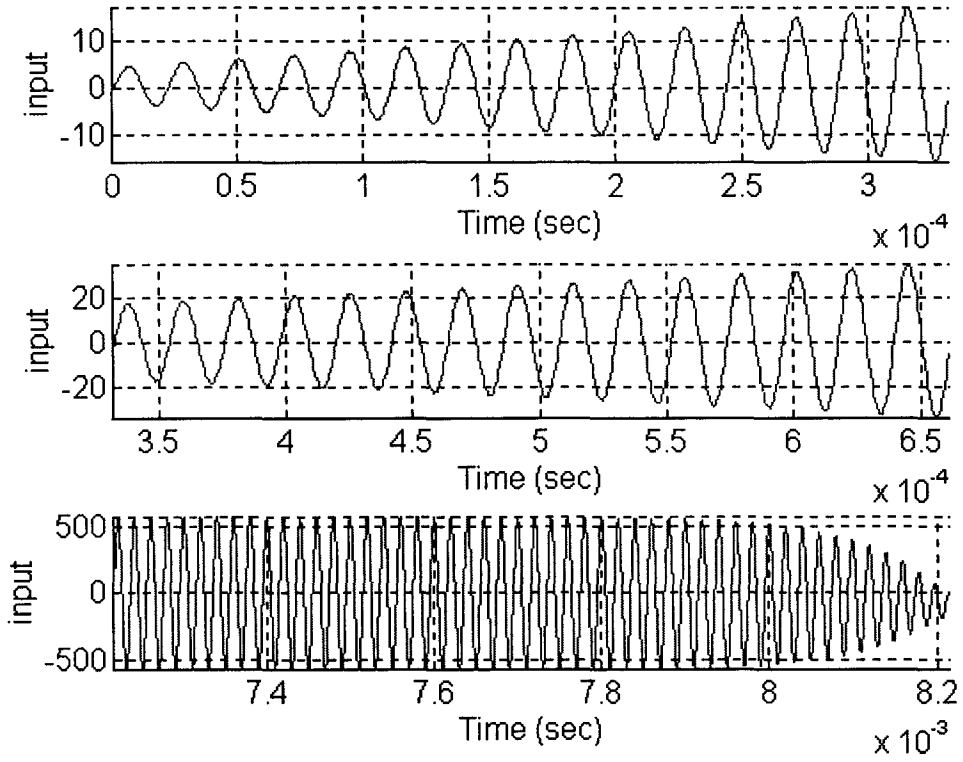


**Fig. 75 System Input Signal**

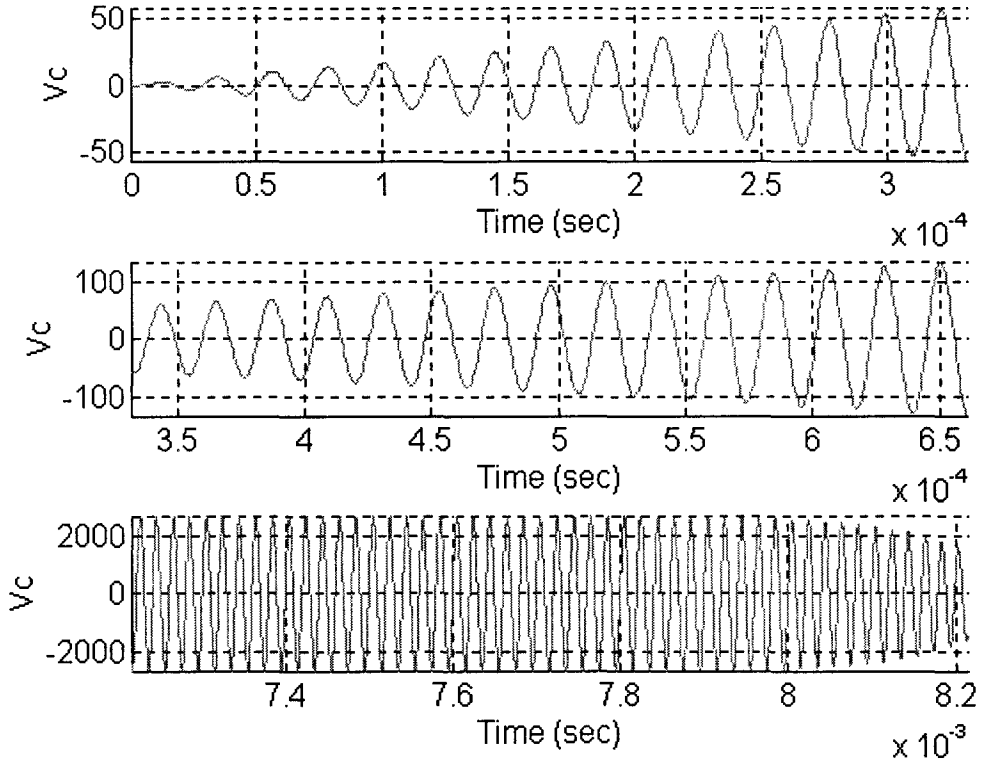


**Fig. 76 Waveform of the Tank Voltage Vc**

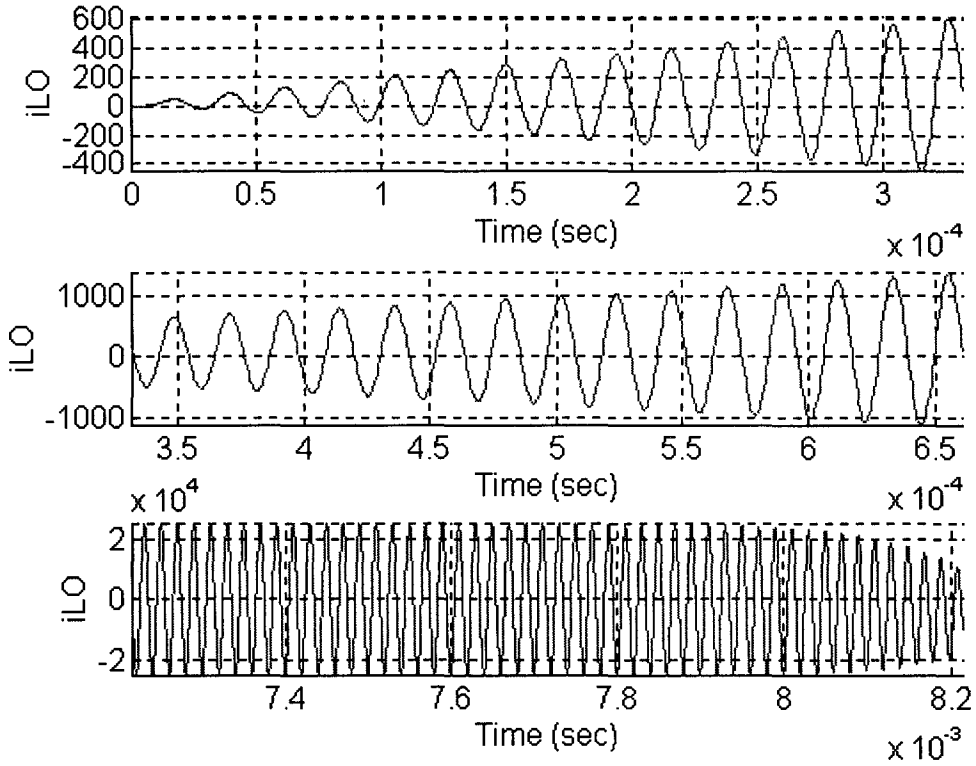


**Fig. 77 Waveform of the Induction Current $i_{LO}$**

## 6.3 Implementation of the LQT Controller

In the real world, the output of the inverter section is square wave, so the input to the load section cannot be a perfect sinusoid waveform. As shown in the system flow chart Fig. 2, the LQT controller only send the firing signals $\alpha$, $\phi$ and operating frequency to the High Frequency Power Supply. So the following requirements has to be made:

a. The firing angle $\alpha$ keeps at $0^o$, and changing the firing angle $\phi$, such that the actual rms value of the inverter section output (square waveform) equals to the optimum $i_{SE}$ (sinusoid waveform).

b. The switching frequency of the inverter section is equal to the optimum operation frequency.

In order to satisfy requirement a, the waveform of the firing angle $\phi$ vs. time is shown as Fig. 78. The firing angle $\phi$ is starting near $180^o$, where the rms value of $V_d$ is close to zero, i.e. there is almost no power output, so the power losses on the switching device is closing to zero. Then $\phi$ decreases, and eventually reaches the steady state value $6.2^o$, where the High Frequency Power Supply run into steady state.

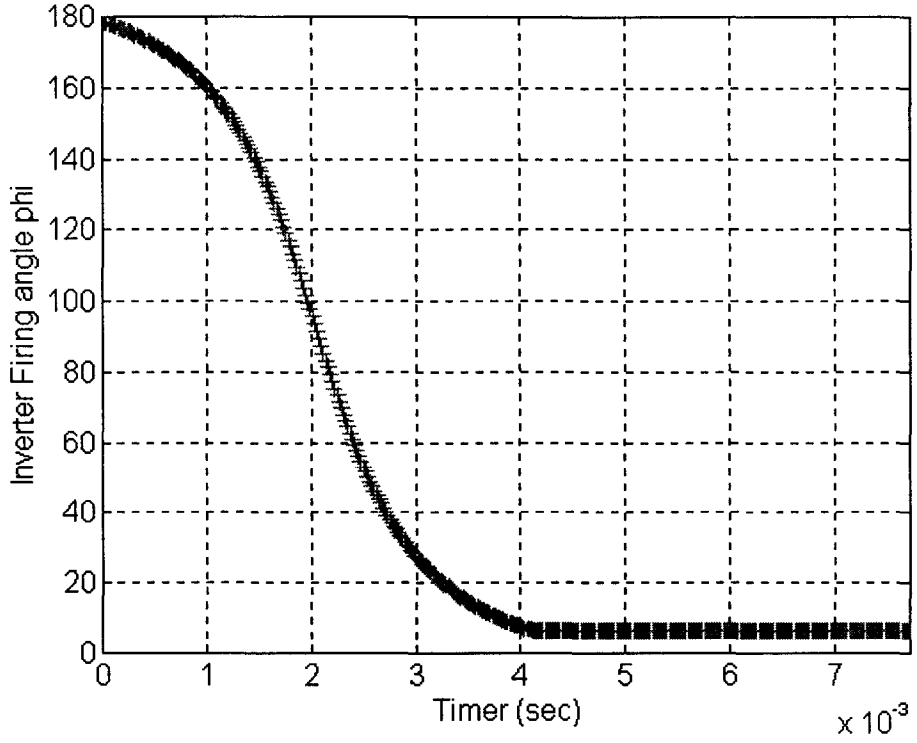


**Fig. 78 Firing Angle $\phi$ vs. Time**

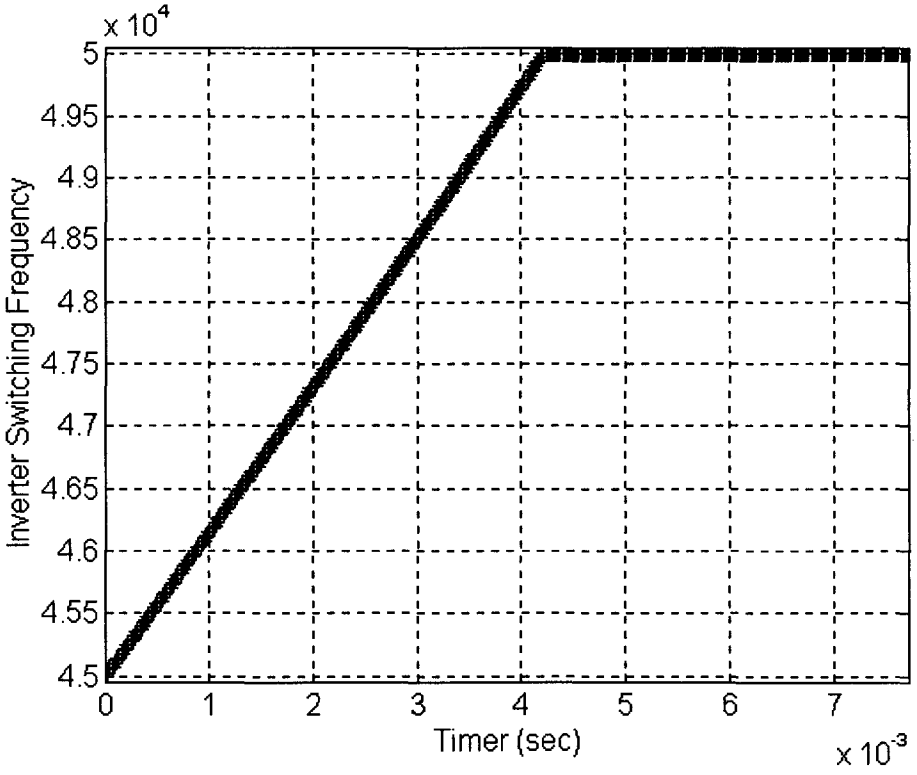


**Fig. 79 Switching Frequency vs. Time**

The switching frequency for the inverter section starts at 45 kHz, then increase linearly to 50 kHz, the waveform of switching frequency vs. time is shown as Fig. 79.

The reason to vary the switching frequency is to force the impedance of the load section higher at the power supply start up period, such that the power losses on the transmission line will be smaller.

The comparison of the optimum and actual waveform of Vd is shown as Fig. 80. Where the actual waveform of $V_d$ is square waveform, but the rms value for the actual and optimum $V_d$ is the same.

Since the sampling rate of this design is 40 points per period, when calculate the firing angle $\phi$, some very small rms value will be ignored. Therefore, there is a very short period in the beginning, there is no output from the inverter section.

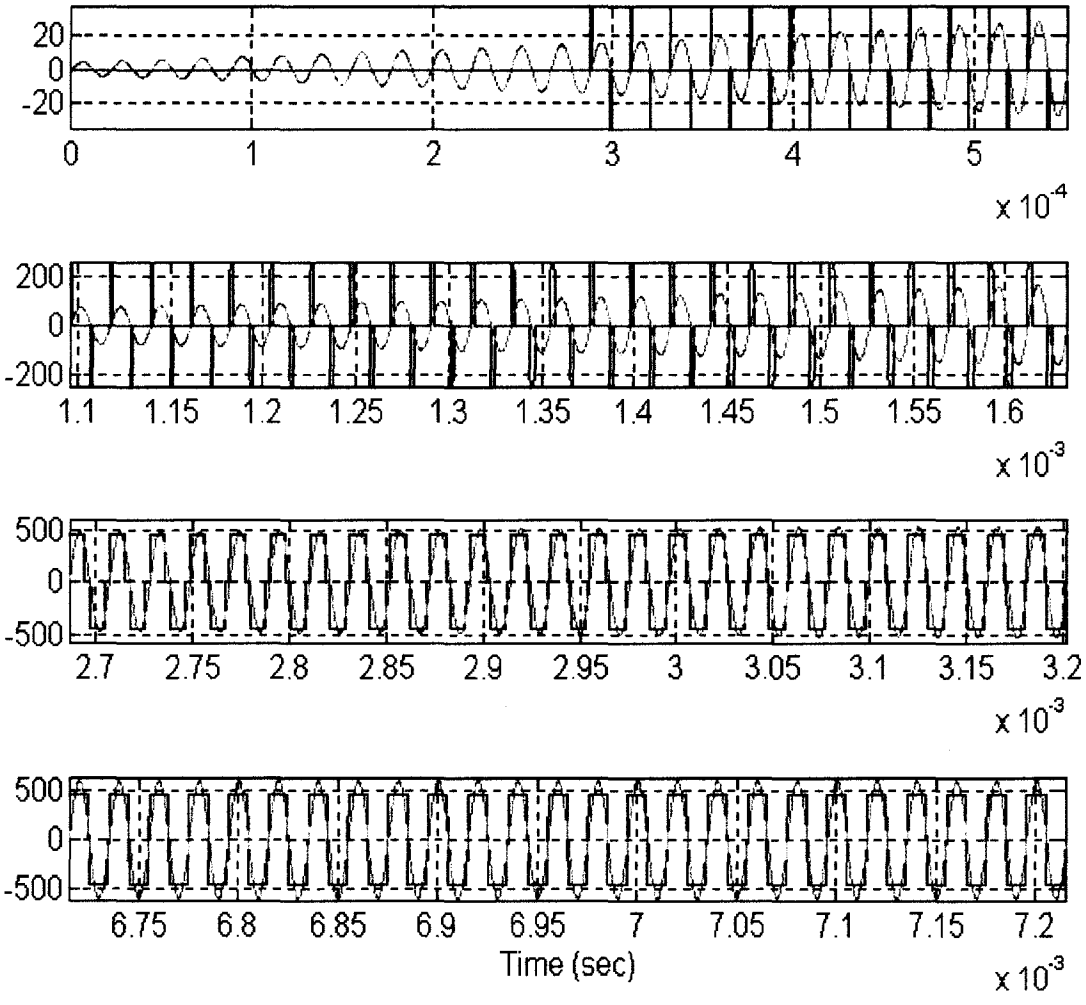


**Fig. 80 Comparison of Ideal and Actual Optimum Output Voltage of the Inverter Section**

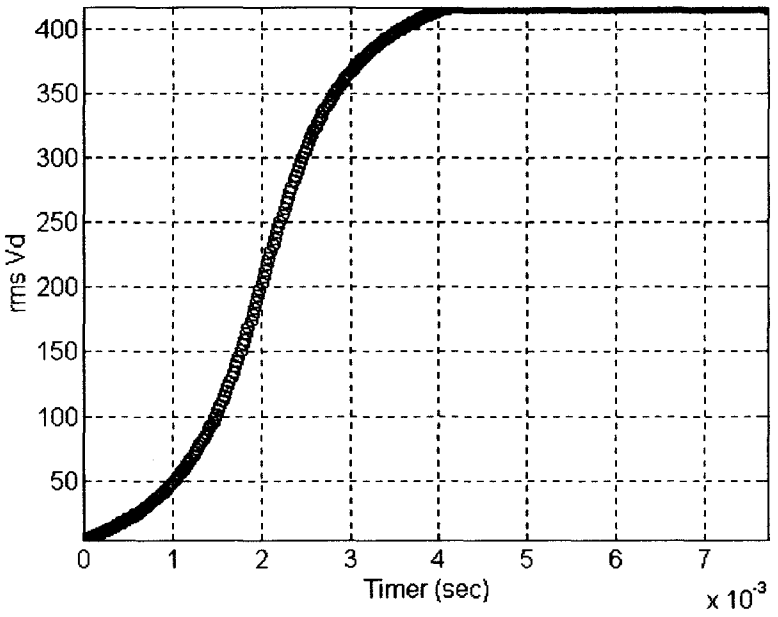


**Fig. 81 Plot for the rms Value of $V_d$ vs. time**

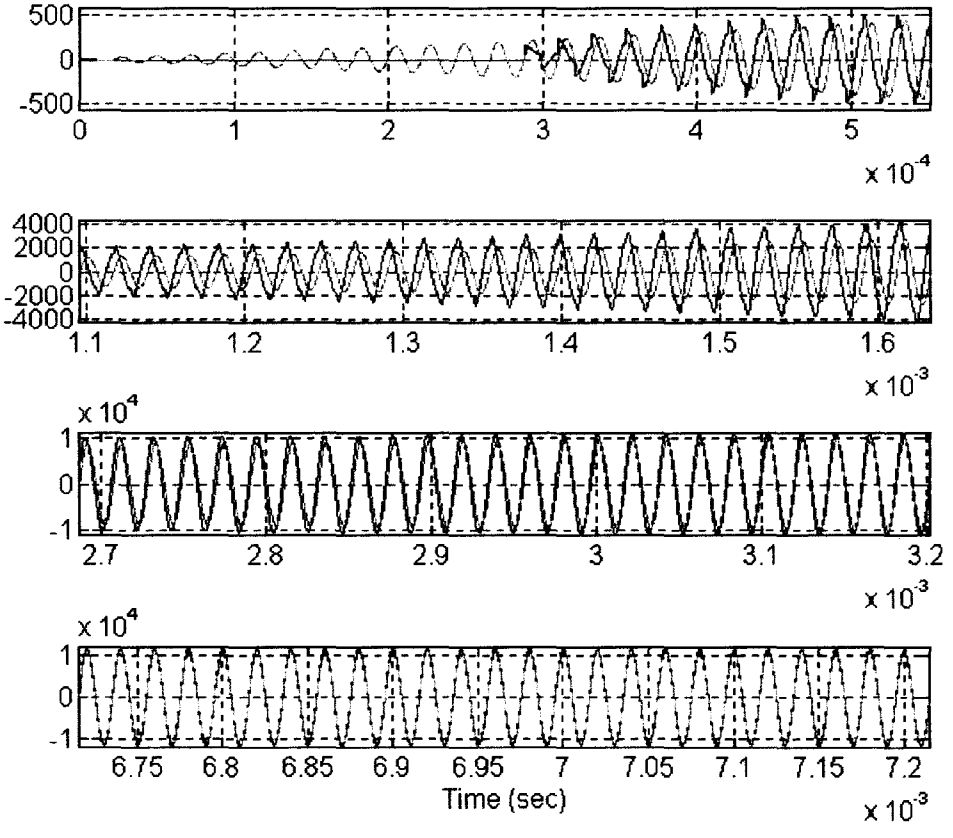


**Fig. 82 Comparison of Actual $i_{SE}$ (w/ Switching Device) and Reference Signal**

From Fig. 81, the rms value of $V_d$ starts from a very small value then increases gradually. At time 4 ms, $V_d$ reaches to the steady state. The pattern of rms value of Vd follows the reference input.

By using Matlab, simulate the discrete time system with actual inverter section output voltage $V_d$. The comparison of the actual and optimum load section input current $i_{SE}$ is shown in Fig. 82.

The actual waveform of $i_{SE}$ is not match the desired reference signal exactly at the beginning, because of the discontinuous square waveform of $V_d$, there is discontinuity in the $i_{SE}$ waveform. The value of the discontinuous current is very small, so that the switching devices can be protected.

After the transient period, the actual $i_{SE}$ waveform will match the reference signal when the system run into steady state. The system output is tracking the reference signal closely. Therefore, the optimum controller is working properly.

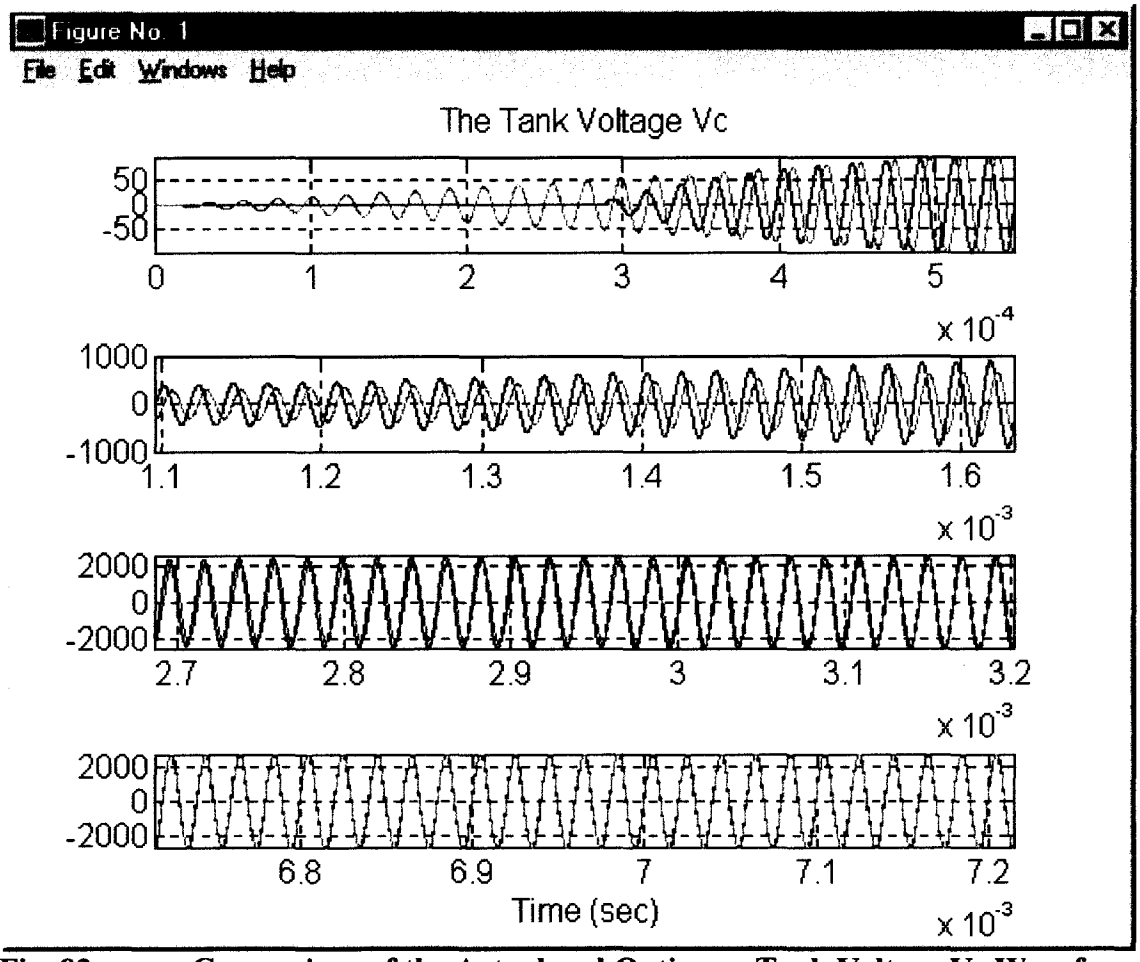


**Fig. 83 Comparison of the Actual and Optimum Tank Voltage Vc Waveform**

The comparison of the optimum and real waveforms with switching devices of the tank voltage ($V_c$) is shown in Fig. 83. Since tank voltage is across a large capacitance, Vc can not be discontinuous, therefore, there is no discontinuity in the waveform of Vc. The actual tank voltage does not follow the optimum tank voltage at the beginning because of the actual input Vd is zero. Before reaching the steady state, the actual Vc is lagging the optimum Vc. From the plot, when the power supply running into steady state, the actual Vc follows the optimum Vc exactly.

The rms value for Vc is increasing from a very small value to the steady state value, the waveform of Vc rms value vs. time is shown in Fig. 84. The plot of rms value of $i_{LO}$ vs. time is shown in Fig. 85, the shape of the plot is similar to the one of $V_C$ and $V_d$.

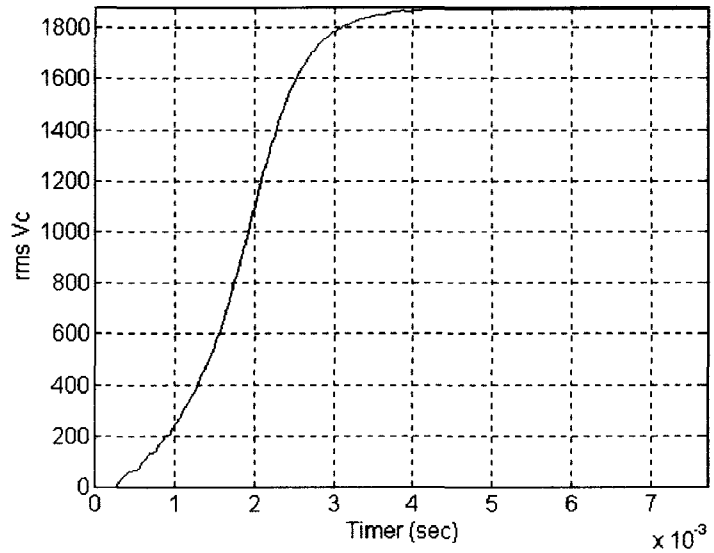


**Fig. 84 Rms Value of Vc vs. Time**

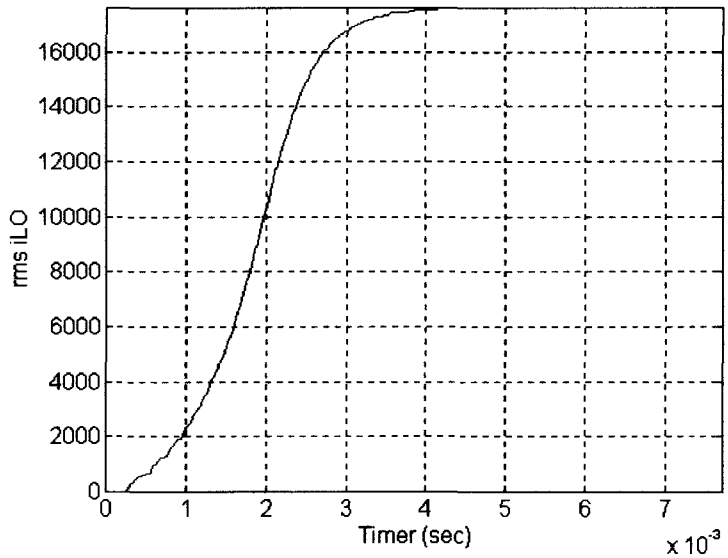


**Fig. 85 Rms Value of $i_{LO}$ vs. Time**

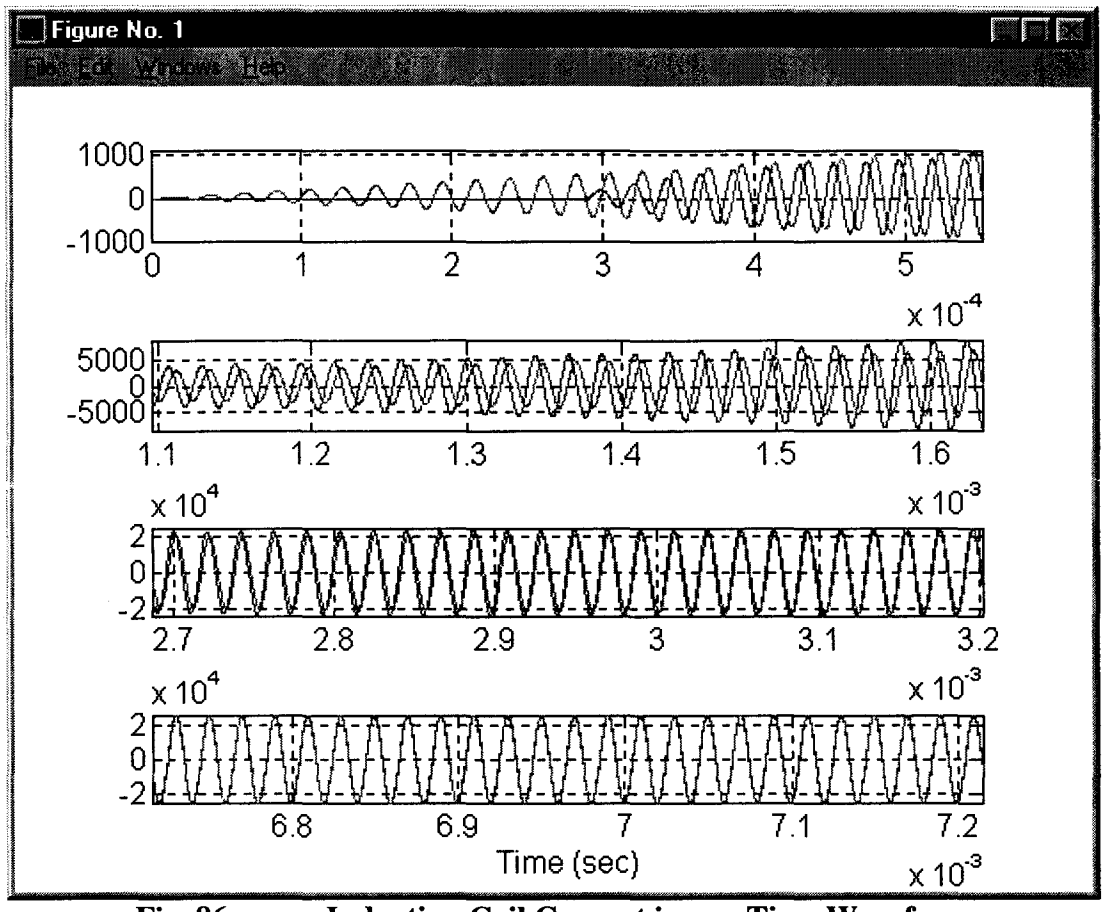


**Fig. 86 Induction Coil Current $i_{LO}$ vs. Time Waveform**

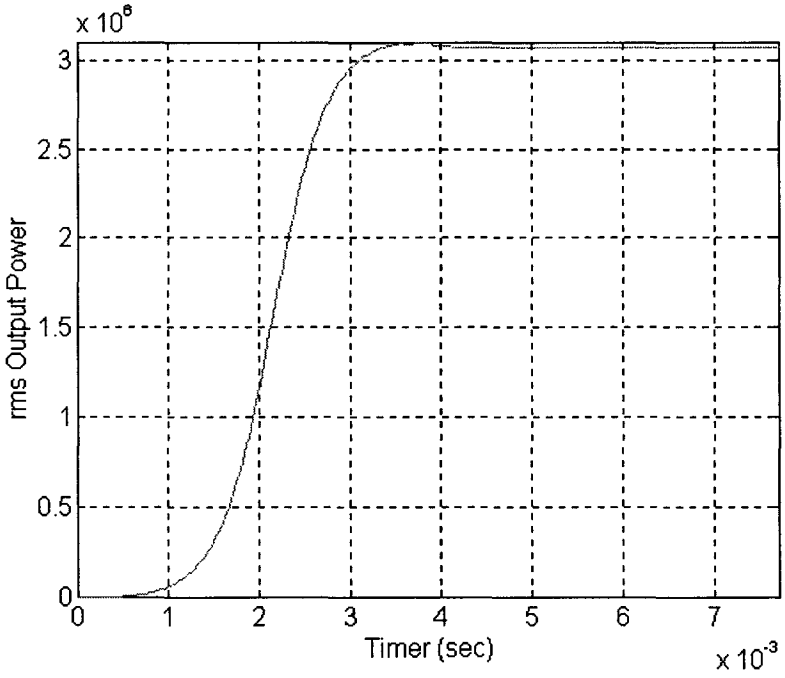


**Fig. 87 Actual Power Supply Power Output vs. Time**

The comparison of the linear optimum and the nonlinear real system waveforms for the induction coil current $i_{LO}$ is shown in Fig. 86. The power supply output kW vs. time plot is shown in Fig. 87. The kW output is starting from zero, then gradually increases to the steady state value.

This kW output curve can be changed by adjust the reference signal, i.e. the Power Supply output kW also follows the reference signal. After 4ms, the Power Supply has steady power output.

# Chapter 7

# High Frequency Power Supply Power Control

Due to different induction heating applications, the HFPS is required to run at different power level. This can be done easily by changing the reference signal accordingly. The simulation of different reference signals is shown in this Chapter.

## 7.1 HFPS Startup Power Control

Using the following equation for the reference signal

$$\begin{aligned} r_1(k) &= i_{SE}(k) \\ &= \sqrt{2} \cdot 6000 \cdot \sin(2 \cdot \pi \cdot 5E4 \cdot kh) \end{aligned} \tag{7-1-1}$$

The rms value of the reference is changed while the frequency keeps the same. The reference plot is shown in Fig. 88. The LQT controller generates appropriate firing angle $\phi$ for the inverter section accordingly, the plot of $\phi$ vs. time is shown in Fig. 89.

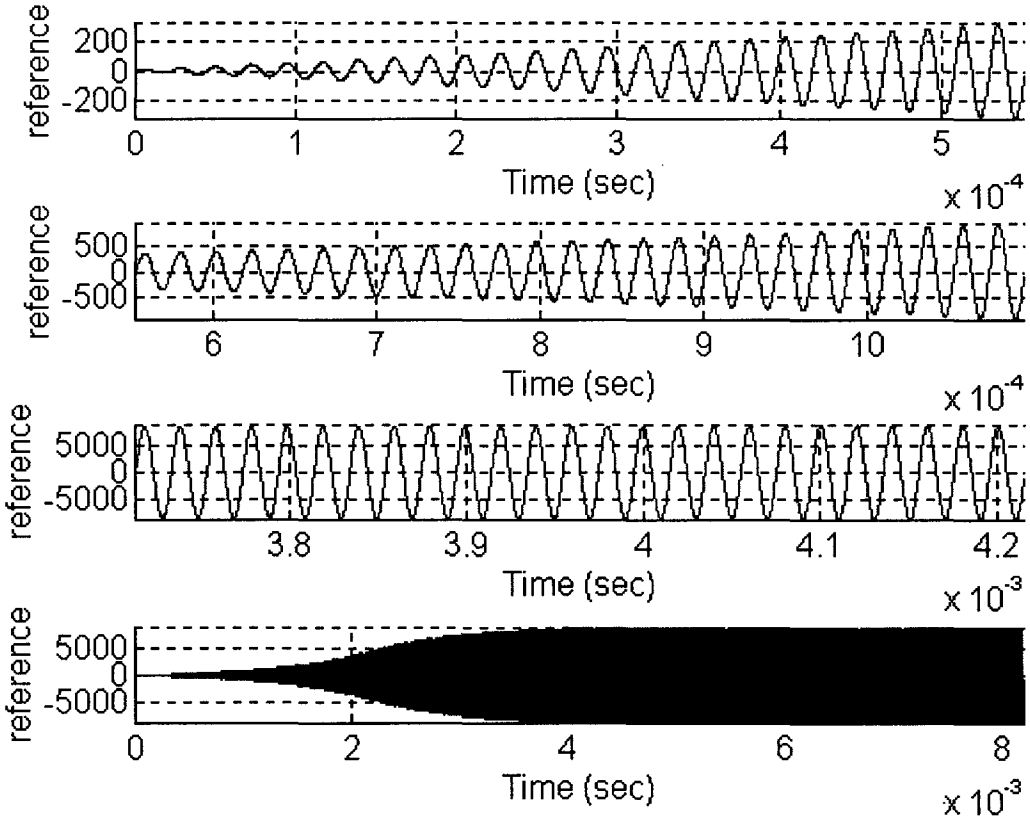


**Fig. 88 Desired Reference Signal Plot**

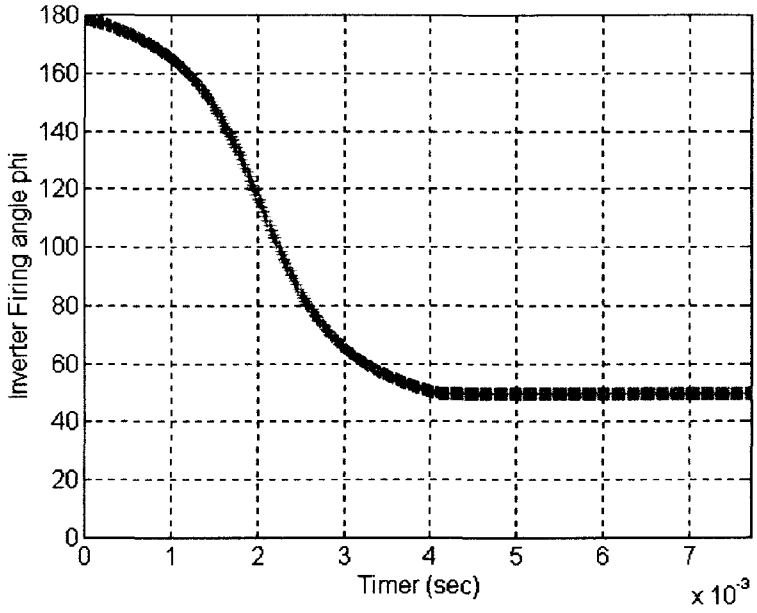


**Fig. 89 Plot of the Firing Angle $\phi$**

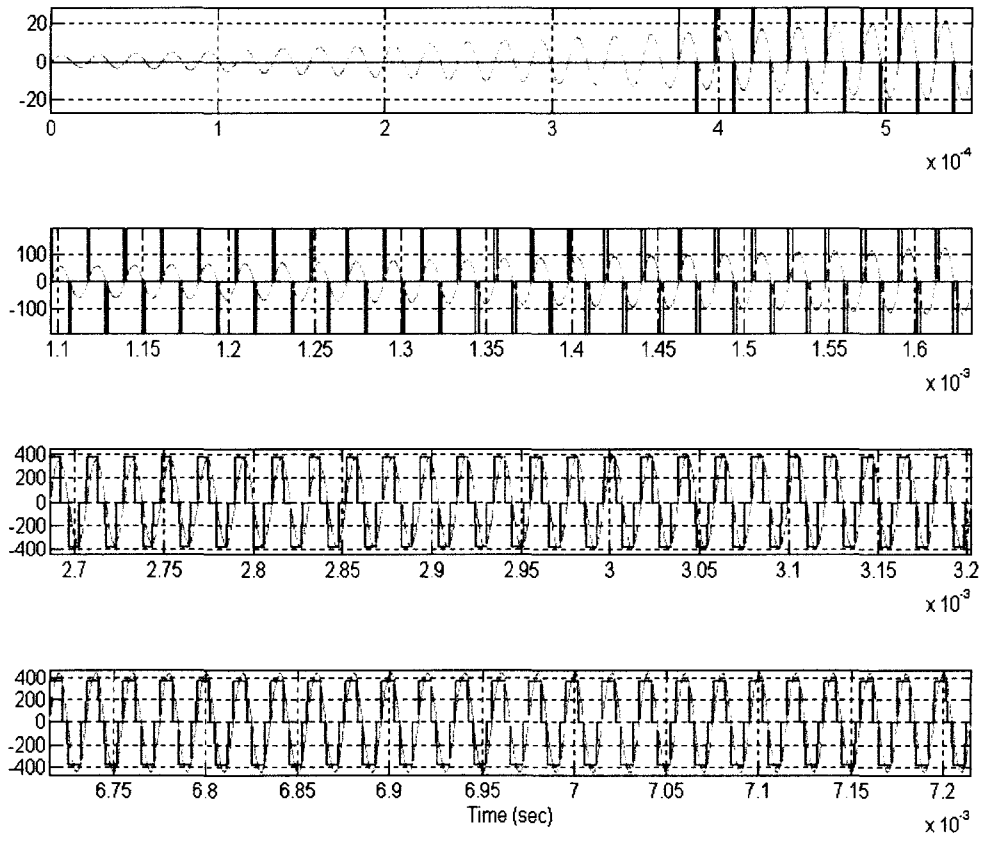


**Fig. 90 Comparison of the Ideal and Actual Optimum Load Section Input**

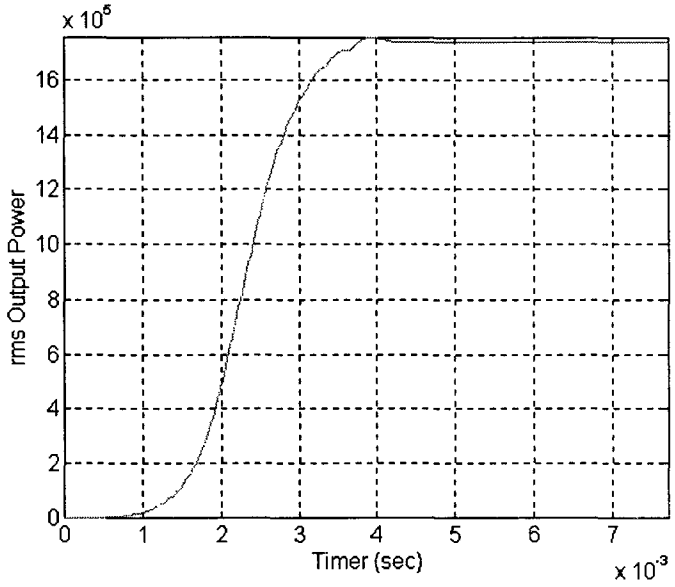


**Fig. 91 Plot of Power (*kW*) vs. Time**

The comparison of the ideal and actual inverter section output is shown in Fig. 90. The width of the square wave is increasing from zero, then keep a constant width when the system is in steady state. By using the new reference signal, from Fig. 91, the steady state output power level is lower.

## 7.2 HFPS Process Power Control

When the Power Supply running at steady state, in order to lower the kW level, the only operation for the LQT controller is to change the reference signal.

The rms value of the new desired system output is smaller, but the frequency is the same. From Fig. 92, the rms value of the reference signal is changed, while the frequency keeps the same.

Based on the change of the reference signal, the LQT controller changes the firing angle $\phi$ for the inverter section, accordingly. In this case, the firing angle increases and the rms value of the inverter section output voltage and the system output power decreases. The plot for the firing angle $\phi$ is shown in Fig. 93.

The value of $\phi$ continues to increase, therefore, the rms value of the input ($V_d$) is decreasing, and the power supply output kW level is decreasing too. The transition of the firing angle is smooth, therefore, the power transition will be smooth too, and no spike will be generated during the output power level changing. From Fig. 94, after 4ms the width of the square wave $V_d$ is decreasing. When the reference signal changes, the rms value of the inverter section Output $V_d$ changes accordingly. From Fig. 95, the kW adjustment will be very smooth and easy to implement.

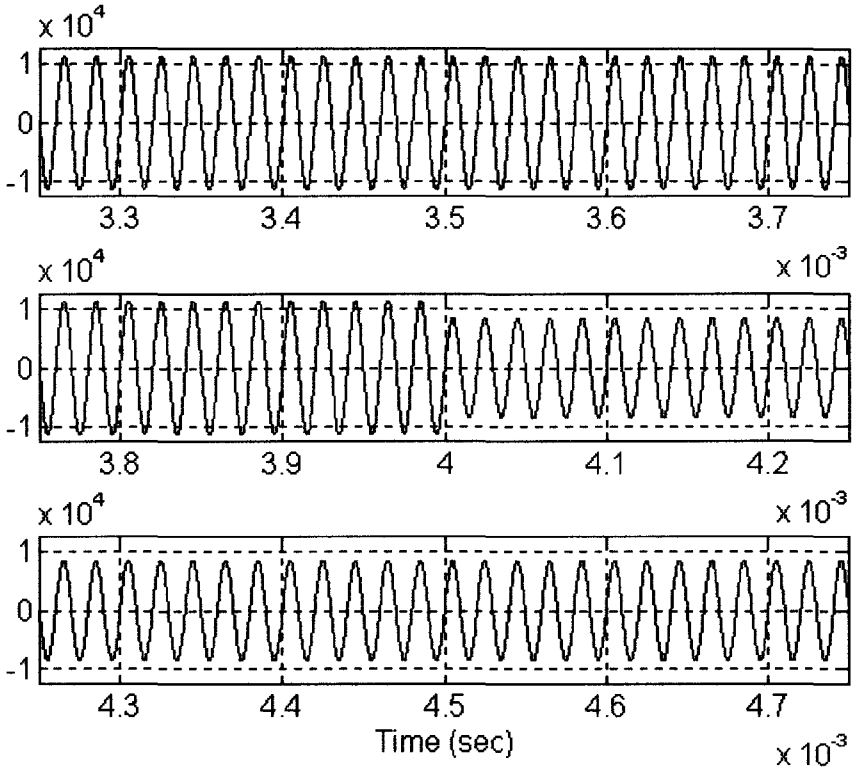


**Fig. 92 Reference Signal**

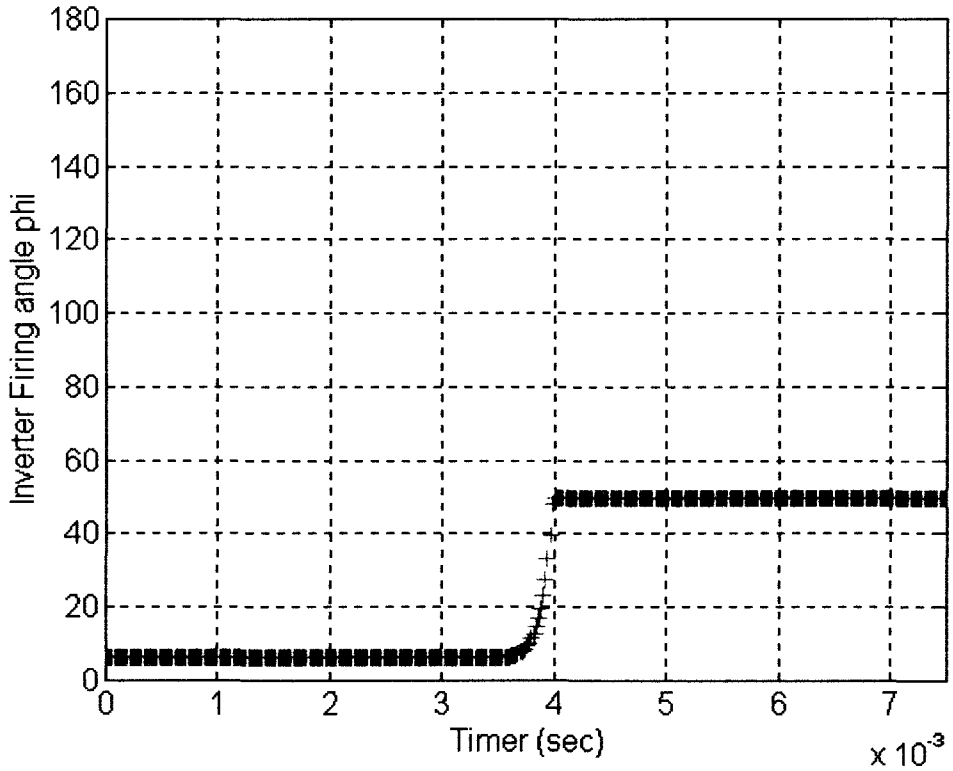


**Fig. 93 Firing Angle for the Inverter Section $\phi$**

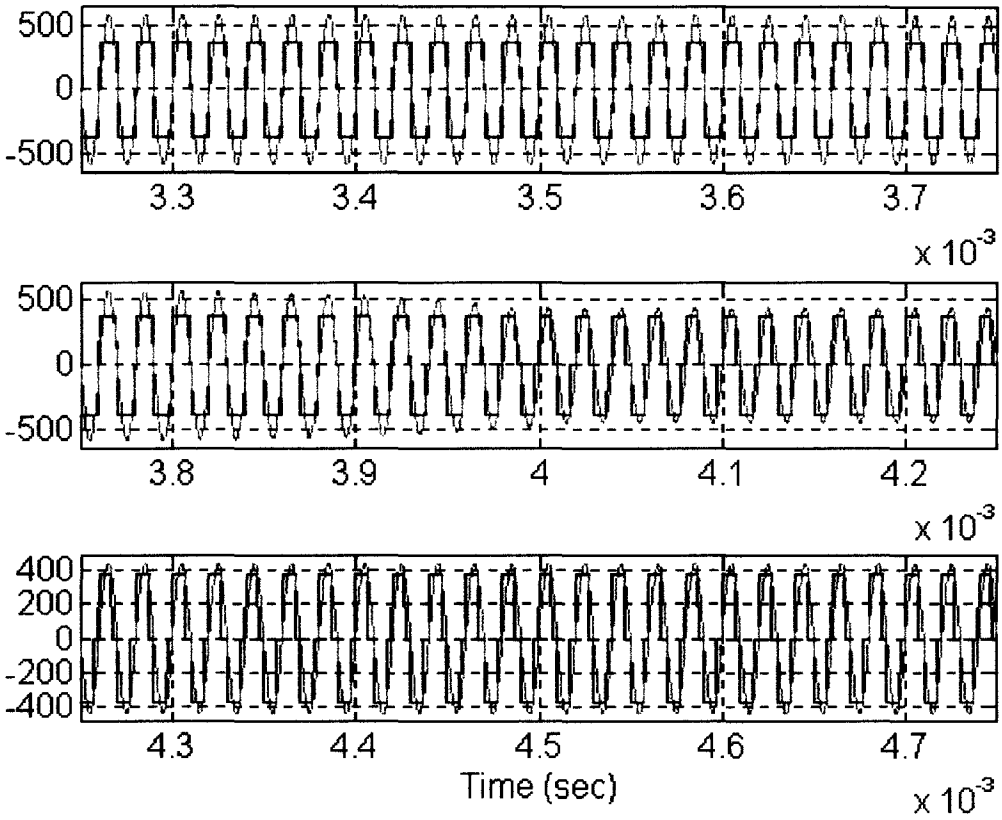


**Fig. 94 Comparison the Ideal and Actual Load Section Input**

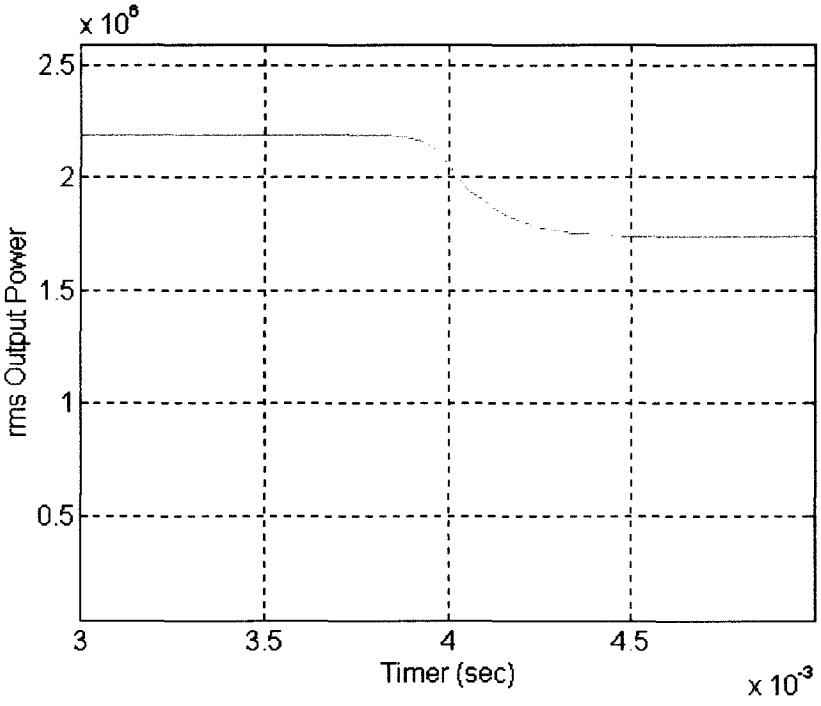


**Fig. 95 Power Level vs. Time Plot**

# Chapter 8

## Summary and Conclusion

An optimal controller design for a HFPS system was presented in this thesis. By using LQT method, the system performance has been optimized. The LQT Controller generates optimal firing angles and switching frequency for the HFPS, that reduces the system loss, eliminates the harmful harmonics, and makes a uniform depth of penetration on the induction load. In the discrete time domain, the desired reference signal can be easily to construct with high accuracy. By changing the reference signal, the HFPS power level and operating frequency can be easily controlled. The LQT controller has the advantage of the closed loop system, it is stable, accurate, and easy to implement. The rms values of the system state variables have been compared with a real system, and the results are matched.

The rms values of the system state variables have been compared with ©**Ajax Magnethermic Corp.** ©PACER HF 2700kW, 50kHz commercial Power Supply, the result are close to the practical result as shown in Table 7.

**Table 7 Comparison of the Value of the State Variables**

| | **Linear Model (w/o Switching Devices)** | **Non-Linear Model (w/ Switching Devices)** | **Real Power Supply** |
|---|---|---|---|
| **$i_{SE}$ (kA)** | 8.00 | 8.00 | 8.10 |
| **$V_C$ (V)** | 2120 | 2120 | 2164 |
| **$i_{LO}$ (kA)** | 17.7 | 17.7 | 16.8 |
| **Frequency (kHz)** | 50.0 | 50.0 | 51.1 |

# References

[1] N. Mohan, T. M. Undeland, W. P. Robbins, "*Power Electronics*", 2nd edition, ISBN 0-471-58408-8, 1995.

[2] K. Astrom, B. Wittenmark, "*Computer Controlled Systems Theory and Design*", 3rd edition, Prentice Hall, Saddle River, NJ. ISBN 0-13-314899-8, 1997.

[3] C. A. Tudbury, "*Basics of Induction Heating*", Library of Congress Cat. Number 60-8958 May, 1960.

[4] B. D. Anderson, J.B. Moore, "Optimum Control, Linear Quadratic Methods", Prentice Hall, Englewood Cliffs, NJ 07632, ISBN 0-13-638560-5, 1990.

[5] C. L. Phillips, R. D. Harbor, "Feedback Control Systems", Prentice Hall, Englewood Cliffs, NJ 07632, ISBN 0-13-313917-4, 1988.

[6] F. L. Lewis, V. L. Syrmos, "Optimal Control", 2nd edition, John Wiley & Sons, INC, ISBN 0-471-03378-2, 1995.

The comparison of the optimum and real waveforms with switching devices of the tank voltage ($V_c$) is shown in Fig. 83. Since tank voltage is across a large capacitance, Vc can not be discontinuous, therefore, there is no discontinuity in the waveform of Vc. The actual tank voltage does not follow the optimum tank voltage at the beginning because of the actual input Vd is zero. Before reaching the steady state, the actual Vc is lagging the optimum Vc. From the plot, when the power supply running into steady state, the actual Vc follows the optimum Vc exactly.

The rms value for Vc is increasing from a very small value to the steady state value, the waveform of Vc rms value vs. time is shown in Fig. 84. The plot of rms value of $i_{LO}$ vs. time is shown in Fig. 85, the shape of the plot is similar to the one of $V_C$ and $V_d$.

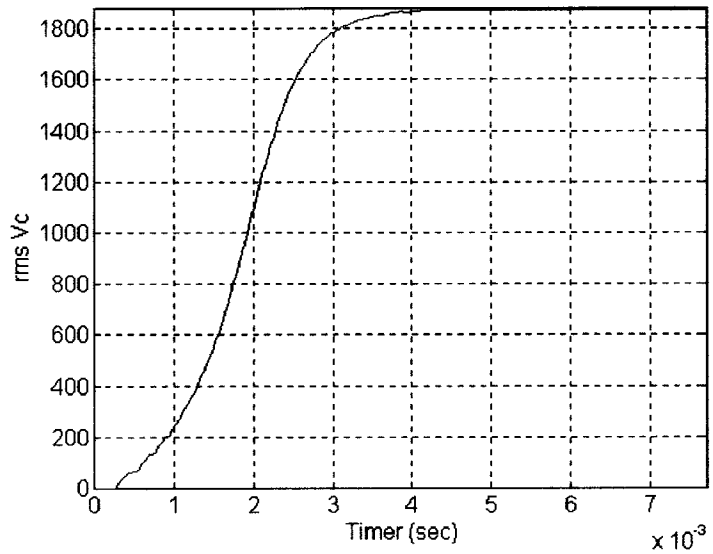


**Fig. 84 Rms Value of Vc vs. Time**

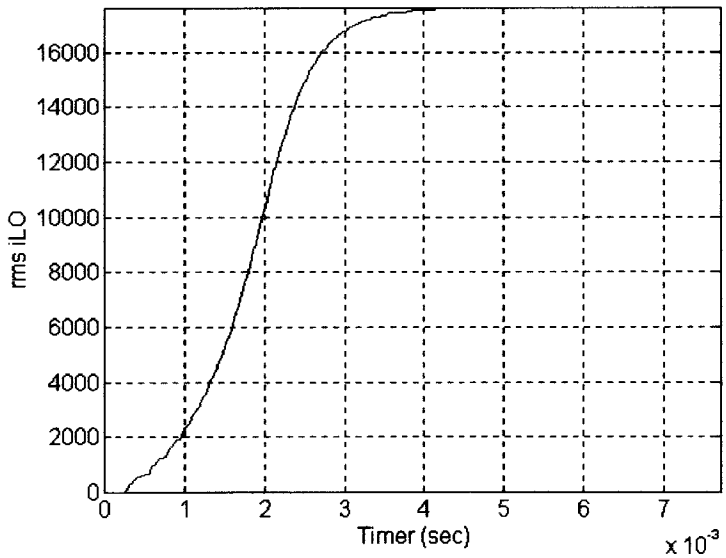


**Fig. 85 Rms Value of $i_{LO}$ vs. Time**

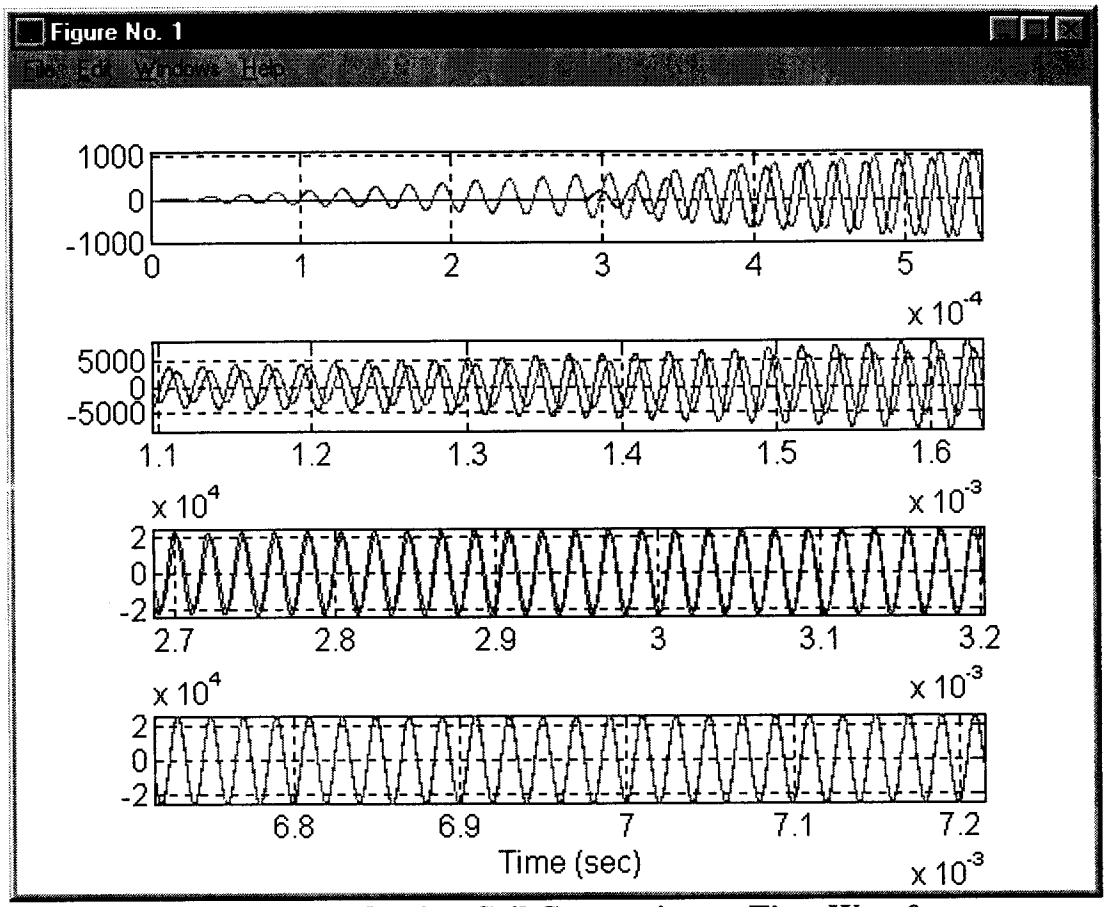


**Fig. 86 Induction Coil Current $i_{LO}$ vs. Time Waveform**

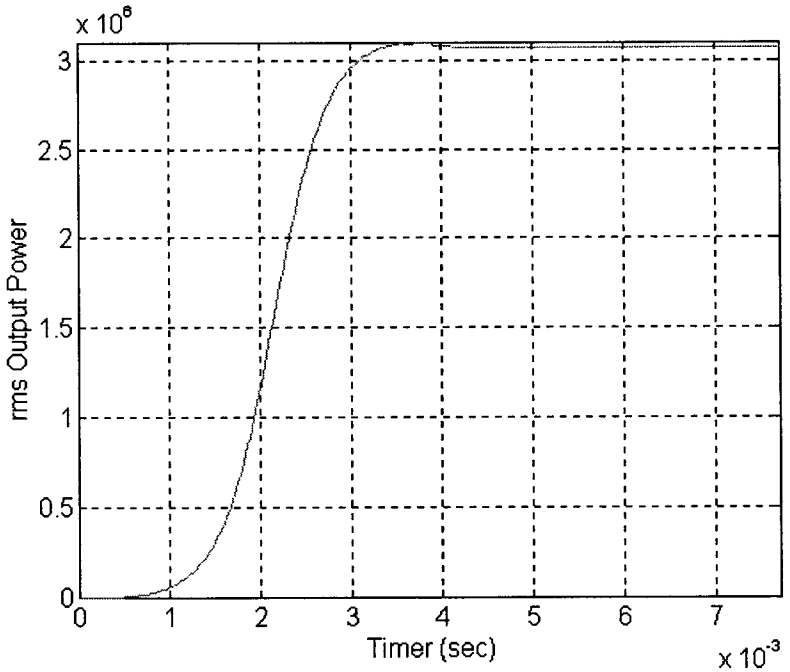


**Fig. 87 Actual Power Supply Power Output vs. Time**

The comparison of the linear optimum and the nonlinear real system waveforms for the induction coil current $i_{LO}$ is shown in Fig. 86. The power supply output kW vs. time plot is shown in Fig. 87. The kW output is starting from zero, then gradually increases to the steady state value.

This kW output curve can be changed by adjust the reference signal, i.e. the Power Supply output kW also follows the reference signal. After 4ms, the Power Supply has steady power output.

# Chapter 7

# High Frequency Power Supply Power Control

Due to different induction heating applications, the HFPS is required to run at different power level. This can be done easily by changing the reference signal accordingly. The simulation of different reference signals is shown in this Chapter.

## 7.1 HFPS Startup Power Control

Using the following equation for the reference signal

$$\begin{aligned} r_1(k) &= i_{SE}(k) \\ &= \sqrt{2} \cdot 6000 \cdot \sin(2 \cdot \pi \cdot 5E4 \cdot kh) \end{aligned} \tag{7-1-1}$$

The rms value of the reference is changed while the frequency keeps the same. The reference plot is shown in Fig. 88. The LQT controller generates appropriate firing angle $\phi$ for the inverter section accordingly, the plot of $\phi$ vs. time is shown in Fig. 89.

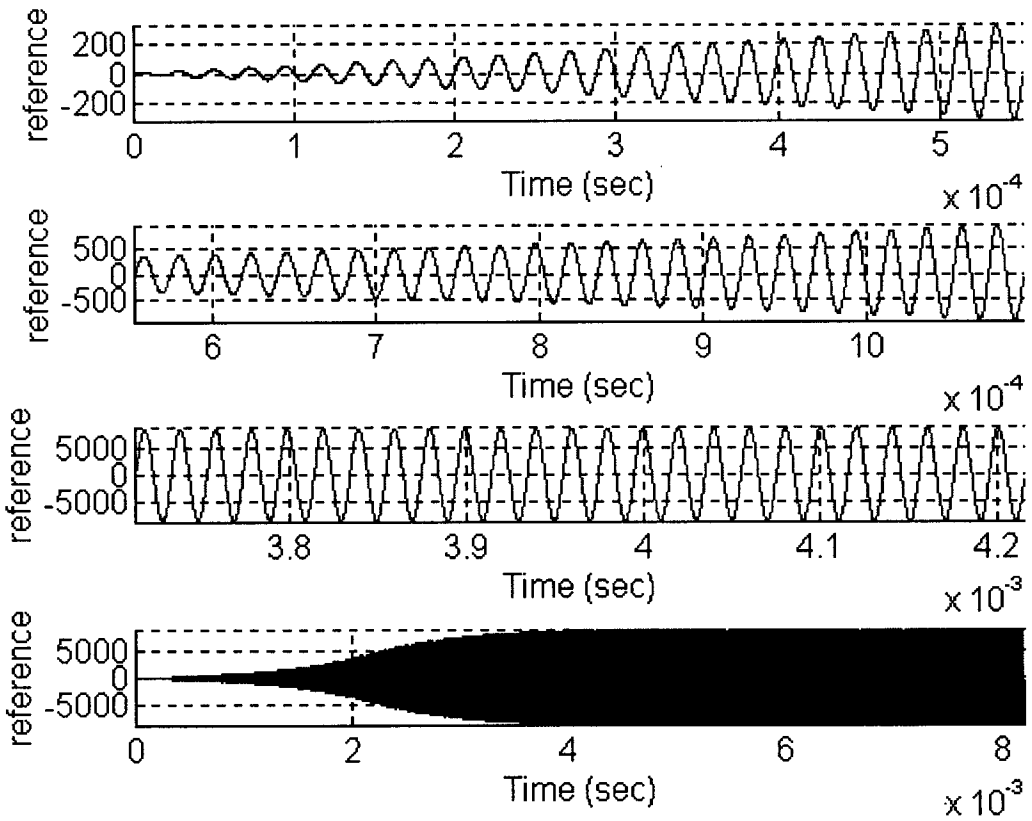


**Fig. 88 Desired Reference Signal Plot**

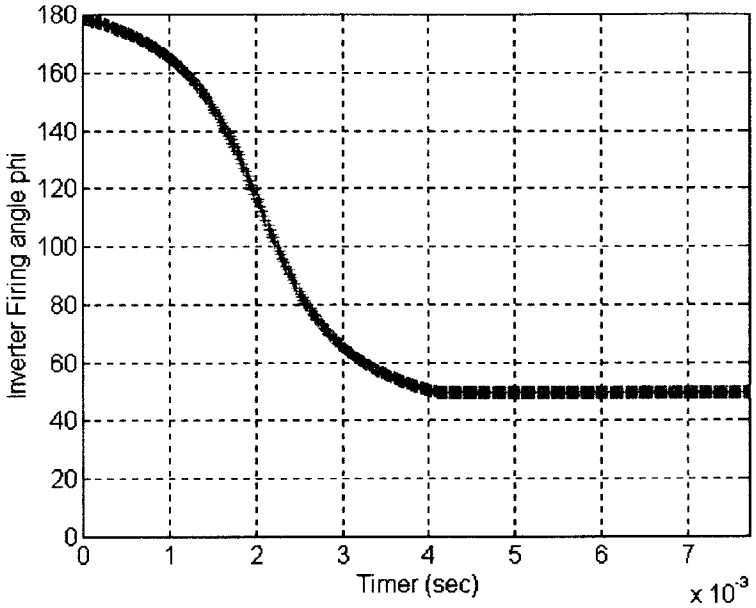


**Fig. 89 Plot of the Firing Angle $\phi$**

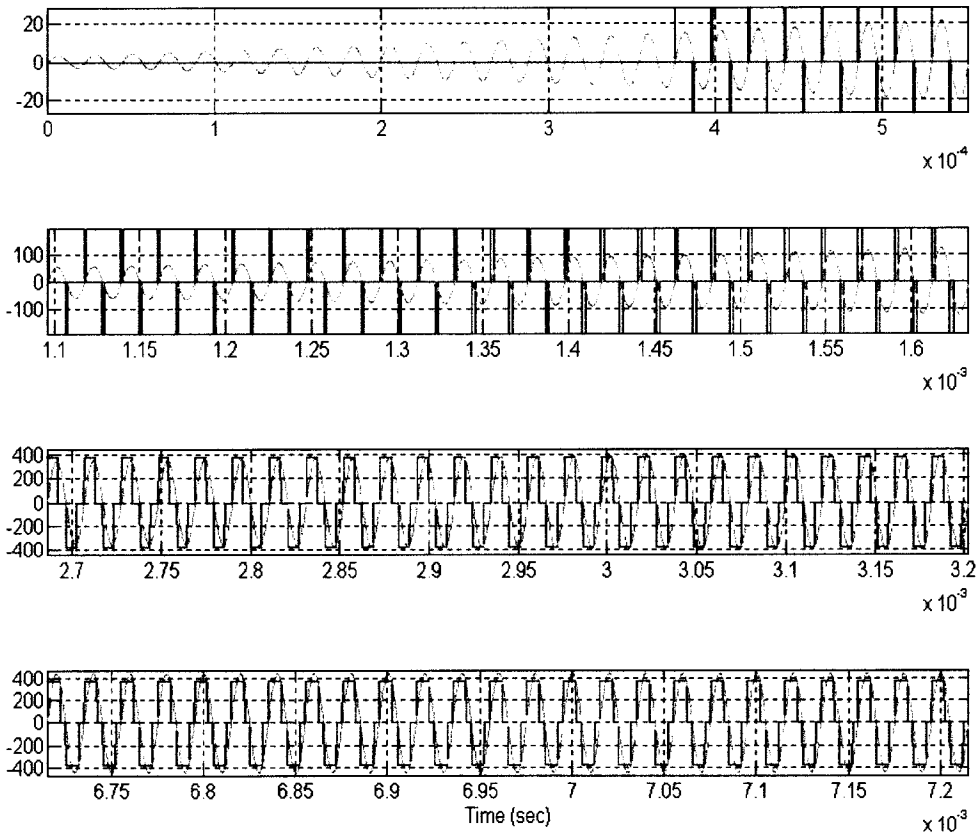


**Fig. 90 Comparison of the Ideal and Actual Optimum Load Section Input**

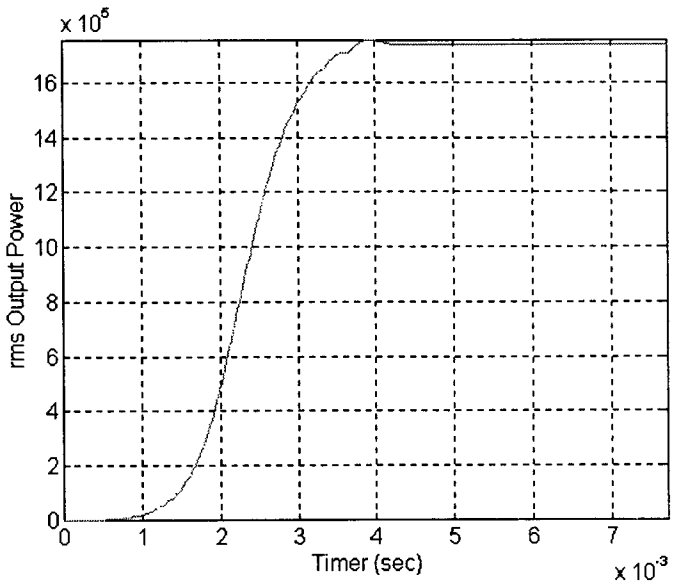


**Fig. 91 Plot of Power (*kW*) vs. Time**

The comparison of the ideal and actual inverter section output is shown in Fig. 90. The width of the square wave is increasing from zero, then keep a constant width when the system is in steady state. By using the new reference signal, from Fig. 91, the steady state output power level is lower.

## 7.2 HFPS Process Power Control

When the Power Supply running at steady state, in order to lower the kW level, the only operation for the LQT controller is to change the reference signal.

The rms value of the new desired system output is smaller, but the frequency is the same. From Fig. 92, the rms value of the reference signal is changed, while the frequency keeps the same.

Based on the change of the reference signal, the LQT controller changes the firing angle $\phi$ for the inverter section, accordingly. In this case, the firing angle increases and the rms value of the inverter section output voltage and the system output power decreases. The plot for the firing angle $\phi$ is shown in Fig. 93.

The value of $\phi$ continues to increase, therefore, the rms value of the input ($V_d$) is decreasing, and the power supply output kW level is decreasing too. The transition of the firing angle is smooth, therefore, the power transition will be smooth too, and no spike will be generated during the output power level changing. From Fig. 94, after 4ms the width of the square wave $V_d$ is decreasing. When the reference signal changes, the rms value of the inverter section Output $V_d$ changes accordingly. From Fig. 95, the kW adjustment will be very smooth and easy to implement.

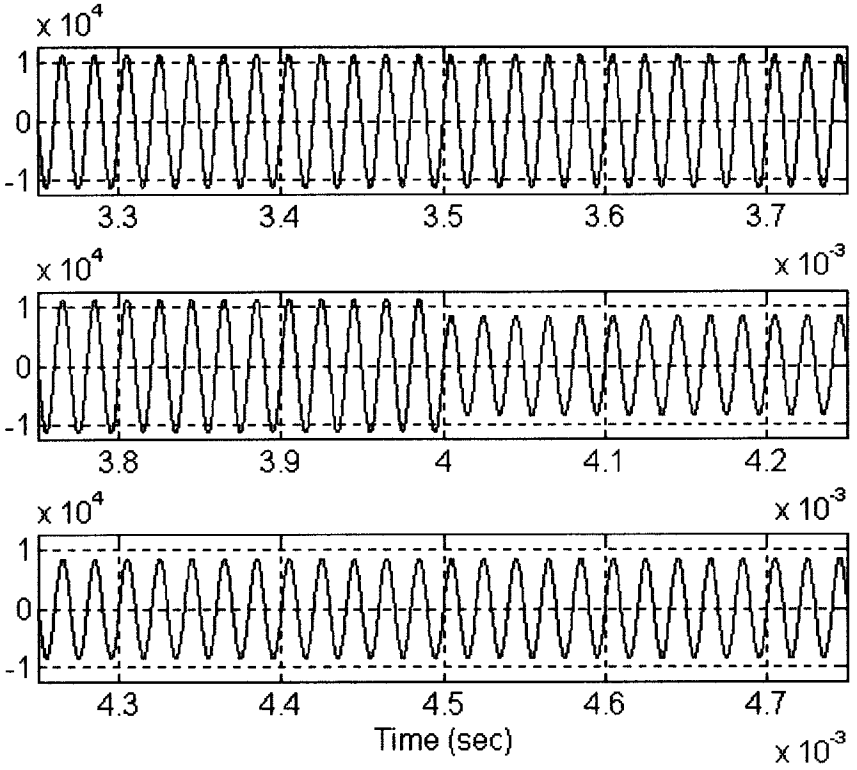


**Fig. 92 Reference Signal**

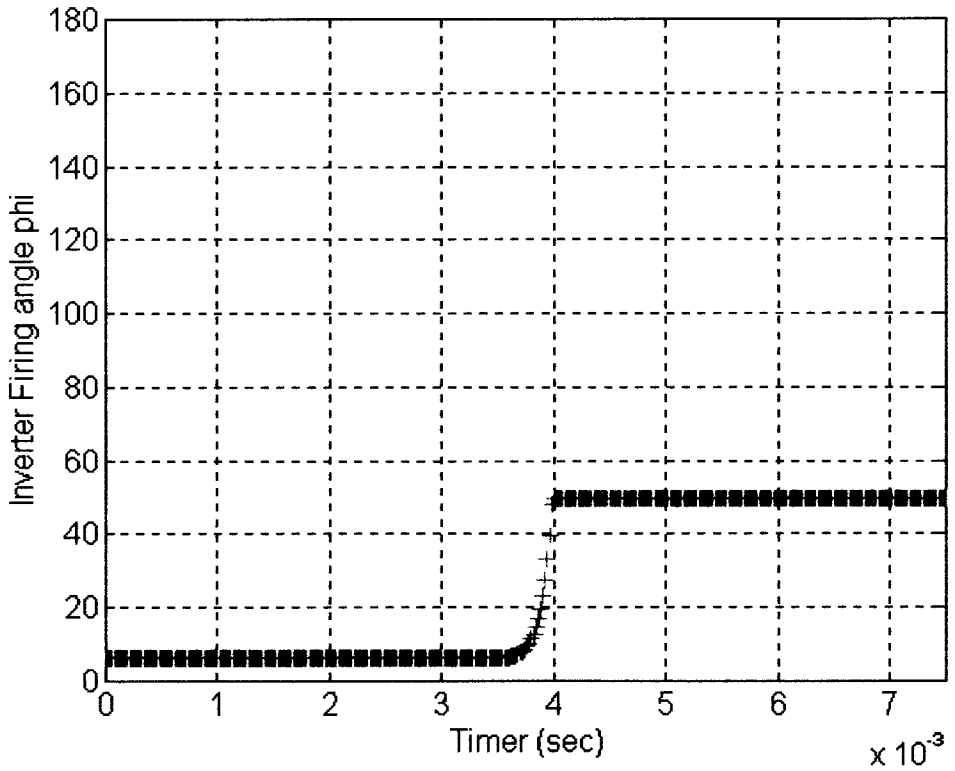


**Fig. 93 Firing Angle for the Inverter Section $\phi$**

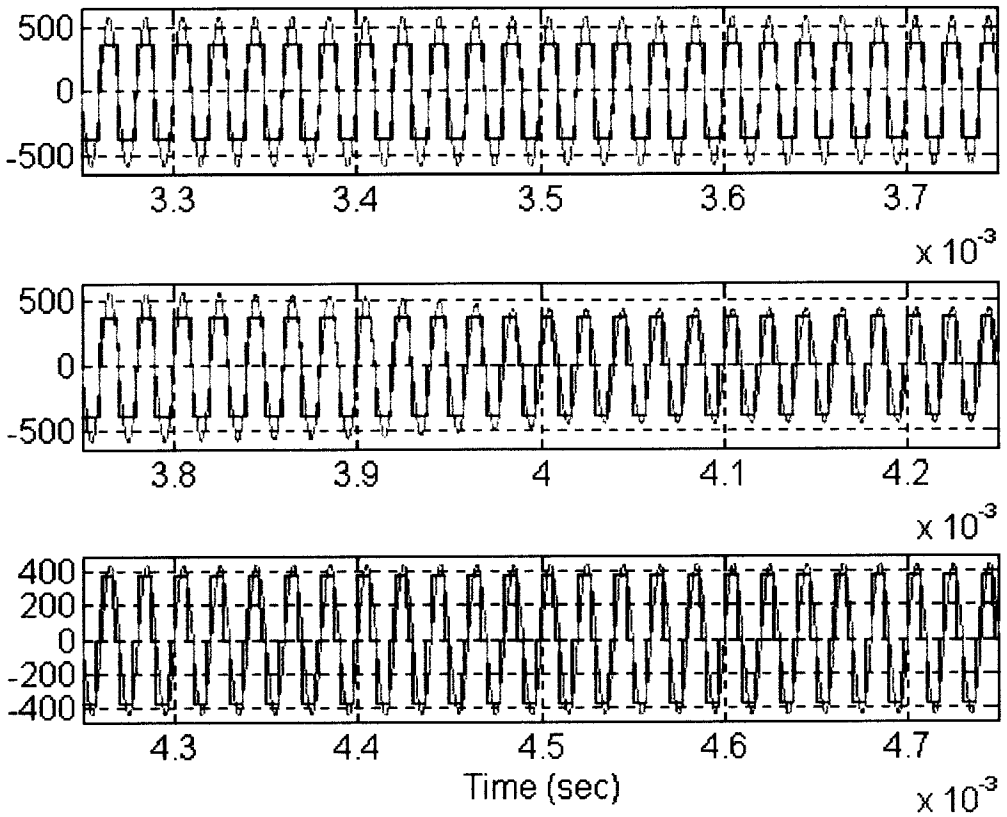


**Fig. 94 Comparison the Ideal and Actual Load Section Input**

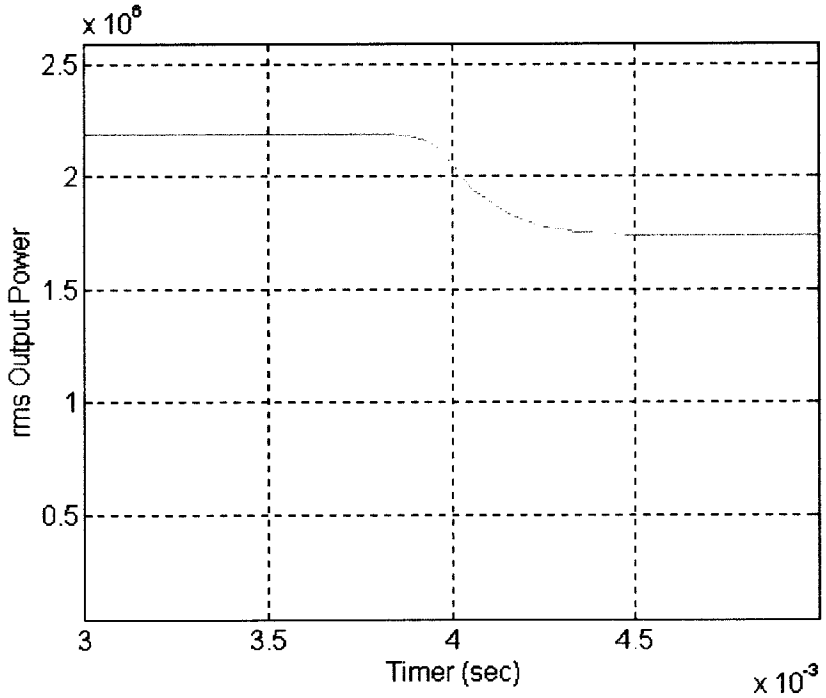


**Fig. 95 Power Level vs. Time Plot**

# Chapter 8

## Summary and Conclusion

An optimal controller design for a HFPS system was presented in this thesis. By using LQT method, the system performance has been optimized. The LQT Controller generates optimal firing angles and switching frequency for the HFPS, that reduces the system loss, eliminates the harmful harmonics, and makes a uniform depth of penetration on the induction load. In the discrete time domain, the desired reference signal can be easily to construct with high accuracy. By changing the reference signal, the HFPS power level and operating frequency can be easily controlled. The LQT controller has the advantage of the closed loop system, it is stable, accurate, and easy to implement. The rms values of the system state variables have been compared with a real system, and the results are matched.

The rms values of the system state variables have been compared with ©**Ajax Magnethermic Corp.** ©PACER HF 2700kW, 50kHz commercial Power Supply, the result are close to the practical result as shown in Table 7.

**Table 7 Comparison of the Value of the State Variables**

| | **Linear Model (w/o Switching Devices)** | **Non-Linear Model (w/ Switching Devices)** | **Real Power Supply** |
|---|---|---|---|
| $i_{SE}$ **(kA)** | 8.00 | 8.00 | 8.10 |
| $V_C$ **(V)** | 2120 | 2120 | 2164 |
| $i_{LO}$ **(kA)** | 17.7 | 17.7 | 16.8 |
| **Frequency (kHz)** | 50.0 | 50.0 | 51.1 |

# References

[1] N. Mohan, T. M. Undeland, W. P. Robbins, "*Power Electronics*", 2nd edition, ISBN 0-471-58408-8, 1995.

[2] K. Astrom, B. Wittenmark, "*Computer Controlled Systems Theory and Design*", 3rd edition, Prentice Hall, Saddle River, NJ. ISBN 0-13-314899-8, 1997.

[3] C. A. Tudbury, "*Basics of Induction Heating*", Library of Congress Cat. Number 60-8958 May, 1960.

[4] B. D. Anderson, J.B. Moore, "Optimum Control, Linear Quadratic Methods", Prentice Hall, Englewood Cliffs, NJ 07632, ISBN 0-13-638560-5, 1990.

[5] C. L. Phillips, R. D. Harbor, "Feedback Control Systems", Prentice Hall, Englewood Cliffs, NJ 07632, ISBN 0-13-313917-4, 1988.

[6] F. L. Lewis, V. L. Syrmos, "Optimal Control", 2nd edition, John Wiley & Sons, INC, ISBN 0-471-03378-2, 1995.